(12) INTERNATIONAL APPLICATION PUBLISHED UNDER THE PATENT COOPERATION TREATY (PCT)

(19) World Intellectual Property Organization
International Bureau

(43) International Publication Date
16 January 2025 (16.01.2025)

WIPO | PCT

(10) International Publication Number
WO 2025/015302 A2

(51) International Patent Classification:
Not classified

(21) International Application Number:
PCT/US2024/037897

(22) International Filing Date:
12 July 2024 (12.07.2024)

(25) Filing Language: English

(26) Publication Language: English

(30) Priority Data:

63/526,278	12 July 2023 (12.07.2023)	US
63/641,318	01 May 2024 (01.05.2024)	US
63/643,053	06 May 2024 (06.05.2024)	US

(71) Applicant: **TRIAD NATIONAL SECURITY, LLC** [US/US]; c/o Los Alamos National Laboratory, P.O. Box 1663, Los Alamos, New Mexico 87545 (US).

(72) Inventors: **NGUYEN, Hau Thi Bich**; c/o Los Alamos National Laboratory, P.O. Box 1663 MS A187, Los Alamos, New Mexico 87545 (US). **GROSECLOSE, Thomas M.**; c/o Los Alamos National Laboratory, P.O. Box 1663 MS A187, Los Alamos, New Mexico 87545 (US).

(74) Agent: **GRAF, Susan W.** et al.; Klarquist Sparkman, LLP, One World Trade Center, 121 SW Salmon St., Suite 1600, Portland, Oregon 97204 (US).

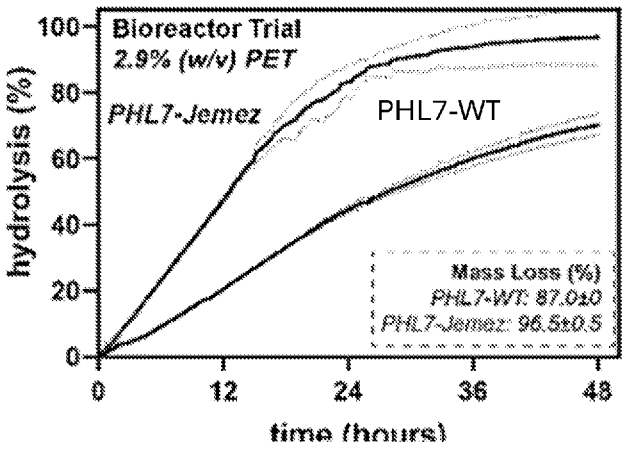
(81) Designated States *(unless otherwise indicated, for every kind of national protection available)*: AE, AG, AL, AM, AO, AT, AU, AZ, BA, BB, BG, BH, BN, BR, BW, BY, BZ, CA, CH, CL, CN, CO, CR, CU, CV, CZ, DE, DJ, DK, DM, DO, DZ, EC, EE, EG, ES, FI, GB, GD, GE, GH, GM, GT, HN, HR, HU, ID, IL, IN, IQ, IR, IS, IT, JM, JO, JP, KE, KG, KH, KN, KP, KR, KW, KZ, LA, LC, LK, LR, LS, LU, LY, MA, MD, MG, MK, MN, MU, MW, MX, MY, MZ, NA, NG, NI, NO, NZ, OM, PA, PE, PG, PH, PL, PT, QA, RO, RS, RU, RW, SA, SC, SD, SE, SG, SK, SL, ST, SV, SY, TH, TJ, TM, TN, TR, TT, TZ, UA, UG, US, UZ, VC, VN, WS, ZA, ZM, ZW.

(84) Designated States *(unless otherwise indicated, for every kind of regional protection available)*: ARIPO (BW, CV, GH, GM, KE, LR, LS, MW, MZ, NA, RW, SC, SD, SL, ST, SZ, TZ, UG, ZM, ZW), Eurasian (AM, AZ, BY, KG, KZ, RU, TJ, TM), European (AL, AT, BE, BG, CH, CY, CZ, DE, DK, EE, ES, FI, FR, GB, GR, HR, HU, IE, IS, IT, LT, LU, LV, MC, ME, MK, MT, NL, NO, PL, PT, RO, RS, SE, SI, SK, SM, TR), OAPI (BF, BJ, CF, CG, CI, CM, GA, GN, GQ, GW, KM, ML, MR, NE, SN, TD, TG).

Published:
— *without international search report and to be republished upon receipt of that report (Rule 48.2(g))*
— *with sequence listing part of description (Rule 5.2(a))*

(54) Title: MODIFIED POLYESTER HYDROLASE POLYPEPTIDES WITH IMPROVED POLYETHYLENE TEREPHTHALATE DEGRADING ACTIVITY

FIG. 7A



(57) Abstract: Modified polyester hydrolase Leipzig #7 (PHL7) polypeptides with improved polyethylene terephthalate degrading activity are provided. Nucleic acids and vectors encoding the modified PHL7 polypeptides are also provided. Also provided are fusion proteins including a PHL7 polypeptide fused to a reporter protein, such as a green fluorescent protein or portion thereof, and nucleic acids and vectors encoding the fusion proteins.

WO 2025/015302 A2

MODIFIED POLYESTER HYDROLASE POLYPEPTIDES WITH IMPROVED POLYETHYLENE TEREPHTHALATE DEGRADING ACTIVITY

CROSS REFERENCE TO RELATED APPLICATIONS

This application claims priority to U.S. Provisional Application No. 63/526,278, filed July 12, 2023; U.S. Provisional Application No. 63/641,318, filed May 1, 2024; and U.S. Provisional Application No. 63/643,053, filed May 6, 2024; each of which is incorporated by reference in its entirety.

FIELD

This disclosure relates to modified enzymes that degrade polyethylene terephthalate with improved activities, particularly modified polyester hydrolase enzymes.

ACKNOWLEDGMENT OF GOVERNMENT SUPPORT

This invention was made with government support under 89233218CNA000001 awarded by the National Nuclear Security Administration. The government has certain rights in the invention.

SEQUENCE LISTING INCORPORATION BY REFERENCE

The Sequence Listing is submitted as an XML file in the form of the file named "8472-110491-06_Sequence_Listing.xml" (22,327 bytes), which was created on July 11, 2024, which is incorporated by reference herein.

BACKGROUND

Just as plastic has become an integral part of modern life, so too has plastic waste become a global crisis. Driven by an increasing need for these versatile, robust, inexpensive, and largely inert materials, worldwide plastic production is estimated at about 460 million metric tons (MT) per year – more mass than all humans on the planet. Almost 80% of this plastic ends up in landfills and the environment, where plastic pollution threatens terrestrial and aquatic ecosystems alike, and has been found in the air and human blood. The 10% of plastic that manages to be recycled (mechanically) is usually "downcycled" into lesser value materials, doing little to mitigate demand for new plastic. This crisis presents an impetus for improving the means to recycle plastic waste. Presently, there is no sustainable way to continue producing plastic at increasing scales, with few options to deal with it at end of life.

Chemical recycling has emerged as a promising potential way to establish a circular plastics economy. Here, discarded plastic can be broken down to its chemical precursors, which can then be used to synthesize new plastic with little, to no, loss of material properties, thus mitigating the need to synthesize virgin plastic from petroleum-based feedstocks, or "up-cycled" to higher valued materials. Polyethylene terephthalate (PET), with an estimated worldwide production of 25 million MT per year and used commonly to make products such as food and beverage containers, clothing, and carpeting, is one such plastic that has been targeted for chemical recycling, where PET can be depolymerized into its terephthalic acid (TPA) and ethylene glycol (EG) precursors. However, typical methods of PET chemical recycling (hydrolysis, solvolysis) are energy- and resource-intensive and characteristically generate complex and/or toxic waste streams. Enzymatic depolymerization is a more sustainable alternative to conventional chemical recycling methods. Thus, there remains a need to develop enzyme variants with improved PET degradation and other properties.

SUMMARY

Provided herein are modified polyester hydrolase Leipzig #7 (PHL7) polypeptides with improved activity, such as increased degradation of PET compared to wild-type or previously described PHL7 enzymes, such as increased polyethylene terephthalate hydrolase activity compared to SEQ ID NO: 1.

In some aspects, a modified PHL7 polypeptide of the disclosure includes at least one amino acid substitution at one or more of positions corresponding to amino acids 32, 35, 64, 80, 111, 112, 175, 185, and 205 of SEQ ID NO: 1. In some examples, the at least one amino acid substitution includes one or more of R32P, A35V, T64S, Q80H, R111H, T112I, T112A, Q175E, H185N, and R205K. In particular examples, the at least one amino acid substitution includes A35V, T112I, Q175E, and H185N; Q80H, Q175E, H185N, and R205K; T112A, Q175E, and H185N; or R32P, T64S, R111H, Q175E, and H185N. In additional examples, the modified polypeptide further includes the amino acid substitution Q95Y. In some examples, the modified PHL7 polypeptide includes A35V, Q95Y, T112I, Q175E, and H185N or Q80H, Q95Y, Q175E, H185N, and R205K. In some examples, the modified PHL7 polypeptide includes or consists of the amino acid sequence of SEQ ID NO: 2, SEQ ID NO: 3, SEQ ID NO: 4, or SEQ ID NO: 5.

In additional aspects, nucleic acid molecules encoding the disclosed modified PHL7 polypeptides are provided. In some examples, the nucleic acid encodes a polypeptide including one or more of R32P, A35V, T64S, Q80H, R111H, T112I, T112A, Q175E, H185N, and R205K. In particular examples, the nucleic acid encodes a polypeptide including A35V, Q95Y, T112I, Q175E,

and H185N; Q80H, Q95Y, Q175E, H185N, and R205K; T112A, Q175E, and H185N; or R32P, T64S, R111H, Q175E, and H185N. In some examples, the nucleic acid includes or consists of the nucleic acid sequence of SEQ ID NO: 8, SEQ ID NO: 9, SEQ ID NO: 10, or SEQ ID NO: 11.

Also provided are vectors including a disclosed nucleic acid encoding a modified PHL7 polypeptide. In some examples, the vector is a plasmid vector. Host cells including a disclosed vector are also provided. In some examples, the host cell is a bacterial cell, such as an *Escherichia coli* cell.

In additional aspects, fusion proteins including a PHL7 polypeptide fused to a reporter protein are provided. In some examples, the reporter protein is a green fluorescent protein or a portion thereof. In one example, the reporter protein is a GFP11 tag. In particular examples, the PHL7 polypeptide portion of the fusion protein includes or consists of the amino acid sequence of SEQ ID NO: 1, SEQ ID NO: 2, SEQ ID NO: 3, SEQ ID NO: 4, or SEQ ID NO: 5. Nucleic acid molecules encoding the fusion proteins and vectors including the nucleic acid molecules are also provided.

In other aspects, methods of degrading PET are provided. In some examples, the methods include contacting PET with a disclosed modified PHL7 polypeptide under conditions sufficient for degrading the PET.

The foregoing and other features of the disclosure will become more apparent from the following detailed description, which proceeds with reference to the accompanying figures.

BRIEF DESCRIPTION OF THE DRAWINGS

FIGS. 1A-1C illustrate improved biocatalytic recycling *via* improved PET hydrolases. FIG. 1A: Envisioning a circular PET economy. Discarded PET can be chemically deconstructed with enzymes to PET precursors, which can then be used to synthesize like-new PET by upcycling/recycling. FIG. 1B: Deconstruction scheme of PET using enzymes (PETases, or PET hydrolases). PET polymer is broken down to monomers BHET, MHET, and TPA and EG (PET precursors). MHETases efficiently convert accumulated MHET to TPA and EG. FIG. 1C: Directed evolution cycle for PET hydrolases. In a particular example, a natural enzyme, PHL7, is used as a scaffold for enhancement of attribute(s) for which it is screened. Large, diverse libraries of enzymes are generated, which are then screened in a high-throughput co-screening assay. Putative, improved variants from screening are isolated and sequenced and can be used as parents for the next round of directed evolution. Once significantly improved enzymes are identified, they can be chosen for large-scale production and thorough characterization.

FIGS. 2A-2C show initial enzymatic rates of PET hydrolases. FIG. 2A: Workflow for sampling PET reactions. Enzymes were added to reactions with PET, which were sampled over time. Samples were analyzed with HPLC, with monomers TPA, MHET, and BHET, and the sum of the three quantified. FIGS. 2B-2D: Quantified products of reactions up to 8 hours, with 0.69 μM enzyme, 2.9% (w/v) PET coupons, at 70°C and pH 8, for benchmarks PHL7-WT, LCC-ICCG, and four engineered PHL7 mutants. Points display the average of n = 3 reactions, while error bars display ±1 S.D. FIG. 2B: Concentration of summed aromatic products. FIG. 2C: Concentration of TPA. FIG. 2D: Concentration of MHET. The engineered PHL7 mutants show the highest initial rates.

FIGS. 3A-3C show deconstruction of PET over time by PET hydrolases. Plots show products of reactions up to 72 hours, quantified with HPLC, with 0.345 μM enzyme, 2.9% (w/v) PET coupons, at 70°C and pH 8, for benchmarks PHL7-WT, LCC-ICCG, and four engineered PHL7 mutants. Points display the average of n = 3 reactions, while error bars display ±1 S.D. FIG. 3A: Concentration of summed aromatic products, TPA, MHET, and BHET. FIG. 3B: Concentration of TPA. FIG. 3C: Concentration of MHET.

FIGS. 4A-4F show PET hydrolase activity at lower pH. Plots show products of reactions up to 72 hours, quantified with HPLC, with 0.69 μM enzyme, 2.9% (w/v) PET coupons, at 70°C, for benchmarks PHL7-WT, LCC-ICCG, and four engineered PHL7 mutants at pH 6 and pH 7. Points display the average of n = 3 reactions, while error bars display ±1 S.D. FIG. 4A: Concentration of summed aromatic products, TPA, MHET, and BHET, at pH 7. FIG.4B: Concentration of TPA, at pH 7. FIG. 4C: Concentration of MHET, at pH 7. FIG. 4D: Concentration of summed aromatic products, TPA, MHET, and BHET, at pH 6. FIG. 4E: Concentration of TPA, at pH 6. FIG. 4F: Concentration of MHET, at pH 6. Engineered PHL7 mutants had higher activities at lower pHs compared to benchmarks.

FIGS. 5A-5C show structural modeling to analyze engineered mutations of PHL7. FIG. 5A: AlphaFold predicted structures of PHL7 variants aligned to the crystal structure of the native PHL7. The regions of maximum variability in the backbone were observed in the loops consisting of residues 46-54 and 111-124. PHL7-L93F/Q95Y was also modeled and overlayed on the crystal structure of native PHL7. The catalytic triad residues S131, D177 and H209 are highlighted. FIG. 5B: ROSETTA modeling shows stabilizing effect of Q → E and R→K mutations at positions 175 and 205 respectively. A hydrogen bond is formed only in case of the double mutation Q175E and R205K. FIG. 5C: Space filling mutation A35V shows improved packing with F38. Native PHL7 (left) and mutant PHL7 (right).

FIGS. 6A-6D show computational docking of PET model substrate in the vicinity of the catalytic triad. FIG. 6A: Surface representation of native PHL7 with a bound PET model substrate (PET3mer). FIG. 6B: PET3mer substrate can be divided into three subsites (-2, -1, +1) where subsite -2 is the leaving group resulting from the esterase activity. Key residues interacting with the PET3mer, that include L210/I179 packing against the leaving group (subsite -2), W156/F63 pi-stacking against subsite -1 and L93/Q95 packing against subsite +1. In this pose, Q95 is also shown to form an H-bond with the ester bond of subsite +1. FIG. 6C: Surface representation of PHL7-Jemez with a bound PET3mer. FIG. 6D: Key residues interacting with the PET3mer include L210/I179 (subsite -2), W156/F63 (subsite -1) and Y95 pi-stacking against subsite +1. Q95Y mutation in PHL7-Jemez results in a preference of an alternate binding mode for the PET3mer substrate, especially at the subsite +1. The catalytic triad consists of S131, D177 and H209.

FIGS. 7A-7C show PET deconstructions by PHL7-WT and PHL7-Jemez in bioreactors. Enzymes (1 mg enzyme/g PET) PHL7-WT and PHL7-Jemez were added to reactions of PET coupons in bioreactors. Bioreactors were monitored for hydrolysis of PET over a 48 hour reaction, with total mass loss observed at the end of the reaction (boxed). Data points and percentages are average of n = 2 bioreactors, while dotted lines represent ±1 S.D. PET coupon solids loading was varied. FIG. 7A: Reaction with 2.9% (w/v) PET. FIG. 7B: Reaction with 5.8% (w/v) PET. FIG. 7C: Reaction with 20% (w/v) PET.

FIG. 8 shows comparison of PET hydrolysis by benchmark enzymes in pH-controlled bioreactors. Enzymes PHL7-Jemez, LCC-LANL, LCC-ICCG, and PHL7-WT were added to reactions of PET coupons [2.9% (w/v)] in bioreactors. Bioreactors were monitored for hydrolysis of amorphous PET coupons over a 48-hour reaction at 65°C, with total mass loss observed after the end of the reaction. Data points show average of n = 2 bioreactors, while dotted lines represent ±1 S.D. Results were plotted for comparison at the conditions: pH 8, 65°C. LCC-LANL and LCC-ICCG reactions were in 100 mM sodium phosphate buffer and 16.5% (w/v) PET, while PHL7-Jemez and PHL7-WT were in 1 M sodium phosphate buffer and 20% (w/v) PET.

FIGS. 9A-9B show activity and thermostability of rationally-designed PHL7 mutants. Data is shown for PHL7-WT, active site mutant PHL7-Q95Y, salt-bridge mutants PHL7-Q175E and PHL7-Q175E/R205K, and disulfide bond mutant PHL7-R205C/S251C. FIG. 9A: Activity of the enzymes, measured by UV absorbance, expressed as equivalents of BHET, in reactions of cell lysates (containing enzymes) with PET. Reactions included 0.5μM enzyme, 2.9% (w/v) PET coupons, 1 M potassium phosphate buffer, pH 8, and incubated at 70°C. PHL7-Q95Y, PHL7-Q175E, and PHL7-Q175E/R205K all had increased activity compared to PHL7-WT over 72 hours. FIG. 9B: Thermostability of the mutants, measured by quantifying enzyme retained in solution pre-

and post-heat treatment for 1 hour at varied temperatures. Fraction of protein retained is the ratio of final protein concentration, quantified by split-GFP complementation, to initial, 0.5 μM. Points display the average of n = 3 reactions, while error bars display ±1 S.D.

FIGS. 10A-10B show comparison of UV absorbance and HPLC techniques for estimation of PET hydrolase activity. Data is shown for PHL7-WT, LCC-ICCG, and four engineered PHL7 mutants. Reactions included 0.69 μM purified enzyme, 2.9% (w/v) PET coupons, at 70°C and pH 8, over 8 hours. FIG. 10A: Activity of the enzymes, measured by UV absorbance, expressed as equivalents of BHET. UV absorbance measures aggregate aromatic products. FIG. 10B: Activity of the enzymes, measured by HPLC. Individual monomers quantified were summed. The two analysis methods gave similar results. Points display the average of n = 3 reactions, while error bars display ±1 S.D.

FIG. 11 shows an SDS PAGE gel of purified proteins. Samples of purified PHL7-WT, PHL7-Jemez, PHL7-Santa Fe, PHL7-Taos, PHL7-Tusas, PHL7-L93F/Q95Y, and LCC-ICCG proteins were run on SDS PAGE gels alongside marker (molecular weights denoted). Samples were boiled in Laemmli buffer for 1 hour at 100°C prior to loading on the gel.

FIG. 12 shows a schematic of evolutionary trajectory of evolved PHL7 mutants. Mutations of the parent enzymes (from rational/semi-rational design) are shown, along with random mutagenesis mutations acquired over four rounds of directed evolution to produce the final evolved mutants.

FIGS. 13A-13F show comparison of LCC and PHL7 benchmarks. Data show activity of benchmarks PHL7-WT, PHL7-L93F/Q95Y, and LCC-ICCG, along with top mutant PHL7-Jemez. Sums of aromatic products (from HPLC analysis) are shown for reactions at varied pH. All experiments were conducted with 2.9% (w/v) PET coupons at 70°C. Points display the average of n = 3 reactions, while error bars display ±1 S.D. FIG. 13A: Initial rate, pH 8. FIG. 13B: Activity over time, pH 8. FIG. 13C: Initial rate, pH 9. FIG. 13D: Activity over time, pH 9. FIG. 13E: Activity over time, pH 7. FIG. 13F: Activity over time, pH 6.

FIGS. 14A-14F show activity of PET hydrolases with powder substrates. Data shows activity of PHL7-WT, LCC-ICCG, and four engineered PHL7 mutants. Product concentrations (from HPLC analysis) are shown for reactions with powder (milled) PET substrates, either amorphous (FIGS. 14A-14C) or high-crystallinity (FIGS. 14D-14F), over 72 hours. The substrate loading was 2.9% (w/v), the enzyme loading was 0.69 μM, and the temperature was 70°C for all experiments. Points display the average of n = 3 reactions, while error bars display ±1 S.D. FIG. 14A: Activity as sum of aromatic products with amorphous PET powder. FIG. 14B: TPA concentration, with amorphous PET powder. FIG. 14C: MHET concentration, with amorphous

PET powder. FIG. 14D: Activity as sum of aromatic products with high-crystallinity PET powder. FIG. 14E: TPA concentration, with high-crystallinity PET powder. FIG. 14F: MHET concentration, with high-crystallinity PET powder.

FIGS. 15A-15B show comparison of LCC and PHL7 benchmarks on powder PET substrates. Data shows activity of benchmarks PHL7-WT, PHL7-L93F/Q95Y, and LCC-ICCG, along with top mutant PHL7-Jemez. Sums of aromatic products (from HPLC analysis) are shown for reactions on 2.9% (w/v) low- and high-crystallinity PET powder over 72 hours at 70°C and pH 8 with 0.69 μM enzyme. Points display the average of n = 3 reactions, while error bars display ±1 S.D . FIG. 15A: Sum of aromatic products, on amorphous PET powder. FIG. 15B: Sum of aromatic products, on high-crystallinity PET powder. While PHL7-Jemez outperformed all benchmarks up to 72 hours on amorphous PET powder, LCC-ICCG had the highest activity on high-crystallinity PET powder.

FIGS. 16A-16F show enzyme activity at pH 9. Activity is shown over 8 hours (0.69 μM enzyme loading) and 72 hours (0.345 μM enzyme loading) for PHL7-WT, LCC-ICCG, and engineered enzyme mutants, with reactions with 2.9% (w/v) PET coupons at 7 °C. Points display the average of n = 3 reactions, while error bars display ±1 S.D. FIG. 16A: Initial rate sum of aromatic products. FIG. 16B: Initial rate TPA concentration. FIG. 16C: Initial rate MHET concentration. FIG. 16D: Sum of aromatic products, activity over time. FIG. 16E: TPA concentration, activity over time. FIG. 16F: MHET concentration, activity over time.

FIGS. 17A-17F show enzyme activity at 65°C. Activity is shown over 8 hours (0.69 μM enzyme loading) and 72 hours (0.345 μM enzyme loading) for PHL7-WT, LCC-ICCG, and engineered enzyme mutants, with reactions with 2.9% (w/v) PET coupons at 65°C. FIG. 17A: Initial rate sum of aromatic products. FIG. 17B: Initial rate TPA concentration. FIG. 17C: Initial rate MHET concentration. FIG. 17D: Sum of aromatic products, activity over time. FIG. 17E: TPA concentration, activity over time. FIG. 17F: MHET concentration, activity over time. Points display the average of n = 3 reactions, while error bars display ±1 S.D.

FIGS. 18A-18F show enzyme activity at 68°C. Activity is shown over 8 hours (0.69 μM enzyme loading) and 72 hours (0.345 μM enzyme loading) for PHL7-WT, LCC-ICCG, and engineered enzyme mutants, with reactions with 2.9% (w/v) PET coupons at 68°C. FIG. 18A: Initial rate sum of aromatic products. FIG. 18B: Initial rate TPA concentration. FIG. 18C: Initial rate MHET concentration. FIG. 18D: Sum of aromatic products, activity over time. FIG. 18E: TPA concentration, activity over time. FIG. 18F: MHET concentration, activity over time. Points display the average of n = 3 reactions, while error bars display ±1 S.D.

FIGS. 19A-19F show comparison of LCC and PHL7 benchmarks at varied temperatures. Data shows activity of benchmarks PHL7-WT, PHL7-L93F/Q95Y, and LCC-ICCG, along with top mutant PHL7-Jemez. Sums of aromatic products (from HPLC analysis) are shown for reactions with 2.9% (w/v) PET coupons over 8 hours (0.69 μM enzyme) and 72 hours (0.345 μM enzyme) at varied temperatures. Points display the average of n = 3 reactions, while error bars display ±1 S.D. FIG. 19A: Initial rate, 65°C. FIG. 19B: Activity over time, 65°C. FIG. 19C: Initial rate, 68°C. FIG. 19D: Activity over time, 68°C. FIG. 19E: Initial rate, 72 °C. FIG. 19F: Activity over time, 72 °C.

FIGS. 20A-20F show enzyme activity at 72°C. Activity is shown over 8 hours (0.69 μM enzyme loading) and 72 hours (0.345 μM enzyme loading) for PHL7-WT, LCC-ICCG, and engineered enzyme mutants, with reactions with 2.9% (w/v) PET coupons at 72°C. FIG. 20A: Initial rate sum of aromatic products. FIG. 20B: Initial rate TPA concentration. FIG. 20C: Initial rate MHET concentration. FIG. 20D: Sum of aromatic products, activity over time. FIG. 20E: TPA concentration, activity over time. FIG. 20F: MHET concentration, activity over time. Points display the average of n = 3 reactions, while error bars display ±1 S.D.

FIGS. 21A-21F show product inhibition of PHL7-WT and PHL7-Jemez. Activity (from HPLC analysis) over 8 hours as sum of aromatic products is shown for PHL7-WT and PHL7-Jemez with product monomers TPA, EG, or MHET initially added at varied concentrations 0 g/L (open circles), 0.5 g/L (light grey circles), 1 g/L (dark grey circles), and 2.5 g/L (black circles). Points display the average of n = 3 reactions, while error bars display ±1 S.D. DMSO [10% (v/v)] was added to TPA and MHET reactions as a consequence of solubilizing monomers. Reactions were at 70°C, pH 8, with 0.69 μM enzyme, 2.9% (w/v) PET coupons. FIG. 21A: PHL7-WT with initial TPA. FIG. 21B: PHL7-Jemez with initial TPA. FIG. 21C: PHL7-WT with initial EG. FIG. 21D: PHL7-Jemez with initial EG. FIG. 21E: PHL7-WT with initial MHET. FIG. 21F: PHL7-Jemez with initial MHET.

FIGS. 22A-22B show computational docking of PET model substrate in the vicinity of the catalytic triad of PHL7-L93F/Q95Y. FIG. 22A: Surface representation of PHL7-L93F/Q95Y with a bound PET model substrate (PET3mer). FIG. 22B: Key residues interacting with the PET3mer, that include L210/I179 packing against the leaving group (subsite -2), W156/F63 pi-stacking against subsite -1 and Y95 packing against subsite +1. T158 sidechain and backbone also show hydrogen bonding with the substrate. F93 fails to show any role in substrate recruitment. The catalytic triad consists of S131, D177 and H209.

SEQUENCE LISTING

The nucleic acid and amino acid sequences provided herein and listed in the accompanying sequence listing are shown using standard letter abbreviations for nucleotide bases, and single letter code for amino acids, as defined in 37 C.F.R. 1.822. Only one strand of each nucleic acid sequence is shown, but the complementary strand is understood as included by any reference to the displayed strand.

In the accompanying sequence listing:

SEQ ID NO: 1 is the amino acid sequence of an exemplary wild type PHL7 polypeptide:

MANPYERGPDPTESSIEAVRGPFAVAQTTVSRLQADGFGGGTIYYPTDTSQGTFGAVAISP
GFTAGQESIAWLGPRIASQGFVVITIDTITRLDQPDSRGRQLQAALDHLRTNSVVRNRIDP
NRMAVMGHSMGGGGALSAAANNTSLEAAIPLQGWHTRKNWSSVRTPTLVVGAQLDTIAPVS
SHSEAFYNSLPSDLDKAYMELRGASHLVSNTPDTTTAKYSIAWLKRFVDDDLRYEQFLCPA
PDDFAISEYRSTCPF

SEQ ID NO: 2 is the amino acid sequence of PHL7-Jemez (modified amino acids in bold type):

MANPYERGPDPTESSIEAVRGPFAVAQTTVSRLQ**V**DGFGGGTIYYPTDTSQGTFGAVAISP
GFTAGQESIAWLGPRIASQGFVVITIDTITRLD**Y**PDSRGRQLQAALDHLR**I**NSVVRNRIDP
NRMAVMGHSMGGGGALSAAANNTSLEAAIPLQGWHTRKNWSSVRTPTLVVGA**E**LDTIAPVS
S**N**SEAFYNSLPSDLDKAYMELRGASHLVSNTPDTTTAKYSIAWLKRFVDDDLRYEQFLCPA
PDDFAISEYRSTCPF

SEQ ID NO: 3 is the amino acid sequence of PHL7-Santa Fe (modified amino acids in bold type):

MANPYERGPDPTESSIEAVRGPFAVAQTTVSRLQADGFGGGTIYYPTDTSQGTFGAVAISP
GFTAGQESIAWLGPRIAS**H**GFVVITIDTITRLD**Y**PDSRGRQLQAALDHLRTNSVVRNRIDP
NRMAVMGHSMGGGGALSAAANNTSLEAAIPLQGWHTRKNWSSVRTPTLVVGA**E**LDTIAPVS
S**N**SEAFYNSLPSDLDKAYMEL**K**GASHLVSNTPDTTTAKYSIAWLKRFVDDDLRYEQFLCPA
PDDFAISEYRSTCPF

SEQ ID NO: 4 is the amino acid sequence of PHL7-Taos (modified amino acids in bold type):

MANPYERGPDPTESSIEAVRGPFAVAQTTVSRLQADGFGGGTIYYPTDTSQGTFGAVAISP
GFTAGQESIAWLGPRIASQGFVVITIDTITRLDQPDSRGRQLQAALDHLR**A**NSVVRNRIDP
NRMAVMGHSMGGGGALSAAANNTSLEAAIPLQGWHTRKNWSSVRTPTLVVGA**E**LDTIAPVS
S**N**SEAFYNSLPSDLDKAYMELRGASHLVSNTPDTTTAKYSIAWLKRFVDDDLRYEQFLCPA
PDDFAISEYRSTCPF

SEQ ID NO: 5 is the amino acid sequence of PHL7-Tusas (modified amino acids in bold type):

MANPYERGPDPTESSIEAVRGPFAVAQTTVS**P**LQADGFGGGTIYYPTDTSQGTFGAVAISP
GF**S**AGQESIAWLGPRIASQGFVVITIDTITRLDQPDSRGRQLQAALDHL**H**TNSVVRNRIDP
NRMAVMGHSMGGGGALSAAANNTSLEAAIPLQGWHTRKNWSSVRTPTLVVGA**E**LDTIAPVS
S**N**SEAFYNSLPSDLDKAYMELRGASHLVSNTPDTTTAKYSIAWLKRFVDDDLRYEQFLCPA
PDDFAISEYRSTCPF

SEQ ID NO: 6 is the amino acid sequence of PHL7- L93F/Q95Y (modified amino acids in bold type):

MANPYERGPDPTESSIEAVRGPFAVAQTTVSRLQADGFGGGTIYYPTDTSQGTFGAVAISP
GFTAGQESIAWLGPRIASQGFVVITIDTITR**F**D**Y**PDSRGRQLQAALDHLRTNSVVRNRIDP
NRMAVMGHSMGGGGALSAAANNTSLEAAIPLQGWHTRKNWSSVRTPTLVVGAQLDTIAPVS
SHSEAFYNSLPSDLDKAYMELRGASHLVSNTPDTTTAKYSIAWLKRFVDDDLRYEQFLCPA
PDDFAISEYRSTCPF

SEQ ID NO: 7 is a nucleic acid sequence encoding an exemplary wild type PHL7:

ATGGCGAATCCGTATGAGCGTGGCCCGGACCCGACCGAGAGCAGCATTGAAGCGGTTCGTG
GCCCGTTTGCGGTTGCGCAGACCACCGTTAGCCGTCTGCAGGCGGATGGCTTCGGTGGTGG
CACCATCTACTATCCGACCGACACCAGCCAAGGCACCTTCGGTGCGGTGGCGATTAGCCCG
GGCTTTACCGCGGGTCAGGAGAGCATTGCGTGGCTGGGTCCGCGTATTGCGAGCCAAGGTT
TTGTGGTTATCACCATTGATACCATCACCCGTCTGGATCAGCCGGACAGCCGTGGCCGTCA
GCTGCAAGCGGCGCTGGATCACCTGCGTACCAACAGCGTGGTTCGTAACCGTATTGACCCG
AACCGTATGGCGGTTATGGGTCACAGCATGGGCGGTGGtGGTGCGCTGAGCGCTGCGGCGA
ACAACACCAGCCTGGAAGCGGCGATCCCGCTGCAGGGTTGGCACACCCGTAAGAACTGGAG
CAGCGTGCGTACCCCGACCCTGGTGGTTGGTGCGCAACTGGATACCATTGCGCCGGTTAGC
AGCCACAGCGAGGCGTTCTACAACAGCCTGCCGAGCGATCTGGACAAAGCGTATATGGAAC
TGCGTGGTGCGAGCCACCTGGTGAGCAACACCCCGGACACCACCACcGCGAAGTACAGCAT
CGCGTGGCTGAAACGTTTTGTTGACGATGACCTGCGTTATGAGCAATTTCTGTGCCCGGCG
CCGGACGACTTTGCGATTAGCGAATACCGTAGCACCTGCCCGTTC

SEQ ID NO: 8 is a nucleic acid sequence encoding PHL7-Jemez (modified nucleotides in bold type):

ATGGCGAATCCGTATGAGCGTGGCCCGGACCCGACCGAGAGCAGCATTGAAGCGGTTCGTG
GCCCGTTTGCGGTTGCGCAGACCACCGTTAGCCGTCTGCAGG**T**GGATGGCTTCGGTGGTGG
CACCATCTACTATCCGACCGACACCAGCCAAGGCACCTTCGGTGCGGTGGCGATTAGCCCG
GGCTTTACCGCGGGTCAGGAGAGCATTGCGTGGCTGGGTCCGCGTATTGCGAGCCAAGGTT

TTGTGGTTATCACCATTGATACCATCACCCGTCTGGAT**T**A**T**CCGGACAGCCGTGGCCGTCA
GCTGCAAGCGGCGCTGGATCACCTGCGTA**T**CAACAGCGTGGTTCGTAACCGTATTGACCCG
AACCGTATGGCGGTTATGGGTCACAGCATGGGCGGTGGTGGTGCGCTGAGCGCTGCGGCGA
ACAACACCAGCCTGGAAGCGGCGATCCCGCTGCAGGGTTGGCACACCCGTAAGAACTGGAG
CAGCGTGCGTACCCCGACCCTGGTGGTTGGTGCG**G**AACTGGATACCATTGCGCCGGTTAGC
AGC**A**ACAGCGAGGCGTTCTACAACAGCCTGCCGAGCGATCTGGACAAAGCGTATATGGAAC
TGCGTGGTGCGAGCCACCTGGTGAGCAACACCCCGGACACCACCACCGCGAAGTACAGCAT
CGCGTGGCTGAAACGTTTTGTTGACGATGACCTGCGTTATGAGCAATTTCTGTGCCCGGCG
CCGGACGACTTTGCGATTAGCGAATACCGTAGCACCTGCCCGTTC

SEQ ID NO: 9 is a nucleic acid sequence encoding PHL7-Santa Fe (modified nucleotides in bold type):

ATGGCGAATCCGTATGAGCGTGGCCCGGACCCGACCGAGAGCAGCATTGAAGCGGTTCGTG
GCCCGTTTGCGGTTGCGCAGACCACCGTTAGCCGTCTGCAGGCGGATGGCTTCGGTGGTGG
CACCATCTACTATCCGACCGACACCAGCCAAGGCACCTTCGGTGCGGTGGCGATTAGCCCG
GGCTTTACCGCGGGTCAGGAGAGCATTGCGTGGCTGGGTCCGCGTATTGCGAGCCA**T**GGTT
TTGTGGTTATCACCATTGATACCATCACCCGTCTGGAT**T**A**T**CCGGACAGCCGTGGCCGTCA
GCTGCAAGCGGCGCTGGATCACCTGCGTACCAACAGCGTGGTTCGTAACCGTATTGACCCG
AACCGTATGGCGGTTATGGGTCACAGCATGGGCGGTGGTGGTGCGCTGAGCGCTGCGGCGA
A**T**AACACCAGCCTGGAAGCGGCGATCCCGCTGCAGGGTTGGCACACCCGTAAGAACTGGAG
CAGCGTGCGTACCCCGAC**T**CTGGTGGTTGGTGCG**G**AACTGGATACCATTGCGCCGGTTAGC
AGC**A**ACAGCGAGGCGTTCTACAACAGCCTGCCGAGCGATCTGGACAAAGCGTATATGGAAC
TG**AAA**GGTGCGAGCCACCTGGTGAGCAACACCCCGGACACCACCACCGCGAAGTACAGCAT
CGCGTGGCTGAAACGTTTTGTTGACGATGACCTGCGTTATGAGCAATTTCTGTGCCCGGCG
CCGGACGACTTTGCGATTAGCGAATACCGTAGCACCTGCCCGTTC

SEQ ID NO: 10 is a nucleic acid sequence encoding PHL7-Taos (modified nucleotides in bold type):

ATGGCGAATCCGTATGAGCGTGGCCCGGACCCGACCGAGAGCAGCATTGAAGCGGTTCGTG
GCCCGTTTGCGGTTGCGCAGACCACCGTTAGCCGTCTGCAGGCGGATGGCTTCGGTGGTGG
CACCATCTACTATCCGACCGACACCAGCCAAGGCACCTTCGGTGCGGTGGCGATTAGCCCG
GGCTTTACCGCGGGTCAGGAGAGCATTGCGTGGCTGGGTCCGCGTATTGCGAGCCAAGGTT
TTGTGGTTATCACCATTGATACCATCACCCGTCTGGATCAGCCGGACAGCCGTGGCCGTCA
GCTGCAAGCGGCGCTGGATCACCTGCGT**G**CCAACAGCGTGGTTCGTAACCGTATTGACCCG
AACCGTATGGCGGTTATGGGTCACAGCATGGGCGGTGG**C**GGTGCGCTGAGCGCTGCGGCGA
ACAACACCAGCCTGGAAGCGGCGATCCCGCTGCAGGGTTGGCACACCCGTAAGAACTGGAG

CAGCGTGCGTACCCCGACCCTGGTGGTTGGTGCG**G**AACTGGATACCATTGCGCCGGTTAGC
AGC**A**ACAGCGAGGCGTTCTACAACAGCCTGCCGAGCGATCTGGACAAAGCGTATATGGAAC
TGCGTGGTGCGAGCCACCTGGTGAGCAACACCCCGGACACCACCACCGCGAAGTACAGCAT
CGCGTGGCTGAAACGTTTTGTTGACGATGACCTGCGTTATGAGCAATTTCTGTGCCCGGCG
CCGGACGACTTTGCGATTAGCGAATACCGTAGCACCTGCCCGTTC

SEQ ID NO: 11 is a nucleic acid sequence encoding PHL7-Tusas (modified nucleotides in bold type):

ATGGCGAATCCGTATGAGCGTGGCCCGGACCCGACCGAGAGCAGCATTGAAGCGGTTCGTG
GCCCGTTTGCGGTTGCGCAGACCACCGTTAGCC**C**TCTGCAGGCGGATGGCTTCGGTGGTGG
CACCATCTACTATCCGACCGACACCAGCCAAGGCACCTTCGGTGCGGTGGCGATTAGCCCG
GGCTTTA**G**CGCGGGTCAGGAGAGCATTGCGTGGCTGGGTCCGCGTATTGCGAGCCAAGGTT
TTGTGGTTATCACCATTGATACCATCACCCGTCTGGATCAGCCGGACAGCCGTGGCCGTCA
GCTGCAAGCGGCGCTGGATCACCTGC**A**TACCAACAGCGTGGTTCG**C**AACCG**G**ATTGACCCG
AACCGTATGGCGGTTATGGGTCACAGCATGGGCGGTGG**C**GGTGCGCTGAGCGCTGCGGCGA
ACAACACCAGCCTGGAAGCGGCGATCCCGCTGCAGGGTTGGCACACCCGTAAGAACTGGAG
CAGCGTGCGTACCCCGACCCTGGTGGTTGGTGCG**G**AACTGGATACCATTGCGCCGGTTAGC
AGC**A**ACAGCGAGGCGTTCTACAACAGCCTGCCGAGCGATCTGGACAAAGCGTATATGGAAC
TGCGTGGTGCGAGCCACCTGGTGAGCAACACCCCGGACACCACCACCGCGAAGTACAGCAT
CGCGTGGCTGAAACGTTTTGTTGACGATGACCTGCGTTATGAGCAATTTCTGTGCCCGGCG
CCGGACGACTTTGCGATTAGCGAATACCGTAGCACCTGCCCGTTC

SEQ ID NO: 12 is a nucleic acid sequence encoding PHL7- L93F/Q95Y (modified nucleotides in bold type):

ATGGCGAATCCGTATGAGCGTGGCCCGGACCCGACCGAGAGCAGCATTGAAGCGGTTCGTG
GCCCGTTTGCGGTTGCGCAGACCACCGTTAGCCGTCTGCAGGCGGATGGCTTCGGTGGTGG
CACCATCTACTATCCGACCGACACCAGCCAAGGCACCTTCGGTGCGGTGGCGATTAGCCCG
GGCTTTACCGCGGGTCAGGAGAGCATTGCGTGGCTGGGTCCGCGTATTGCGAGCCAAGGTT
TTGTGGTTATCACCATTGATACCATCACCCGT**T**T**T**GAT**T**A**T**CCGGACAGCCGTGGCCGTCA
GCTGCAAGCGGCGCTGGATCACCTGCGTACCAACAGCGTGGTTCGTAACCGTATTGACCCG
AACCGTATGGCGGTTATGGGTCACAGCATGGGCGGTGGtGGTGCGCTGAGCGCTGCGGCGA
ACAACACCAGCCTGGAAGCGGCGATCCCGCTGCAGGGTTGGCACACCCGTAAGAACTGGAG
CAGCGTGCGTACCCCGACCCTGGTGGTTGGTGCGCAACTGGATACCATTGCGCCGGTTAGC
AGCCACAGCGAGGCGTTCTACAACAGCCTGCCGAGCGATCTGGACAAAGCGTATATGGAAC
TGCGTGGTGCGAGCCACCTGGTGAGCAACACCCCGGACACCACCACcGCGAAGTACAGCAT

CGCGTGGCTGAAACGTTTTGTTGACGATGACCTGCGTTATGAGCAATTTCTGTGCCCGGCG
CCGGACGACTTTGCGATTAGCGAATACCGTAGCACCTGCCCGTTC

SEQ ID NO: 13 is the amino acid sequence of LCC-ICCG:

MSNPYQRGPNPTRSALTADGPFSVATYTVSRLSVSGFGGGVIYYPTGTSLTFGGIAMSPGY
TADASSLAWLGRRLASHGFVVLVINTNSRFDGPDSRASQLSAALNYLRTSSPSAVRARLDA
NRLAVAGHSMGGGGTLRIAEQNPSLKAAVPLTPWHTDKTFNTSVPVLIVGAEADTVAPVSQ
HAIPFYQNLPSTTPKVYVELCNASHIAPNSNNAAISVYTISWMKLWVDNDTRYRQFLCNVN
DPALCDFRTNNRHCQ

SEQ ID NO: 14 is a nucleic acid sequence encoding LCC-ICCG:

ATGTCTAACCCGTACCAGCGCGGACCGAACCCGACCCGTTCTGCGTTAACCGCTGATGGTC
CGTTTTCCGTGGCTACCTACACCGTTTCTCGTCTGTCCGTTTCCGGTTTTGGTGGTGGTGT
TATCTACTATCCGACTGGTACCTCTCTGACCTTCGGCGGTATCGCGATGTCCCCGGGTTAC
ACCGCTGATGCTTCCTCTCTGGCGTGGCTGGGTCGTCGCCTGGCGAGCCACGGTTTTGTTG
TTCTGGTTATCAACACGAACTCTCGTTTCGACGGCCCGGACTCCCGTGCCTCGCAACTGTC
TGCTGCGCTGAACTACCTGCGTACGTCGTCACCTTCAGCGGTCCGTGCACGCCTGGATGCC
AATCGTCTGGCTGTGGCGGGTCACAGCATGGGCGGTGGCGGTACCCTGCGTATTGCTGAAC
AGAACCCGTCCCTGAAAGCTGCAGTGCCACTGACTCCGTGGCATACCGACAAAACGTTCAA
CACCAGTGTTCCGGTACTGATCGTAGGCGCAGAAGCGGACACCGTAGCACCGGTTTCCCAG
CACGCAATCCCGTTCTACCAGAACCTGCCGAGCACCACTCCAAAAGTATACGTTGAACTGT
GCAACGCCTCGCACATTGCTCCGAACTCGAACAACGCTGCGATTAGCGTGTACACCATCTC
CTGGATGAAACTGTGGGTTGATAACGATACCCGTTATCGCCAATTCCTGTGTAACGTGAAC
GATCCGGCTCTCTGCGATTTTCGTACCAACAACCGTCATTGCCAA

SEQ ID NO: 15 is the nucleic acid sequence of an expression cassette for PHL7-WT-GFP11 (nucleotides 1-19, T7 promoter; nucleotides 20-44, *lac* operator; nucleotides 59-81, RBS; underlined, restriction sites NdeI and BamHI; nucleotides 89-865, PHL7; nucleotides 872-901, linker; nucleotides 902-949, GFP11; nucleotides 1052-1099, T7 terminator):

TAATACGACTCACTATAGGGGAATTGTGAGCGGATAACAATTCCCCTCTAGAAATAATTTT
GTTTAACTTTAAGAAGGAGATATACATATGGCGAATCCGTATGAGCGTGGCCCGGACCCGA
CCGAGAGCAGCATTGAAGCGGTTCGTGGCCCGTTTGCGGTTGCGCAGACCACCGTTAGCCG
TCTGCAGGCGGATGGCTTCGGTGGTGGCACCATCTACTATCCGACCGACACCAGCCAAGGC
ACCTTCGGTGCGGTGGCGATTAGCCCGGGCTTTACCGCGGGTCAGGAGAGCATTGCGTGGC
TGGGTCCGCGTATTGCGAGCCAAGGTTTTGTGGTTATCACCATTGATACCATCACCCGTCT
GGATCAGCCGGACAGCCGTGGCCGTCAGCTGCAAGCGGCGCTGGATCACCTGCGTACCAAC
AGCGTGGTTCGTAACCGTATTGACCCGAACCGTATGGCGGTTATGGGTCACAGCATGGGCG

GTGGtGGTGCGCTGAGCGCTGCGGCGAACAACACCAGCCTGGAAGCGGCGATCCCGCTGCA
GGGTTGGCACACCCGTAAGAACTGGAGCAGCGTGCGTACCCCGACCCTGGTGGTTGGTGCG
CAACTGGATACCATTGCGCCGGTTAGCAGCCACAGCGAGGCGTTCTACAACAGCCTGCCGA
GCGATCTGGACAAAGCGTATATGGAACTGCGTGGTGCGAGCCACCTGGTGAGCAACACCCC
GGACACCACCACcGCGAAGTACAGCATCGCGTGGCTGAAACGTTTTGTTGACGATGACCTG
CGTTATGAGCAATTTCTGTGCCCGGCGCCGGACGACTTTGCGATTAGCGAATACCGTAGCA
CCTGCCCGTTCGGATCCGATGGAGGGTCTGGTGGCGGATCAACTAGTCGTGACCACATGGT
CCTTCATGAGTACGTAAATGCTGCTGGGATTACATAAGGTACCTAACTCGAGCACCACCAC
CACCACCACTGAGATCCGGCTGCTAACAAAGCCCGAAAGGAAGCTGAGTTGGCTGCTGCCA
CCGCTGAGCAATAACTAGCATAACCCCTTGGGGCCTCTAAACGGGTCTTGAGGGGTTTTTT
G

DETAILED DESCRIPTION

As disclosed herein, directed evolution and rational design engineering approaches, coupled with a high-throughput screening platform (FIG. 1C), were used to engineer high-performance PET hydrolases that, surpass the catalytic properties of current state-of-the-art enzymes. Polyester Hydrolase Leipzig #7 (PHL7), a thermophilic polyester hydrolase (Sonnendecker *et al., ChemSusChem*, 15:e202101062, 2022) that was reported to outperform previously-reported PET hydrolases (Richter *et al., Nature Commun.* 14:1905, 2023), was conferred with improved activity, enhanced stability, and higher expression, yielding enzyme variants that were able to better break down PET more efficiently, providing a vital technology for sustainable, biocatalytic chemical recycling, as well as demonstrating the ability to evolve diverse PET hydrolases for a range of engineering goals.

I. Summary of Terms

Unless otherwise noted, technical terms are used according to conventional usage. Definitions of many common terms in molecular biology may be found in Krebs *et al.* (eds.), *Lewin's genes XII*, published by Jones & Bartlett Learning, 2017. As used herein, the singular forms "a," "an," and "the," refer to both the singular as well as plural, unless the context clearly indicates otherwise. For example, the term "a protein" includes singular or plural proteins and can be considered equivalent to the phrase "at least one protein." As used herein, the term "comprises" means "includes." It is further to be understood that any and all base sizes or amino acid sizes, and all molecular weight or molecular mass values, given for nucleic acids or polypeptides are approximate, and are provided for descriptive purposes, unless otherwise indicated. Although

many methods and materials similar or equivalent to those described herein can be used, particular suitable methods and materials are described herein. In case of conflict, the present specification, including explanations of terms, will control. In addition, the materials, methods, and examples are illustrative only and not intended to be limiting.

To facilitate review of the various aspects, the following explanations of terms are provided:

Heterologous: Originating from a different genetic source or species. A gene or nucleic acid that is heterologous to a prokaryotic cell originates from an organism or species other than the prokaryotic cell in which it is expressed or in a different genetic location, orientation, or in any other way modified from its natural sequence and location in the genome. Methods for introducing a heterologous gene or nucleic acid in a cell or organism are well known in the art, for example transformation with a nucleic acid, including electroporation, lipofection, particle gun acceleration, and homologous recombination.

Isolated: An "isolated" biological component (such as a nucleic acid molecule, protein, or cell) has been substantially separated or purified away from other biological components, such as in the cell of the organism, or the organism itself, in which the component occurs, such as other chromosomal and extra-chromosomal DNA and RNA, proteins and cells. Nucleic acid molecules and proteins that have been "isolated" include nucleic acid molecules and proteins purified by standard purification methods. The term also embraces nucleic acid molecules and proteins prepared by recombinant expression in a host cell as well as chemically synthesized nucleic acid molecules and proteins.

It is understood that the term "isolated" does not imply that the component is free of trace contamination, and can include molecules that are at least 50% isolated, such as at least 50%, 55%, 60%, 65%, 70%, 75%, 80%, 85%, 90%, 95%, 98%, 99%, or even 100% isolated.

Modified: A "modified" nucleic acid or polypeptide is one that has a sequence that is not naturally occurring or has a sequence that is made by an artificial combination of two or more otherwise separated segments of sequence. A modified nucleic acid or polypeptide may be produced by chemical synthesis or artificial manipulation of isolated segments of nucleic acids, *e.g.,* by genetic engineering or genetic editing techniques.

Operably linked: A first nucleic acid is operably linked to a second nucleic acid when the first nucleic acid is placed in a functional relationship with the second nucleic acid. For instance, a regulatory element is operably linked to a coding sequence if the regulatory element affects the transcription or expression of the coding sequence. Regulatory elements include regions such as promoters or portions thereof (such as -35 and/or -10 sites), transcription factor binding sites,

operators, terminators and the like, that may be located upstream or downstream of a coding sequence.

Polyester hydrolase Leipzig #7 (PHL7): A polyester-hydrolyzing enzyme first discovered and isolated from plant compost through a metagenomic study from different compost sites located in Leipzig, Germany (Sonnendecker *et al.*, *ChemSusChem* 15:e202101062, 2022). PHL7 efficiently degrades PET. Exemplary wild type PHL7 amino acid and nucleic acid sequences are provided as SEQ ID NOs: 1 and 7, respectively.

Promoter: Promoters are sequences of DNA near the 5′ end of a gene that act as a binding site for RNA polymerase, and from which transcription is initiated. A promoter includes necessary nucleic acid sequences near the start site of transcription, such as, in the case of a polymerase II type promoter, a TATA element. In one aspect, a promoter includes an enhancer. In another aspect, a promoter includes a repressor element. In one example, a promoter is a T7 promoter.

Transduced and **Transformed:** A vector "transduces" a cell when it transfers nucleic acid into the cell. A cell is "transformed" by a nucleic acid transduced into the cell when the DNA becomes stably replicated by the cell, either by incorporation of the nucleic acid into the cellular genome, or by episomal replication. As used herein, the term transformation encompasses all techniques by which a nucleic acid molecule is introduced into such a cell, including transformation with plasmid vectors, and introduction of naked DNA by electroporation, lipofection, and particle gun acceleration.

Vector: A nucleic acid molecule that can be introduced into a host cell, thereby producing a transformed or transduced host cell. Recombinant DNA vectors are vectors including recombinant DNA. A vector can include nucleic acid sequences that permit it to replicate in a host cell, such as an origin of replication. A vector can also include one or more selectable marker genes, a cloning site for introduction of heterologous nucleic acids, a promoter (for example for expression of an operably linked nucleic acid), and/or other genetic elements known in the art. Vectors include plasmid vectors, including plasmids for expression in Gram negative and Gram positive bacterial cells. Exemplary vectors include those for use in *E. coli.*

II. Modified PHL7 Polypeptides and Fusion Proteins

Provided herein are modified PHL7 polypeptides. In some aspects, the modified PHL7 polypeptides have improved qualities (such as increased PET hydrolase activity) compared to a wild type PHL7 (such as SEQ ID NO: 1) or previously described modified PHL7s (such as PHL7-L93F/Q95Y, for example, SEQ ID NO: 6).

In some aspects, the modified PHL7 polypeptide includes one or more amino acid substitutions (such as 1, 2, 3, 4, 5, 6, 7, 8, 10, or more substitutions). In some examples, the amino acid substitutions include a substitution at one or more of positions corresponding to amino acids 32, 35, 64, 80, 111, 112, 175, 185, and 205 of SEQ ID NO: 1. In some examples, amino acid substitution includes one or more of R32P, A35V, T64S, Q80H, R111H, T112I, T112A, Q175E, H185N, and R205K. In particular examples, the modified PHL7 polypeptide includes amino acid substitutions A35V, T112I, Q175E, and H185N; Q80H, Q175E, H185N, and R205K; T112A, Q175E, and H185N; or R32P, T64S, R111H, Q175E, and H185N.

In additional aspects, the modified polypeptide further includes the amino acid substitution Q95Y. In some examples, the modified PHL7 polypeptide includes A35V, Q95Y, T112I, Q175E, and H185N; or includes Q80H, Q95Y, Q175E, H185N, and R205K.

In some examples, the modified PHL7 polypeptide includes amino acid substitutions A35V, Q95Y, T112I, Q175E, and H185N and has an amino acid sequence with at least 85% sequence identity (such as at least 85%, 86%, 87%, 88%, 89%, 90%, 91%, 92%, 93%, 94%, 95%, 96%, 97%, 98%, 99%, or 100% identity) to SEQ ID NO: 2. In other examples, the modified PHL7 polypeptide includes or consists of the amino acid sequence of SEQ ID NO: 2.

In some examples, the modified PHL7 polypeptide includes amino acid substitutions Q80H, Q95Y, Q175E, H185N, and R205K and has an amino acid sequence with at least 85% sequence identity (such as at least 85%, 86%, 87%, 88%, 89%, 90%, 91%, 92%, 93%, 94%, 95%, 96%, 97%, 98%, 99%, or 100% identity) to SEQ ID NO: 3. In other examples, the modified PHL7 polypeptide includes or consists of the amino acid sequence of SEQ ID NO: 3.

In some examples, the modified PHL7 polypeptide includes amino acid substitutions T112A, Q175E, and H185N and has an amino acid sequence with at least 85% sequence identity (such as at least 85%, 86%, 87%, 88%, 89%, 90%, 91%, 92%, 93%, 94%, 95%, 96%, 97%, 98%, 99%, or 100% identity) to SEQ ID NO: 4. In other examples, the modified PHL7 polypeptide includes or consists of the amino acid sequence of SEQ ID NO: 4.

In some examples, the modified PHL7 polypeptide includes amino acid substitutions R32P, T64S, R111H, Q175E, and H185N and has an amino acid sequence with at least 85% sequence identity (such as at least 85%, 86%, 87%, 88%, 89%, 90%, 91%, 92%, 93%, 94%, 95%, 96%, 97%, 98%, 99%, or 100% identity) to SEQ ID NO: 5. In other examples, the modified PHL7 polypeptide includes or consists of the amino acid sequence of SEQ ID NO: 5.

In some aspects, a modified PHL7 polypeptide has increased polyethylene terephthalate hydrolase activity compared to a control, such as a wild type PHL7 polypeptide (such as SEQ ID NO: 1) or PHL7-L93F/Q95Y (such as SEQ ID NO: 6). In some examples, the increased

polyethylene terephthalate hydrolase activity includes increased activity against PET or a model substrate (such as bis(2-hydroxyethyl) terephthalate (BHET) or impranil) compared to a wild type PHL7 polypeptide (such as SEQ ID NO: 1) or PHL7-L93F/Q95Y (such as SEQ ID NO: 6). In other examples, the increased polyethylene terephthalate hydrolase activity includes increased production of ethylene glycol (EG), terephthalic acid (TPA), mono(2-hydroxyethyl) terephthalic acid (MHET), and/or BHET from PET compared to a wild type PHL7 polypeptide (such as SEQ ID NO: 1) or PHL7-L93F/Q95Y (such as SEQ ID NO: 6). In some examples, a modified PHL7 polypeptide has an increase of in PET hydrolase activity of at least 10%, at least 20%, at least 30%, at least 40%, at least 50%, at least 60%, at least 70%, at least 80%, at least 90%, at least 2-fold, at least 2.5-fold, at least 3-fold, at least 4-fold, at least 5-fold, or more compared to a control (such as a wild type PHL7 polypeptide (such as SEQ ID NO: 1) or PHL7-L93F/Q95Y (such as SEQ ID NO: 6). In other examples, the modified PHL7 polypeptide has increased thermostability compared to a control, such as a wild type PHL7 polypeptide (such as SEQ ID NO: 1) or PHL7-L93F/Q95Y (such as SEQ ID NO: 6). In further examples, the modified PHL7 polypeptide has increased expression compare compared to a control, such as a wild type PHL7 polypeptide (such as SEQ ID NO: 1) or PHL7-L93F/Q95Y (such as SEQ ID NO: 6). n some examples, a modified PHL7 polypeptide has an increase expression of at least 10%, at least 20%, at least 30%, at least 40%, at least 50%, at least 60%, at least 70%, at least 80%, at least 90%, at least 2-fold, at least 2.5-fold, at least 3-fold, at least 4-fold, at least 5-fold, at least 10-fold or more compared to a control (such as a wild type PHL7 polypeptide (such as SEQ ID NO: 1) or PHL7-L93F/Q95Y (such as SEQ ID NO: 6). Exemplary methods for determining PET hydrolase activity, thermostability, and/or expression are provided in Example 1. Additional methods can be identified by one of ordinary skill in the art.

Also provided are fusion proteins including a PHL7 polypeptide fused to a reporter protein. In some aspects the PHL7 polypeptide is a wild type PHL7 polypeptide. In other aspects the PHL7 polypeptide is a modified PHL7 polypeptide disclosed herein. In some aspects, the PHL7 polypeptide has at least 85% sequence identity (such as at least 85%, 86%, 87%, 88%, 89%, 90%, 91%, 92%, 93%, 94%, 95%, 96%, 97%, 98%, 99%, or 100% identity) to the amino acid sequence of any one of SEQ ID NO: 1, SEQ ID NO: 2, SEQ ID NO: 3, SEQ ID NO: 4, SEQ ID NO: 5, or SEQ ID NO: 6. In other examples, the PHL7 polypeptide includes or consists of any one of SEQ ID NO: 1, SEQ ID NO: 2, SEQ ID NO: 3, SEQ ID NO: 4, SEQ ID NO: 5, or SEQ ID NO: 6.

In some aspects, the reporter protein is a fluorescent protein or a portion thereof. In some examples, the reporter is a fluorescent protein or a portion thereof. Exemplary fluorescent proteins include green fluorescent protein (GFP), a superfolder GFP (sfGFP), eGFP, red fluorescent protein (RFP), superfolder RFP (sfRFP), mCherry, or sfCherry, mStrawberry, mOrange, or dTomato). In

other examples, the reporter protein is a split or fragmented protein that can be used in a protein fragment complementation assay (PCA). In further examples, the reporter protein is an enzyme, for example, β-lactamase, horseradish peroxidase, β-galactosidase, luciferase, or dihydrofolate reductase. In one example, the reporter protein is a green fluorescent protein (GFP) or a portion thereof. In a particular example, the GFP protein or portion thereof is a GFP11 tag. Exemplary, non-limiting split GFP systems are described in U.S. Pat. No. 9,081,014 and U.S. Pat. Publ. No. 2015/0099271. In some examples, the reporter protein is linked to the C-terminus of PHL7. In other examples, the reporter protein is linked to the N-terminus of PHL7.

III. Nucleic Acids and Vectors

Also provided herein are nucleic acids and vectors encoding a disclosed modified PHL7 polypeptide. In some aspects, the nucleic acid encodes a modified PHL7 polypeptide including one or more amino acids substitutions (such as 1, 2, 3, 4, 5, 6, 7, 8, 10, or more substitutions). In some examples, the nucleic acid encodes a modified PHL7 polypeptide with amino acid substitution(s) at one or more of positions corresponding to amino acids 32, 35, 64, 80, 111, 112, 175, 185, and 205 of SEQ ID NO: 1. In some examples, nucleic acid encodes a PHL7 polypeptide with amino acid substitutions including one or more of R32P, A35V, T64S, Q80H, R111H, T112I, T112A, Q175E, H185N, and R205K. In particular examples, the nucleic acid encodes a modified PHL7 polypeptide including amino acid substitutions A35V, T112I, Q175E, and H185N; Q80H, Q175E, H185N, and R205K; T112A, Q175E, and H185N; or R32P, T64S, R111H, Q175E, and H185N.

In additional aspects, the nucleic acid encodes modified PHL7 polypeptide further including the amino acid substitution Q95Y. In some examples, the nucleic acid encodes a modified PHL7 polypeptide including A35V, Q95Y, T112I, Q175E, and H185N; or a modified PHL7 polypeptide including Q80H, Q95Y, Q175E, H185N, and R205K.

In some examples, the nucleic acid encodes a modified PHL7 polypeptide including amino acid substitutions A35V, Q95Y, T112I, Q175E, and H185N and having an amino acid sequence with at least 85% sequence identity (such as at least 85%, 86%, 87%, 88%, 89%, 90%, 91%, 92%, 93%, 94%, 95%, 96%, 97%, 98%, 99%, or 100% identity) to SEQ ID NO: 2. In other examples, the nucleic acid encodes a modified PHL7 polypeptide including or consisting of the amino acid sequence of SEQ ID NO: 2. In particular examples, the nucleic acid encodes a modified PHL7 polypeptide with amino acid substitutions A35V, Q95Y, T112I, Q175E, and H185N and the nucleic acid sequence has at least 80% sequence identity (such as at least 80%, 81%, 82%, 83%, 84%, 85%, 86%, 87%, 88%, 89%, 90%, 91%, 92%, 93%, 94%, 95%, 96%, 97%, 98%, 99%, or

100% identity) to SEQ ID NO: 8. In additional examples, the nucleic acid includes or consists of the nucleic acid sequence of SEQ ID NO: 8.

In some examples, the nucleic acid encodes a modified PHL7 polypeptide including amino acid substitutions Q80H, Q95Y, Q175E, H185N, and R205K and having an amino acid sequence with at least 85% sequence identity (such as at least 85%, 86%, 87%, 88%, 89%, 90%, 91%, 92%, 93%, 94%, 95%, 96%, 97%, 98%, 99%, or 100% identity) to SEQ ID NO: 3. In other examples, the nucleic acid encodes a modified PHL7 polypeptide including or consisting of the amino acid sequence of SEQ ID NO: 3. In particular examples, the nucleic acid encodes a modified PHL7 polypeptide with amino acid substitutions Q80H, Q95Y, Q175E, H185N, and R205K and the nucleic acid sequence has at least 80% sequence identity (such as at least 80%, 81%, 82%, 83%, 84%, 85%, 86%, 87%, 88%, 89%, 90%, 91%, 92%, 93%, 94%, 95%, 96%, 97%, 98%, 99%, or 100% identity) to SEQ ID NO: 9. In additional examples, the nucleic acid includes or consists of the nucleic acid sequence of SEQ ID NO: 9.

In some examples, the nucleic acid encodes a modified PHL7 polypeptide including amino acid substitutions T112A, Q175E, and H185N and having an amino acid sequence with at least 85% sequence identity (such as at least 85%, 86%, 87%, 88%, 89%, 90%, 91%, 92%, 93%, 94%, 95%, 96%, 97%, 98%, 99%, or 100% identity) to SEQ ID NO: 4. In other examples, the nucleic acid encodes a modified PHL7 polypeptide including or consisting of the amino acid sequence of SEQ ID NO: 4. In particular examples, the nucleic acid encodes a modified PHL7 polypeptide with amino acid substitutions T112A, Q175E, and H185N and the nucleic acid sequence has at least 80% sequence identity (such as at least 80%, 81%, 82%, 83%, 84%, 85%, 86%, 87%, 88%, 89%, 90%, 91%, 92%, 93%, 94%, 95%, 96%, 97%, 98%, 99%, or 100% identity) to SEQ ID NO: 10. In additional examples, the nucleic acid includes or consists of the nucleic acid sequence of SEQ ID NO: 10.

In some examples, the nucleic acid encodes a modified PHL7 polypeptide including amino acid substitutions R32P, T64S, R111H, Q175E, and H185N and having an amino acid sequence with at least 85% sequence identity (such as at least 85%, 86%, 87%, 88%, 89%, 90%, 91%, 92%, 93%, 94%, 95%, 96%, 97%, 98%, 99%, or 100% identity) to SEQ ID NO: 5. In other examples, the nucleic acid encodes a modified PHL7 polypeptide including or consisting of the amino acid sequence of SEQ ID NO: 5. In particular examples, the nucleic acid encodes a modified PHL7 polypeptide with amino acid substitutions R32P, T64S, R111H, Q175E, and H185N and the nucleic acid sequence has at least 80% sequence identity (such as at least 80%, 81%, 82%, 83%, 84%, 85%, 86%, 87%, 88%, 89%, 90%, 91%, 92%, 93%, 94%, 95%, 96%, 97%, 98%, 99%, or

100% identity) to SEQ ID NO: 11. In additional examples, the nucleic acid includes or consists of the nucleic acid sequence of SEQ ID NO: 11.

In some aspects, a nucleic acid encoding a modified PHL7 polypeptide provided herein is incorporated into a vector, into an autonomously replicating plasmid or virus, or into the genomic DNA of a host cell, or which exists as a separate molecule independent of other sequences. In some non-limiting examples, the vector also includes one or more of an origin of replication, a nucleic acid encoding a replication initiator protein (such as RepA or a temperature-sensitive RepA), a nucleic acid encoding an antibiotic resistance gene (such as chloramphenicol resistance or apramycin resistance), a transcription terminator (such as a dual transcription terminator), or other features. In particular examples, the vector encodes a replicase. One of ordinary skill in the art will recognize that these portions of the vector can be altered (for example, modified or replaced) with other appropriate components.

Vectors for cloning, replication, and/or expression of the disclosed nucleic acid molecules include bacterial plasmids, such as bacterial cloning or expression plasmids. Exemplary bacterial plasmids into which the nucleic acids can be cloned include *E. coli* plasmids, such as pBR322, pUC plasmids (such as pUC18 or pUC19), pBluescript, pACYC184, pCD1, pGEM® plasmids (such as pGEM®-3, pGEM®-4, pGEM-T® plasmids; Promega, Madison, WI), TA-cloning vectors, such as pCR® plasmids (for example, pCR® II, pCR® 2.1, or pCR® 4 plasmids; Life Technologies, Grand Island, NY) or pcDNA plasmids (for example pcDNA™3.1 or pcDNA™3.3 plasmids; Life Technologies). In some examples, the vector includes a heterologous promoter which allows protein expression in bacteria. Exemplary vectors include pET vectors (for example, pET21b), pDEST™ vectors (Life Technologies), pRSET vectors (Life Technologies), pBAD vectors, and pQE vectors (Qiagen). The disclosed nucleic acids can also be cloned into *B. subtilis* plasmids, for example, pTA1060 and pHT plasmids (such as pHT01, pHT43, or pHT315 plasmids). In some examples, the vector is a broad host range vector, such as pBTBX vectors (Prior *et al., Biotechnol. Bioeng.* 106:326-332, 2010), pBTL vectors (Lynch *et al., Biotechnol. Bioeng.* 94:151-158, 2006), or BAV1K vectors (Murin *et al., Appl. Env. Microbiol.* 78:280-283, 2012). In some examples, the vector is based on vector pBTL-2 (Addgene plasmid # 22806) or vector pBAV1K- PT5-*gfp* (Addgene plasmid # 26702), or pCRA1 (Kotrba *et al., Biochem. Biophys. Res. Commun.* 289:1307–1313, 2001) or pSFK6 (Nakamura *et al., Plasmid* 56:179–186, 2006), or pBL1 or pUL330 (Santamaria et al, *J. Gen. Microbiol.* 130:2237-2246, 1984), or pEK0 or pEKEx1 (Eikmanns *et al., Gene* 102:93-98, 1991) or their derivatives such as pEKEx2 (JBEI-7909) and pEKEx3.

IV. Host Cells

Also provided are host cells including a nucleic acid encoding one or more of the disclosed modified PHL7 polypeptides or fusion proteins, or vectors including a nucleic acid encoding one or more of the disclosed modified PHL7 polypeptides or fusion proteins. In some aspects, the cells are bacterial cells. Bacterial cells are available from numerous sources, including commercial sources known to those skilled in the art, such as the American Type Culture Collection (ATCC; Manassas, VA). Commercial sources of cells used for recombinant protein expression also provide instructions for usage of such cells. In particular non-limiting examples, the bacterial cells are *Escherichia coli* cells. In other examples the host cells are yeast cells (such as *Pichia pastoris*, for example, *P. pastoris* GS115) or thermophilic bacterial cells (such as *Geobacillus*).

In some examples, the nucleic acid encoding a modified PHL7 polypeptide or fusion protein, or vector including a nucleic acid encoding the modified PHL7 polypeptide or fusion protein is introduced extrachromosomally and replicated within the host cell. In other examples, after introduction of the plasmid, a double homologous recombination event occurs and the one or more genes are inserted into the genome of the host cell.

Transformation of a bacterial cell with recombinant DNA can be carried out by techniques known to those skilled in the art. Where the host is bacterial, competent cells which are capable of DNA uptake can be prepared from cells harvested after exponential growth phase and subsequently treated by the $CaCl_2$ method using procedures well known in the art. Alternatively, $MgCl_2$ or RbCl can be used. Bacteria can also be transformed by methods including heat shock, electroporation, conjugation, or transduction.

V. Methods of Use

Also provided are methods of use of the disclosed modified PHL7 polypeptides. In some aspects, the methods include degrading polyethylene terephthalate (PET), the methods including contacting PET with the modified PHL7 polypeptide of claim 1 under conditions sufficient for degrading the PET. In some examples, the methods are performed in a bioreactor, for example with amorphous or crystalline PET. In some examples, the conditions sufficient for degrading PET include pH 6-9 (such as pH 6, pH 6.5, pH 7, pH 7.5, pH 8, pH 8.5, or pH 9) and/or temperatures of 65-72°C (such as 65°C, 68°C, 70°C, or 72°C). Exemplary conditions sufficient for degrading PET are provided in Example 8. One of ordinary skill in the art can determine additional suitable conditions.

EXAMPLES

The following examples are provided to illustrate particular features of certain aspects of the disclosure, but the scope of the claims should not be limited to those features exemplified.

Example 1

Methods

This example describes the methods utilized in the experiments described in Examples 2-8.

Materials and data analysis: Unless noted, materials were obtained from the following sources. Oligonucleotides were purchased from Integrated DNA Technologies. Genes were synthesized by Twist Biosciences. Sanger sequencing was performed by Genewiz. Enzymes were purchased from New England Biolabs. Amorphous PET films (product ES301445; 8.5% crystallinity) and high crystallinity PET powder (product ES306031; 39.7% crystallinity) were purchased from Goodfellow Cambridge Ltd. A micronized amorphous powder was produced from the PET film by cryo-milling, first in a SM300 cutting mill (Retsch), then in a ZM200 centrifugal mill (Retsch), as described previously (Erickson *et al., Nature Commun.* 13:7850, 2022), but using a ring sieve with a larger pore size (0.5 mm) in the second step. The powder was thoroughly dried at 45°C for over 24 hours before use as a substrate. Chemicals were purchased from Fisher Scientific or Millipore Sigma. Kits were purchased from Qiagen. Data analysis and curation was performed in Microsoft Excel, GraphPad Prism, and Agilent OpenLab CDS. Sequencing and gene design were performed using ApE (M. Wayne Davis) and SnapGene (Dotmatics).

Cloning, mutagenesis, and library creation: A codon-optimized, synthesized gene encoding wild-type PHL7 (Sonnendecker *et al., ChemSusChem*, 15:e202101062, 2021) was cloned into the pET21b(+)-GFP11 screening vector, between the NdeI and BamHI sites. The DNA sequence of this construct is SEQ ID NO: 15. A plasmid encoding LCC-ICCG in the pET21b(+) vector was used from Erickson *et al.* (*Nature Commun.* 13:7850, 2022). A synthesized gene encoding PHL7-L93F/Q95Y (Pfaff *et al., ACS Catalysis* 12:9790-9800, 2022) was cloned into the pET21b(+) vector between the NdeI and XhoI sites. The amino acid and nucleic acid sequences of the wild type PHL7 and variants are provided as SEQ ID NOs: 1-12. Selected engineered mutants were amplified from the pET21b(+)-GFP11 vector with NdeI and XhoI sites and subcloned into pET21b(+), as necessary, for expression and purification using the His_6 system. Plasmids were transformed into *E. coli* BL21 (DE3) Gold cells (B F^- *ompT hsdS*(rB^- mB^-) *dcm*$^+$ Tet^r gal λ(DE3) *endA* Hte). Chemical transformation was used for routine cloning, while library transformations used in-house electrocompetent cells. Cells were cultured either using LB Miller agar or LB Miller liquid media, with relevant antibiotics (carbenicillin, 100 μg/mL).

Site-directed mutagenesis (SDM) was performed by inverse PCRs using 5'-phosphorlyated oligo primers, followed by treatment with DpnI and T4 DNA Ligase at 30°C overnight. Site-saturation mutagenesis (SSM) was performed in the same way, except with the use of degenerate (NNK) oligos at the position of interest. For SDM, single colonies were picked, cultured, subjected to plasmid isolation, and sequence verified. For SSM, 96 colonies were picked for screening into media in a 96-well plate.

Libraries were constructed using a DNA shuffling protocol. Briefly, gene templates were amplified by Q5 DNA Polymerase (NEB), then fragmented with DNAseI (Invitrogen). Fragmented DNA was re-assembled and amplified using Exo(-) Pfu DNA Polymerase (Agilent). Full-length library gene fragments were cloned into pET21b(+)-GFP11 between the NdeI and BamHI sites, after digestion with restriction enzymes and ligation with T4 DNA Ligase. The ligated library was transformed into *E. coli* cells, which was selected for on LB Miller plates with carbenicillin. Colonies on plates were streaked into LB liquid media, were prepared as 1.0 OD_{600} glycerol stocks, and were stored at -80°C until use.

High-throughput co-screening assay: Briefly, transformed bacterial libraries were plated on Durapore PVDF 0.45 µm 47 mm membrane filters (product HVLP14250) on LB agar plates. To yield a well-spread, yet pickable density of cells on the plate, libraries were plated at approximately a 2.5×10^5 dilution from a 1.0 OD_{600} freezer cell stock. Library plates were then grown overnight. The next day, Durapore membranes (with cells) were transferred onto LB agar plates with IPTG (1 mM) and incubated for 2 hours to induce protein expression. Membranes were then transferred to BHET screening plates. To cast BHET screening plates, first, a 0.7% (w/v) agarose in [500 mM potassium phosphate pH 8] buffer solution was made. BHET solution (at a working concentration of 500 mM BHET in 100% DMSO) was then added to the agarose solution (in 50 mL total aliquots) to the appropriate concentration (ranging from 20-120 mM BHET), then mixed well, pouring into a 50 mm petri dish, then cooled. 500 mM buffer was used in screening plates due to solubility limitations of agarose at
1 M buffers.

Library colonies were lysed on screening plates by spraying membranes with BugBuster (Millipore) 4 times from a spray bottle, rotating the plate. This method ensures an even coverage of BugBuster and lysed cells across the plate. Membranes were then removed from plates and stored at 4°C on original LB agar plates. Screening plates were then incubated at relevant heat treatment and screening temperatures. Incubations and reactions were done in VWR Hybridization Ovens (model 5420), for 2 to 24 hours. After reactions were completed, solutions of refolded GFP1-10 in [100 mM Tris-HCl pH 7.4, 150 mM NaCl, 10% (v/v) glycerol] (TNG buffer) were put

on screening plates. GFP1-10 was refolded from inclusion bodies then incubated 4 hours to overnight. Plates were imaged using a ChemiDoc MP Imager, detecting colorimetric blot and Alexa 488 signals. Membranes (with partially-lysed colonies) were then re-aligned on screening plates and colonies were picked into LB in 96-well plates for next steps of screening.

Selected colonies from libraries were grown out in plates overnight, then replica plated (Boekel Scientific) onto Durapore membranes. The screening process was repeated as above, but with 8 µL of BugBuster pipetted onto each colony for cell lysis. Colonies chosen from this fine screening were chosen as putative improved variants.

Medium-throughput screening assays: Putative improved mutants were expressed in small-scale, 2 to 25 mL expressions. Starter cultures of colonies grown overnight in LB were inoculated 1:100 into 2 to 25 mL of 2XYT media with antibiotic in Falcon tubes (Fisher Scientific) or deep-well microwell plates (USA Scientific) and grown to 0.6 to 0.8 OD_{600} at 37°C, 250 rpm. Cultures were then placed on ice or at 4°C for 10 minutes before 1 mM IPTG was added to induce expression, which were then grown for an additional 16-20 hours at 20°C, 150 rpm. Cultures were pelleted at 3500 rpm for 20 minutes, supernatant was removed, and pellets were resuspended in 500 µL of lysis buffer [100 mM potassium phosphate pH 8, 200 mM NaCl] then lysed by sonication with a Fisherbrand Model 50 Sonic Dismembrator (Fisher Scientific). Sonication was 5×20 seconds, on ice, centrifuging at 14,000 rpm for 3 minutes at 4°C between cycles, with a final centrifuge for 30 minutes to clarify cell lysate.

Enzyme concentration in cell lysates was measured *via* plate reader (detecting GFP fluorescence intensity; excitation: 488 nm, emission: 520 nm) after complementation with GFP1-10. Briefly, 20 µL of cell lysate was added to Corning MaxiSorp 96-well plates with 180 µL of refolded GFP1-10 in TNG buffer. Plates were then incubated overnight at room temperature with shaking. Proteins were quantified *via* a standard curve from 2-fold serial dilutions of a purified sulfide reductase-GFP11 construct (from 0.11 to 14.26 µM). Background fluorescence was subtracted from all samples using the cell lysate of an expression construct lacking the GFP11 tag [PHL7 in pET21b(+)]. Fluorescence was measured using a Tecan M Plex Plate Reader. GFP1-10 complementation was performed in triplicate.

Proteins were diluted to 0.5 µM using lysis buffer and added 1:10 (to 0.1 µM, in 500 µL total) in reactions containing [1 M potassium phosphate buffer, pH 8] (PHL7) or [100 mM potassium phosphate buffer, pH 8] (LCC-ICCG) reaction buffer, and 0.92% (w/v) PET coupons as 3 mm hole-punched circles (approximately 2.5 mg each; Fiskars). Reactions were then incubated in deep-well 96-well plates at 70°C, with aliquots drawn at each time point: 2, 4, 6, 8, 24, 48, and 72 hours. Absorbance at 240 nm was measured using a Tecan M Plex Plate Reader to detect

aggregate aromatic products released (Baath *et al., Analytical Biochemistry* 607:113873, 2020), with baseline (t=0) absorbance for each enzyme subtracted from timepoints. BHET equivalent concentrations were determined from a standard curve of absorbance of serially-diluted BHET. Promising enzyme variants were grown out and plasmids were isolated and sequenced. Plasmids from any promising variants were used as parents for additional rounds of evolution.

Protein expression and purification: Proteins were expressed using the pET21b(+) expression vector, using His_6 tag purification with Co TALON Resin (Takara Bio). Colonies were streaked out on LB selection plates, picked, and grown out overnight in LB media at 37°C, 250 rpm. Cultures were then inoculated 1:100 into 500 mL 2XYT media with carbenicillin, grown to 0.6 to 0.8 OD_{600} at 37°C, 250 rpm, and induced with 1 mM IPTG after being cooled for 10 minutes on ice or at 4°C. Cultures were then grown for an additional 16-20 hours at 20°C, 150 rpm. Cells were harvested for 20 minutes at 3,500 rpm and stored at -80°C until purification.

For purification, pellets were thawed and resuspended in 30 mL column buffer [100 mM potassium phosphate pH 8, 200 mM NaCl, 10% (v/v) glycerol], then sonicated using a Branson Digital Sonifier 450 at 80% amplitude for 10 minutes on ice at 20°C. Lysate was clarified by centrifuging 1 hour at 4 °C and 40,000 × g, then filtered with a 0.45 μm syringe filter before loading onto 2.5 mL packed, equilibrated resin. The lysate was incubated with the resin, rocking at 4°C overnight. Purification was performed manually. Flow-through was discarded and the resin was washed with 15 column volumes (CV) of column buffer [100 mM potassium phosphate pH 8, 200 mM NaCl, 10% (v/v) glycerol], 10 CVs of column buffer with 5 mM imidazole, and finally eluted with 5 CVs with column buffer with 250 mM imidazole. Proteins were verified for correct size and purity by SDS PAGE gel by running alongside Protein Kaleidoscope Protein Standards (Bio-Rad). Purified protein samples were boiled in Laemmli Buffer at 100°C for 20 minutes before loading on a gel. Purity of purified proteins was >90% (evaluated with Image Lab, Bio-Rad). Enzymes were then buffer exchanged using an Amicon 10 kDa cutoff filter (Millipore Sigma) with [100 mM potassium phosphate pH 8, 200 mM NaCl], using the manufacturer's protocol. Protein concentration was quantified by Pierce BCA Protein Assay (Fisher Scientific) using the manufacturer's protocol. Aliquots of the enzymes were stored at -80°C.

Protein thermostability assay: Enzymes in cell lysates were normalized to the same concentration, 0.5 μM, and incubated for 1 hour in a thermal cycler (MJ Research; model PTC-200) at a range of temperatures, from 60°C to 85°C, in reaction buffer [1 M potassium phosphate, pH 8] in PCR tubes. Following heat treatment, samples were removed, transferred to 1.5 mL microtubes, and centrifuged at 14,000 × g for 3 minutes to separate aggregated protein and cell debris. Supernatant was removed and GFP complementation was used to quantify the amount of soluble

enzyme remaining by diluting 1:10 in a solution of GFP1-10 in TNG buffer and incubated for 4 hours to overnight, shaking, at room temperature, in the wells of Corning MaxiSorp 96-well plates. Background fluorescence was subtracted from all samples. Fluorescence was measured using a Tecan M Plex Plate Reader (ex: 488 nm, em: 520 nm). All samples were performed in triplicate. Remaining protein was compared to initial concentrations to determine fraction of protein retained.

Small-scale PET hydrolysis reactions: Reactions were performed with 0.69 or 0.345 μM enzyme and 2.9% (w/v) loading PET (0.35 or 0.7 mg enzyme/g PET for PHL7-WT) in 500 μL evaporation-proof cryo-vials (Simport Scientific; product T309-2A). Reactions were composed of PET, enzymes (diluted with lysis buffer), and appropriate potassium phosphate buffer (of varied pH and concentration). PET was either in the form of milled powder (added prior to reaction buffer and aliquoted into reactions after re-suspension) or as film in the form of 3 mm hole-punched circular coupons (Fiskars). Time points were taken at 2, 4, 6, 8, 24, 48, and 72 hours, incubating at the reaction temperature. Samples were taken for absorbance measurement and HPLC analysis. For HPLC, samples were immediately diluted 50% (v/v) with methanol and then filtered using a 0.2 μm plate filter using MultiScreen HTS Filter Plates (Millipore Sigma; product MSGVN2250). Absorbance measurement was performed as above. Samples were stored at -20°C until analysis. As necessary, samples for absorbance and HPLC analysis were diluted with ultrapure water. All reactions were performed in triplicate.

Monomer quantification: Concentrations of monomers TPA, MHET, and BHET were quantified by HPLC using an Agilent Technologies Infinity II 1260, equipped with a G7115A diode array detector (DAD), detecting signal at 240 nm. 10 μL of sample maintained at 10°C were injected onto a Phenomenex Luna C18(2) (100 Å, 150 mm × 4.6 mm, 5 μm) 40°C. The mobile phase consisted of (A) 20 mM phosphoric acid in ultrapure water and (B) 100% methanol. The flow rate was a constant 1.2 mL/min for a total time of 10 min per sample. An A:B gradient program was used, as follows: 80:20 at t = 0 min; a gradient to 35:65 by t = 7.5 min; and held constant at 80:20 from t = 7.51 min to 10 min. A calibration curve, from 0.1 to 500 mg/L, was used for each analyte to determine concentrations.

PET hydrolysis in pH-controlled bioreactors: Enzymatic PET hydrolysis reactions at 200 mL scale were carried out in duplicate using Applikon MiniBio bioreactor systems with 250 mL glass vessels (Getinge AB, Sweden) equipped with one marine impeller. Amorphous PET film of 0.25 mm thickness (Goodfellow) was cut into approximately 10 x 10 mm squares, washed with 70% EtOH, and incubated at 40°C until completely dry. These PET film squares were added to the reactor at a given solids loading [2.9%, 5.8%, or 20% (w/v)] in 1 M sodium phosphate buffer, pH 8. The suspension was pre-equilibrated to 65°C with stirring at 400 rpm. The reaction was

initiated by the addition of enzyme to 1 mg/g PET. Depolymerization reactions proceeded for 48 hours with continuous pH control through the intermittent addition of 6 or 9.5 M NaOH using a peristaltic pump control module (Applikon my-Control). At the end of the reaction, any remaining substrate was recovered by filtration through a Whatman glass microfiber filter (Cytiva) using a Büchner funnel. The retained solid residue was washed with ultrapure water to remove any precipitated salts, and dried at 40°C overnight prior to obtaining the residual dry weight, from which the percentage mass loss was calculated.

Example 2

Rational design to confer enhanced activity and stability in the PHL7 scaffold

Enzymatic PET depolymerization has been reported to be most efficient at temperatures approaching PET's glass transition temperature (T_g), about 70°C. At such temperatures, the otherwise ordered polymer chains are increasingly susceptible to cleavage by the enzymes. It follows that efficient PET hydrolases are those that are able to function at elevated temperatures. PHL7 has reported homologues that function at mesophilic temperatures (such as *Is*PETase), but those that can function at thermophilic temperatures, including PHL7 and LCC, have the highest rates of PET depolymerization. Hence, a major goal of PET hydrolase engineering efforts has been to increase their thermostability, allowing the enzymes to survive at these elevated temperatures for long reaction times to maximize turnover.

Both disulfide bonds and salt bridges were examined in the PHL7 scaffold, focusing on the analogous sites to LCC D238C/S283 (disulfide bond) and *Is*PETase E204/N233K (salt bridge), positing that one would confer increased thermostability, ideally not at the sacrifice of enzyme activity. Testing the disulfide bond variant, PHL7 R205C/S251C, however, no significant increase in activity was observed, but an increase in thermostability was observed, which was also reported by Pfaff *et al.* (*ACS Catalysis* 12:9790-9800, 2022) (FIGS. 9A-9B). Two salt bridge variants, PHL7 Q175E/R205 and PHL7 Q175E/R205K, were constructed with the hypothesis that different sidechains of positively charged residues at position 205 may better facilitate intramolecular electrostatics, and mutating glutamine to glutamate would be amenable to constructing a salt bridge without disrupting enzyme structure. Both Q175E/R205 and Q175E/R205K conferred increased thermostability to PHL7, though the double-mutation construct increased the thermostability more than Q175E alone (FIG. 9B).

Site-saturated mutation of the active site of PHL7 was carried out at five positions at which the sequence of PHL7 and LCC differed: F63, L93, Q95, I179, and L210. These positions span regions of the protein that are responsible for both TPA binding (subsite I), and regions that are

hypothesized to facilitate initial binding of substrate and guidance of the scissile bond towards the active site (subsite II) (Richter *et al., Nature Commun.* 14:1905, 2023). Several of these mutants had increased activity and/or thermostability. However, after shuffling of these mutations after several rounds, only one mutation, Q95Y, which increased both activity and thermostability (FIGS. 9A-9B), was present in the final engineered enzymes, likely as the other active site mutations were not compatible with other random mutations appearing in the library. This incompatibility of mutations has been reported previously, particularly for these types of enzymes (Tournier *et al., Nature* 580:216-219, 2020; Pfaff *et al., ACS Catalysis* 12:9790-9800, 2022). Hence, moving forward with directed evolution of PHL7 several rational design mutations were included in the libraries: Q95Y, Q175E, and R205K.

Example 3

Directed evolution of PHL7

A major bottleneck in PET hydrolase engineering has been caused by the lack of a screen to efficiently evaluate the diversity of large libraries, which are often necessary to discover rare, beneficial mutations in directed evolution, of these types of enzymes. A new platform for engineering PET hydrolases, which is capable of simultaneously screening large, random mutagenesis enzyme libraries for improved (i) protein expression and (ii) activity has been developed. The method is summarized briefly in FIG. 1C. To evaluate expression, enzymes in the libraries are expressed with C-terminal GFP11 tags (exemplary PHL7-WT cassette: SEQ ID NO: 15), which allows their quantification in crude cell lysates, in solutions or on plates, via a fluorescent readout when complemented with GFP1-10 (Cabantous *et al., Nature Biotechnology* 23:102-107, 2005). Activity is evaluated step-wise, on model, then on PET substrates (FIG. 1C). A colorimetric, agar plate screen using bis(2-hydroxyethyl) terephthalate (BHET) as a model substrate screens bacterial colony libraries (with $>10^5$ constituents) simultaneously, monitoring cell lysates causing the appearance of clearing (transparent) zones. Coupling the fluorescence and colorimetric assays, it is possible to quickly and precisely select improved enzymes based on both activity and protein expression. Selected enzymes can then expressed in small scale (2-25 mL) and screened in medium-throughput assays on PET substrates, in solution, with aggregate product concentration measured in microwell plates ($\sim10^2$), with plate-based absorbance protocols. Any superior enzyme compared to the parent enzymes from the previous round were sequenced and selected as parents for the next round of evolution.

Leveraging this high-throughput engineering platform (screening $\geq10^5$ constituents, per round), a directed evolution campaign was performed on PHL7 (FIG. 1C). It was hypothesized that

rare, beneficial mutations that were previously on the periphery of, or intractable to, PET hydrolase engineering due to the limitations in rational and computational designs could be discovered. Each round, mutations were made and combined using DNA shuffling, initially using as a scaffold, PHL7-WT, as well as PHL7 Q95Y, PHL7 Q175E, and PHL7 Q175E/R205K. Selection criteria used for evolution were i) high specific activity on PET substrates and ii) thermostability. In each round of evolution, concentration of BHET on the screening plates was increased and plates were incubated for increasing amounts of time, as higher BHET concentrations required longer times for clearing zones to develop. Then, through medium throughput screens, enzyme variants with enhanced activities were selected by comparison of product release by the library members to the starting sequences for directed evolution. UV absorbance to measure aggregate product concentration trended closely with HPLC results (FIGS. 10A-10B). To evaluate thermostability, screens on plates and in solutions were heat treated at 75°C (T_m of PHL7 is 79.1 °C) for 1-2 hours (rounds 1-2: 1 hour; rounds 3-4: 2 hours) prior to incubation at the reaction temperature, 70°C. The GFP complementation assay additionally allowed for measurement of protein survivability through facile quantification of protein concentration before and after heat treatment (FIGS. 9A-9B).

After four rounds of directed evolution, four mutants, named PHL7-Jemez, PHL7-Santa Fe, PHL7-Taos, and PHL7-Tusas, were selected to proceed with detailed characterization. They were expressed, purified (FIG. 11), and characterized alongside benchmarks from literature, PHL7-WT, LCC-ICCG (Tournier *et al., Nature* 580:216-219, 2020), and PHL7 L93F/Q95Y (Pfaff *et al., ACS Catalysis* 12:9790-9800, 2022). Table 1 shows the amino acid mutations of the enzyme variants, compared to the PHL7-WT scaffold. FIG. 12 shows the evolutionary trajectory of the evolved mutants.

Table 1: Amino acid mutations of evolved enzyme variants.

Variant Name	Wild-type Position/Mutation										
	R32	A35	T64	Q80	L93	Q95	R111	T112	Q175	H185	R205
PHL7-Jemez		V				Y		I	E	N	
PHL7-Santa Fe				H		Y			E	N	K
PHL7-Taos								A	E	N	
PHL7-Tusas	P		S				H		E	N	
PHL7-L93F/Q95Y					F	Y					

Example 4

Benchmarking engineered enzymes against PET hydrolases

Evolved enzyme variants were tested for activity on commercially-available (Goodfellow), amorphous (8.5% crystallinity) PET film coupons at conditions at which PHL7 was initially reported to have the highest activity: 70°C, pH 8 in 1 M potassium phosphate buffer. To evaluate PET deconstruction, enzymes were introduced to reactions with PET substrate and monomer release (TPA, MHET, and BHET) was monitored over time using HPLC (FIG. 2A). In the HPLC analysis, TPA and MHET concentrations for reactions were abundant and readily measured, while BHET concentrations were generally low and are not explicitly discussed, but were factored into calculations of the sum of aromatic products: the sum total concentration of TPA, MHET, and BHET. While PHL7-WT and its mutants were screened in 1 M potassium phosphate buffer, 0.1 M buffer was used for LCC-ICCG reactions.

The engineered enzymes achieved higher initial rates of PET depolymerization compared to PHL7-WT, LCC-ICCG (FIGS. 2B-2D), and the PHL7 double-mutant, PHL7-L93F/Q95Y (FIG. 13A), as well as higher (3-fold, on average) expression levels than PHL7-WT and comparable levels to LCC-ICCG (Table 2). The best performing mutant for these conditions, PHL7-Jemez, achieved 2.4-fold higher conversion than LCC-ICCG by 8 hours (on a basis of sum of total aromatic products), and 4.6- and 7.2-fold higher conversions compared to PHL7-WT and PHL7 L93F/Q95Y, respectively (FIG. 2B, FIG. 13A). Interestingly, much of the increase in total product release appeared to be the result of disproportionate increase in MHET release (FIG. 2D) by the PHL7 mutants. When compared to the product release by LCC-ICCG, all four mutants showed 1.8- to 3-fold increases in MHET release, while TPA release was 2.2-fold or less, the highest observed for PHL7-Jemez (FIG. 2C).

Table 2. Expression yield of purified enzymes, per liter of expression culture, quantified by BCA assay and corrected for purity by SDS PAGE analysis.

Variant Name	**Enzyme Expression Yield [*per L culture*] (mg)**
PHL7-WT	9.50
PHL7-L93F/Q95Y	22.47
LCC-ICCG	31.64
PHL7-Jemez	31.14
PHL7-Santa Fe	31.56

Variant Name	Enzyme Expression Yield [*per L culture*] (mg)
PHL7-Taos	31.08
PHL7-Tusas	23.46

Initial reactions were run with 0.69 μM enzyme loading and 0.7 mg enzyme/g PET, for PHL7-WT, though for the reactions on PET coupons, it was observed that the substrates were fully depolymerized by 24 hours in reactions with several of the PHL7 variants. To evaluate the enzymes over time, the enzyme loading was decreased to 0.345 μM (0.35 mg enzyme/g PET, for PHL7-WT). At lower enzyme concentration, the engineered PHL7 mutants yet again outperformed the benchmark enzymes (FIG. 3; FIG. 13B). The mutants showed approximately 2-fold higher conversion by 72 hours over LCC-ICCG, and 3.4- and 2.6-fold higher conversion than wild-type PHL7-WT and PHL7-L93F/Q95Y, respectively. In addition, it was observed that the mutants had higher activity on MHET compared to LCC-ICCG (FIG. 3C), with MHET concentration depleting from its maximum concentrations (at ~24 to 48 h) at the 72 hour time point, whereas LCC-ICCG showed relatively constant MHET concentration beyond 24 h. Higher activity on MHET is advantageous, as it mitigates the need for additional MHETase enzymes to fully hydrolyze the MHET intermediate to TPA and EG. The higher MHET release we observed by these enzymes could be explained, in part, by the screening method, wherein the first step is the creation of clearing zones, screening for the conversion of BHET to the more water-soluble MHET, TPA, and EG (or, in PET reactions, rapid conversion of polymers/oligomers to small molecules). High MHET release, coupled with apparent higher intrinsic activity on MHET by PHL7 and its mutants, can be a route to higher TPA conversion over time.

Example 5

Characterization of PHL7 mutants at a range of reaction pH and temperature

The enzymes were next characterized beyond the standard testing conditions to evaluate their performance in several altered reaction conditions. Enzymes were tested with a varying a range of: pH (pH 6, 7, 8, 9), temperature (65°C, 68°C, 70°C, 72 °C), substrate form and crystallinity [amorphous coupon (8.5% crystallinity), amorphous powder (8.5%), and high crystallinity powder (39.7%)], and enzyme loading (0.345 μM and 0.69 μM).

An overall decrease in activity comparing amorphous PET film coupons to amorphous PET powder was observed for the mutants (FIG. 2, FIGS. 14A-14C, FIG. 15A). Interestingly, the activities of PHL7-WT, PHL7-L93F/Q95Y, and LCC-ICCG on the two amorphous substrates were

similar, up to 8 hours' reaction, approximately 4 g/L product for PHL7 and PHL7-L93Q/Q95Y and 8 g/L for LCC-ICCG. The mutants, however, showed significantly diminished increases in activity in reactions with the amorphous powder, with product releases reduced to half from up to 20 g/L to 10 g/L. This reduction in activity could be explained by use of PET coupons in the screening method. It was observed that, while amorphous PET films were completely depolymerized in 24 hours, the PET powder required extended reaction time, to 72 hours, to achieve more complete depolymerization. Notwithstanding, this high activity on PET film could eliminate the need for extensive pre-treatment, which is a significant contributor to process economics, energy demands, and greenhouse gas emissions of recycled PET. Another goal for substrate pre-treatment is to reduce the crystallinity of PET. Most post-consumer PET (used for manufacturing, e.g., bottles and textiles) has crystallinities of 30-40%, although some packaging has crystallinities of about 8%.

On high crystallinity (39.7% crystallinity) PET powder, the engineered PHL7 enzymes' activities were reduced by up to 11-fold, while PHL7-WT's was reduced by about 4-fold, and LCC-ICCG's by 3-fold (comparing up to 8 hours) (FIG. 2B, FIGS. 14D-14F, FIG. 15B). As a result, LCC-ICCG had the highest activity of all the enzymes tested on high crystallinity PET, with on average, about 50% higher activity than the mutants by 8 and 72 hour time points. However, the engineered enzymes showed significantly improved activities over PHL7-WT on high crystallinity PET. For example, PHL7-Jemez had a 1.3-fold increase over PHL7 (FIG. 14D). This is likely a consequence of the screening method, as high crystallinity substrates were not used in screening, and despite the high reaction temperatures approaching the T_g of PET (70°C), these enzymes are thought to preferentially depolymerize the amorphous regions of the polymer.

The mutants could also be of use in enzyme cocktails with LCC-ICCG, as it appears that LCC-ICCG, in reactions with high crystallinity PET, accumulates MHET, whereas the mutants appear readily able to convert residual MHET, with concentrations rapidly decreasing after 24 hours (when it appears the more freely-accessible PET becomes limiting, and overall conversion begins to plateau) (FIGS. 14C, 14F). To date, no MHETase exists that can function at 70°C. Synergistic reactions with LCC-ICCG and PHL7 could serve as viable alternatives to facilitate higher extents of total PET conversion.

Catalytic performance over a range of pH is an additional means to increase the economics of recycled PET. The pH of enzymatic PET deconstruction reactions decreases (acidifies) as TPA is generated upon hydrolysis. Hence, pH control by the addition of base (e.g., NaOH) is necessary to maintain activity of the enzymes, which is a significant contributor to the process costs and poor score in life cycle assessment. Additionally, one method to recover TPA from the reaction is to precipitate it out by the addition of acid (e.g., H_2SO_4) to drop the pH below 2.5. Enzyme function,

then, at a broad range of pH, and namely lower than the standard pH 8, would lead to better process economics and environmental compliance for PET recycling, as these acid and base additions would be limited. The performance of the PHL7 variants at reduced pHs was investigated. Activities at pH 6 and pH 7 were reduced significantly compared to pH 8, up to 30-40% less at pH 7 (FIGS. 2B-2D, FIGS. 4A-4C) and 85% less at pH 6 (FIGS. 2B-2D, FIGS. 4D-4F), in the first 8 hours. Results at an increased pH 9 were similar to those at pH 8. For reactions at pH 9, similar results were observed to the reactions at pH 8 (FIG. 16, FIGS. 13C-13D). The total product release between the two conditions were similar for the engineered enzymes (about 15 g/L), and PHL7-WT (about 4.5 g/L). However, LCC-ICCG had initial higher activity than at pH 8, with about 40% higher activity by 8 hours at pH 9 (FIG. 16A). Though, similar to pH 8 with amorphous coupons, complete conversion of the PET by 24 hours by the mutants was observed (the coupons disappeared entirely), prompting run of the time-course reaction to 72 hours, at a reduced enzyme loading (0.345 μM). Here, the engineered enzymes out-performed LCC-ICCG and PHL7-WT over time, namely, with product continuing to be released to 72 hours, while LCC-ICCG's activity appeared to plateau by 24 hours (FIG. 16D). Taken together, it appears that LCC-ICCG's higher apparent activity may be due to the pH in the reaction maintaining for a longer time around its optimum, pH 8, in a reaction starting at pH 9, whereas the PHL7 mutants are stable at a wider range of pH. Interestingly, LCC-ICCG has a predicted isoelectric point (pI) of 8.9, whereas PHL7 has a predicted pI of 5.3.

At pH 7, the engineered enzymes again out-performed all benchmarks, with for instance, PHL7-Santa Fe showing 1.7- and 1.4-fold higher activities in 72 hours than PHL7 and PHL7 L93Q/Q95Y, respectively, and 3-fold higher activities than LCC-ICCG, comparing sums of aromatic products (FIG. 4A, FIG. 13E). Additionally, the activity of LCC-ICCG did not increase significantly beyond 24 hours, whereas the mutants, and PHL7-WT, continued to cause product release for the entire duration of the reaction. At pH 6, dramatic decreases in activity were observed for most of the enzymes, as well as the benchmarks (FIGS. 4D-4F, FIG. 13F). However, at pH 6, PHL7-Tusas showed significantly higher depolymerization, maintaining 27% of its productivity at pH 8 in the first 8 hours, and reaching 100% of equivalent of productivity at pH 8 in 72 h (FIG. 2B, FIG. 4D). Therefore, PHL7-Tusas could serve as a starting point for evolution of PET hydrolases that are more acid tolerant, promoting more economical and less environmentally-impactful PET recycling. More broadly, these engineered enzymes are more pH tolerant and retain higher activity than the benchmarks in the neutral and acidic pH range, even without directed evolution toward catalytic activity at varying pH. This is a potential consequence of the screening method, wherein evolved enzymes are screened for high activity in acidifying batch reactions.

The activities of the enzymes were investigated at different reaction temperatures. While the engineering and screening was at 70°C, the goal was to compare the activities at 65°C, 68°C, and 72°C, a temperature range at which similar thermotolerant enzymes have demonstrated activities, and which is still near the T_g of PET (65°C-80°C), but without reaching a temperature which would rapidly recrystallize the PET.

Compared to activity at 70°C, at 65°C and 68°C, generally, PHL7-WT and the PHL7 mutants' activities were reduced from upwards of 20 g/L by 8 hours (with 0.69 μM enzyme) and 40 g/L by 72 hours (with 0.345 μM) to upwards of 15 g/L after 8 hours (0.69 μM) and upwards of 20 g/L after 72 hours (0.345 μM) (FIG. 2, FIGS. 17-18). The mutants' activities at 65°C and 68°C were similar, with a trend of increasing activity up to 70°C. Meanwhile, the activity of LCC-ICCG remained relatively constant, about 10 g/L after 8 hours and 20 g/L after 72 hours FIGS. 17-18). Consequently, below 70°C, LCC-ICCG outcompeted the exemplar PHL7 variant, PHL7-Jemez, but with the mutants, as a whole, performing better than LCC-ICCG as the temperature increased. In comparison to the benchmark PHL7-L93/Q95Y, PHL7-Jemez showed 2- to 3-fold higher conversion at all tested temperatures and enzyme concentrations (FIG. 19). Despite having decreased initial rates at lower temperatures, several of the enzyme variants achieved the level of conversion of LCC-ICCG by 72 hours, with the product formed from these mutants continuing to increase up to 72 hours (FIG. 19D). This was not observed at 70°C, suggesting that, although the catalytic rate of the enzymes may decrease at lower temperatures, they may persist longer in the reaction. Conversely, at 72°C, initial rates were higher than at 70°C for all of the engineered enzymes, with all activities on par with PHL7-Jemez, the top performer at 70°C (FIGS. 20A-20C). However, over time, for most of the enzyme variants, the activity plateaued by 24 hours (FIGS. 20D-20F). This may be due to increased reaction kinetics at 72°C, but decreased thermostability for the enzymes, which were evolved at a lower temperature. Therefore, 70°C appeared to be the optimal temperature for these enzymes, although interestingly PHL7-Taos showed higher product release (and apparent thermostability) at 72°C compared to itself and the other variants at lower temperatures (FIG. 20D).

Example 6

Evaluating product inhibition of PHL enzymes

Inhibition by product monomer accumulation is another key consideration in engineering PET hydrolases. Accumulation of TPA, EG, and MHET have been shown to affect the substrate hydrolysis rate of PET hydrolases, so potential product inhibition by the top-performing mutant (PHL7-Jemez) and PHL7-WT were tested by determining changes in monomer release in the

presence of initial additions of TPA (FIGS. 21A-21B), EG (FIGS. 21C-21D), and MHET (FIGS. 21E-21F). At high concentrations of TPA, PHL7-WT was observed to have a decrease in initial rate, which appeared relieved in the engineering of PHL7-Jemez (FIGS. 21A-21B). With 2.5g/L TPA addition, PHL7-WT suffered a 22% decrease in activity in 8 hours compared to a reaction with no TPA added. No significant inhibition was observed by MHET and EG (FIGS. 21C-21F). This may, in part, be supported by PHL7's enhanced ability to break down MHET, as it could be able to tolerate higher MHET concentrations and/or better convert accumulated MHET concentrations to TPA and EG. LCC-ICCG was likewise not shown to experience product inhibition by any of MHET, EG, and TPA, with its primary limitation explained by thermal degradation of the protein. It is hypothesized that the same is true for PHL7 and its mutants.

Example 7

Structural basis of PHL7 mutations

The various mutations in the PHL7 variants were investigated via structural modeling. AlphaFold2 (AF2) structure prediction tool showed high confidence in each of the PHL7 variants. PHL7-Jemez, PHL7-SantaFe, PHL7-Taos, PHL7-Tusas showed pLDDT scores ~98, while PHL7-L93F/Q95Y showed a pLDDT score of 96. Overlay of the predicted structures on the native PHL7 crystal structure (PDB code 7NEI), showed RMSD of < 0.6 Å over the full Cα backbone atoms (FIG. 5A). The regions of maximum variation from the crystal structure included loops consisting of residues 46-54 and 111-124, that were also observed in the AF2 predicted structure of the native PHL7. In order to evaluate if the mutations enriched through directed evolution and dual screening of activity and expression were stabilizing, computational modeling using ROSETTA was performed. It was hypothesized that a design/relax protocol with an option to choose from native and the identified mutations will prefer a stabilizing mutation. The T64S mutation was highly represented in the ROSETTA designed sequences. Mutations such as Q80H and Q175E were also preferred in many designs, confirming these mutations to provide stability advantage to the PHL7 variants.

Furthermore, various mutations were threaded on the PHL7 structure, to identify the role of each mutation. The Q175E is most likely to contribute to charge-charge interaction between negatively charge E175 and positively charged R205. The mutation, R205K showed an improved orientation and a formation of hydrogen bond between E175 and K205 (FIG. 5B), a set of mutations that showed an appreciable improvement in the stability of PHL7 protein (FIG. 9B).

In order to gain insight to what other catalytic features might be enhanced due to the mutations in PHL7-Jemez, a docking of a PET model substrate consisting of three terephthalate and

ethylene glycol subunits (PET3mer) was performed. Various conformers around the dihedral angles of PET3mer were created. Using a central point as the gamma oxygen of catalytic serine (S131), the PET3mer ligand was docked within a radius of 10 Å. Top poses for both native and PHL7-Jemez, showed comparable binding affinities, with W156 and F63 being key residues packing to the aromatic ring of TPA in the proximity of the scissile bond. The three PET3mer subsites (subsites -2, -1, +1), showed similarity in the binding mode at the subsite -2 and -1, but the key difference was observed in subsite +1, where the Q95Y mutation in PHL7-Jemez, resulted in flipping outside the groove formed by L93/Q95 in the native protein. While a similar groove is presented with L93/Y95 in the PHL7-Jemez, the subsite +1 aromatic ring in the substrate preferred pi-stacking only with Y95. In order to further understand the role of Y95 in the substrate recruitment and stabilizing the subsite +1, PET3mer docking in the published mutant PHL7-L93F/Q95Y (Pfaff *et al.*, *ACS Catalysis* 12:9790-9800, 2022) was performed. The top binding pose for PET3mer showed a preference for the mode, which was more consistent with the PHL7-Jemez substrate recruitment than the native PHL7 (FIG. 22). The close proximity of two aromatic amino acids (F93/Y95) in the variant failed to provide a suitable interface for subsite +1 of PET3mer.

Example 8

Deployment of PHL7 mutants in bioreactors

To demonstrate the utility of the engineered enzymes in bioreactors, which better represent industrial recycling processes and provide a standardized approach to compare these enzymes, one of the top performing evolved variants, PHL7-Jemez, alongside PHL7-WT, was deployed in bioreactors. PHL7-WT was chosen as the benchmark, as it and PHL7-Jemez share reaction conditions, and to exhibit the enhancement of the mutant from its parent enzyme in bioreactors. Extent of PET hydrolysis over time and final solids mass loss was determined for reactions with PHL7-Jemez and PHL7-WT with PET coupons (FIGS. 7A-7C). PET solids loading was varied to determine its effects on enzyme performance: 2.9% (w/v) was used to mirror small-scale reactions (FIG. 7A), which was also doubled to 5.8% (w/v) (FIG. 7B), and 20% (w/v) was used to mimic levels similar to what would be used industrially (FIG. 7C).

The comparative performance of PHL7-Jemez in bioreactors was similar to that in small-scale reactions, showing improvement over the wild-type enzyme (FIGS. 7A-7C). PHL7-Jemez had approximately 2.5-fold higher initial rates (hydrolysis up to 12 hours) at low PET loadings (2.9% and 5.8%) than PHL7-WT (FIGS. 7A-7B) and nearly 5-fold higher initial rates at high PET loadings (20%) (FIG. 7C). This higher activity was maintained over time for all conditions, with,

for example, nearly 95% hydrolysis in 36 hours by PHL7-Jemez compared to 60% by PHL7-WT (at 2.9% PET) (FIG. 7A). PHL7-Jemez, at all conditions, also showed the highest polymer mass losses, with nearly 96.5% at 2.9% (w/v), 97.5% at 5.8% (w/v), and 70.5% at 20% (w/v) PET loading (FIGS. 7A-7C). Interestingly, however, at higher PET loadings, a diminished hydrolysis by PHL7-Jemez was observed, starting at 5.8% PET, where only 82% hydrolysis was seen in 48 hours, compared to almost 97% at 2.9% PET, even while maintaining approximately the same polymer mass loss, ~97% (FIGS. 7A-7B). Hydrolysis was severely affected at 20% PET, with only 37% hydrolysis and 70.5% mass loss in 48 hours by PHL7-Jemez (FIG. 7C). Still, this is about 3.5-fold higher extent of hydrolysis and mass loss compared to PHL7, at industrially-relevant conditions.

It was hypothesized that the diminished hydrolysis at higher PET loadings, along with the discrepancies between hydrolysis and mass loss in reactions, could be caused by the high reaction buffer concentration. With 1 M phosphate buffer, the reaction's ionic strength begins high, and as the reaction proceeds, high concentrations of soluble oligomers/monomers (e.g., $(Na^{2+})_2TPA^{2-}$) are released, further increasing ionic strength. High ionic strength likely causes precipitation, which was observed in the reaction vessels, along with large amounts of undigested substrates, and hinders the reaction. Much of the reaction products are likely not fully-hydrolyzed to TPA, and are instead soluble oligomers, accounting for relatively high PET mass loss compared to extent of hydrolysis. This may explain, additionally, why PHL7-Jemez does not appear as improved over PHL7-WT at 5.8% PET. While PHL7-WT has similar performance at 2.9% and 5.8% PET (70-74% hydrolysis and 87-84.5% mass loss), PHL7-Jemez has its extent of hydrolysis decrease from 97% to 82%, with nearly identical mass loss (~97%). At 5.8% PET, the reaction is potentially operating near a threshold where only ~80% hydrolysis is possible by these enzymes, as exceeding 80% causes the ionic strength to be too high and hindering of the reaction. Here, then, the higher activity of PHL7-Jemez causes it to be more affected by this phenomenon: PHL7-Jemez can liberate oligomers to nearly 100% mass loss, but the reaction cannot proceed to complete hydrolysis.

In comparison to other, established, PET hydrolase benchmarks in bioreactors (FIG. 8), at 2.9% PET and similar reaction conditions, LCC-ICCG (in 100 mM phosphate buffer) showed up to 65% hydrolysis in 36 hours and 83.5% mass loss in 48 hours, compared here to PHL7-Jemez with 94% hydrolysis and 96.5% weight loss. Against LCC-LANL, PHL7-Jemez had significantly improved catalytic rates, with 36% higher hydrolysis extent in 24 hours, although with similar overall extents of reaction (90-95% hydrolysis in 48 hours) and overall mass loss (94.5-96.5% loss).

It will be apparent that the precise details of the methods or compositions described may be varied or modified without departing from the spirit of the described aspects of the disclosure. We claim all such modifications and variations that fall within the scope and spirit of the claims below.

5

We claim:

1. A modified polyester hydrolase Leipzig #7 (PHL7) polypeptide comprising at least one amino acid substitution at one or more of positions corresponding to amino acids 32, 35, 64, 80, 111, 112, 175, 185, and 205 of SEQ ID NO: 1.

2. The modified PHL7 polypeptide of claim 1, wherein the at least one amino acid substitution comprises one or more of R32P, A35V, T64S, Q80H, R111H, T112I, T112A, Q175E, H185N, and R205K.

3. The modified PHL7 polypeptide of claim 2, wherein the at least one amino acid substitution comprises:

a) A35V, T112I, Q175E, and H185N;

b) Q80H, Q175E, H185N, and R205K;

c) T112A, Q175E, and H185N; or

d) R32P, T64S, R111H, Q175E, and H185N.

4. The modified PHL7 polypeptide of claim 1, wherein the polypeptide further comprises amino acid substitution Q95Y.

5. The modified PHL7 polypeptide of claim 4, wherein the polypeptide comprises or consists of the amino acid sequence of SEQ ID NO: 2, SEQ ID NO: 3, SEQ ID NO: 4, or SEQ ID NO: 5.

6. The modified PHL7 polypeptide of claim 1, wherein the modified polypeptide has increased polyethylene terephthalate hydrolase activity compared to SEQ ID NO: 1.

7. A nucleic acid molecule encoding the modified PHL7 polypeptide of claim 1.

8. The nucleic acid molecule of claim 7, wherein the nucleic acid encodes a polypeptide comprising one or more of R32P, A35V, T64S, Q80H, R111H, T112I, T112A, Q175E, H185N, and R205K.

9. The nucleic acid molecule of claim 8, wherein the nucleic acid encodes a polypeptide comprising:

a) A35V, Q95Y, T112I, Q175E, and H185N;

b) Q80H, Q95Y, Q175E, H185N, and R205K;

c) T112A, Q175E, and H185N; or

d) R32P, T64S, R111H, Q175E, and H185N.

10. The nucleic acid molecule of claim 8, wherein the nucleic acid comprises or consists of the nucleic acid sequence of SEQ ID NO: 8, SEQ ID NO: 9, SEQ ID NO: 10, or SEQ ID NO: 11.

11. A vector comprising the nucleic acid of claim 7.

12. The vector of claim 11, wherein the vector is a plasmid vector.

13. An isolated host cell comprising the vector of claim 12.

14. The isolated host cell of claim 13, wherein the host cell is a bacterial cell.

15. A fusion protein comprising a polyester hydrolase Leipzig #7 (PHL7) polypeptide fused to a reporter protein.

16. The fusion protein of claim 15, wherein the reporter protein is a green fluorescent protein (GFP) or portion thereof.

17. The fusion protein of claim 16, wherein the GFP or portion thereof comprises a GFP11 tag.

18. The fusion protein of claim 15, wherein the PHL7 polypeptide comprises or consists of the amino acid sequence of SEQ ID NO: 1, SEQ ID NO: 2, SEQ ID NO: 3, SEQ ID NO: 4, or SEQ ID NO: 5.

19. A nucleic acid molecule encoding the fusion protein of claim 15 or a vector comprising a nucleic acid encoding the fusion protein.

20. A method of degrading polyethylene terephthalate (PET), comprising:

contacting PET with the modified PHL7 polypeptide of claim 1 under conditions sufficient for degrading the PET.

FIG. 1A

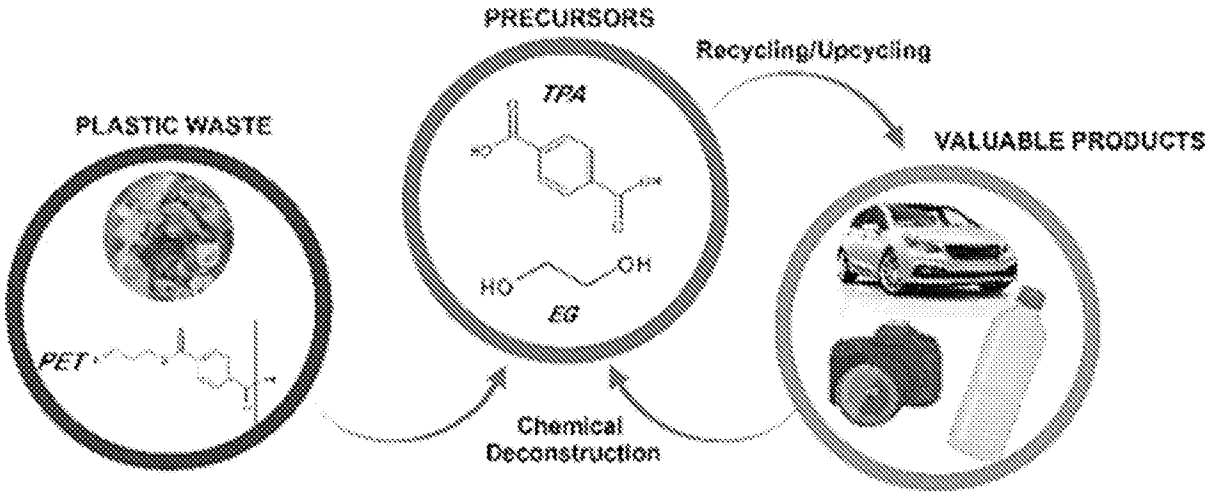
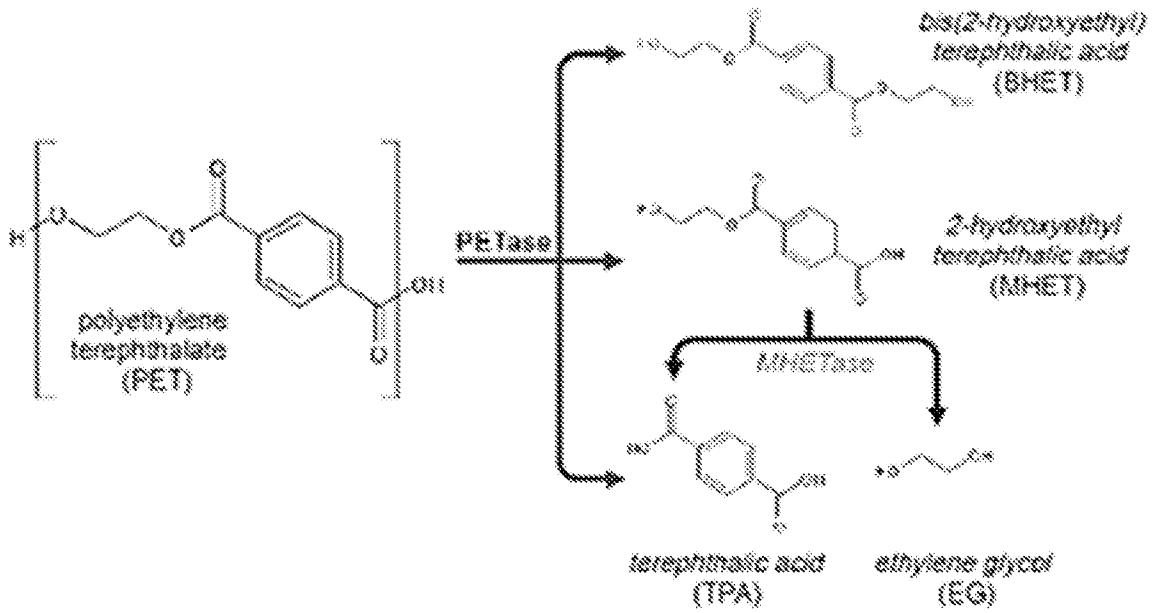
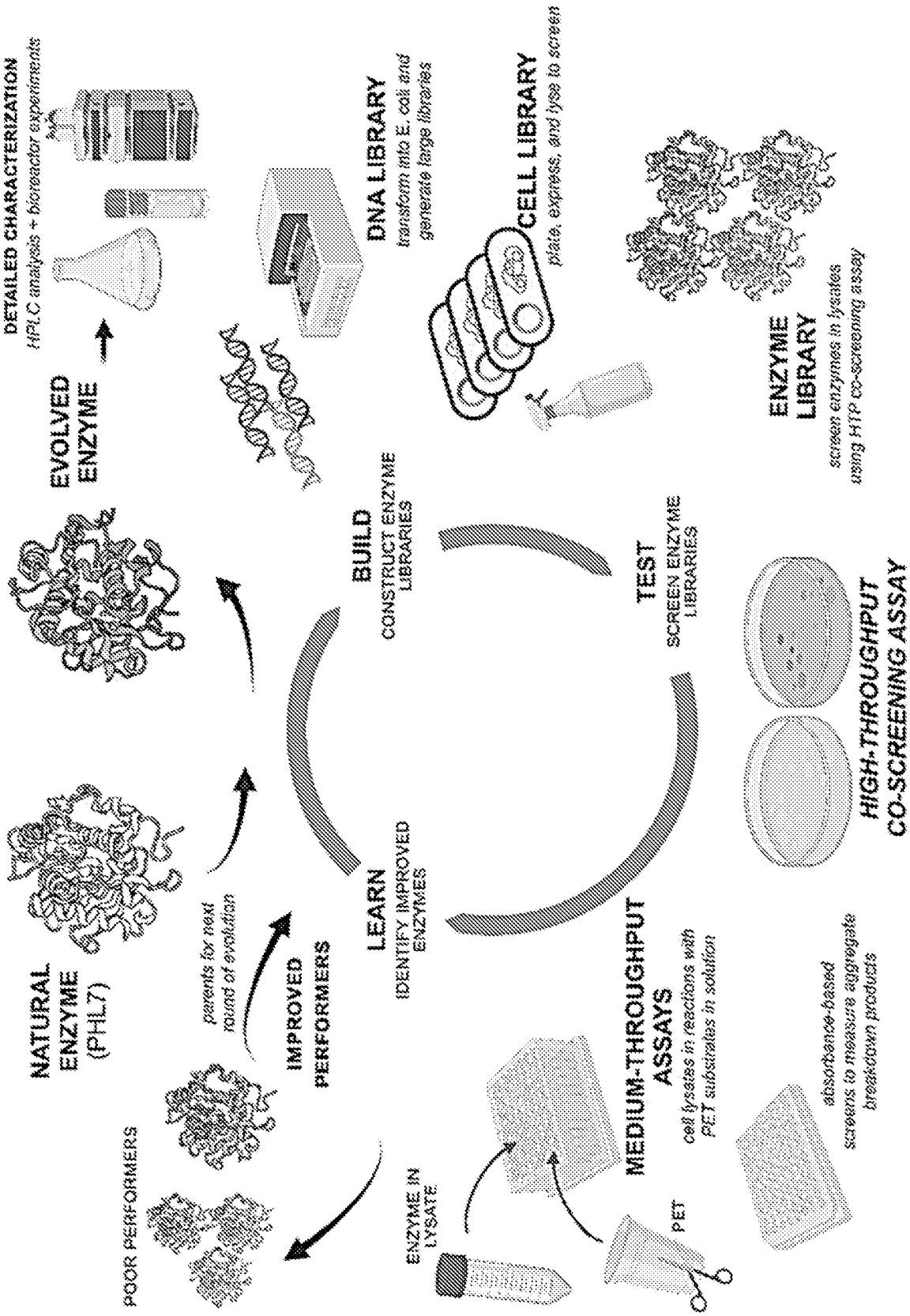


FIG. 1B



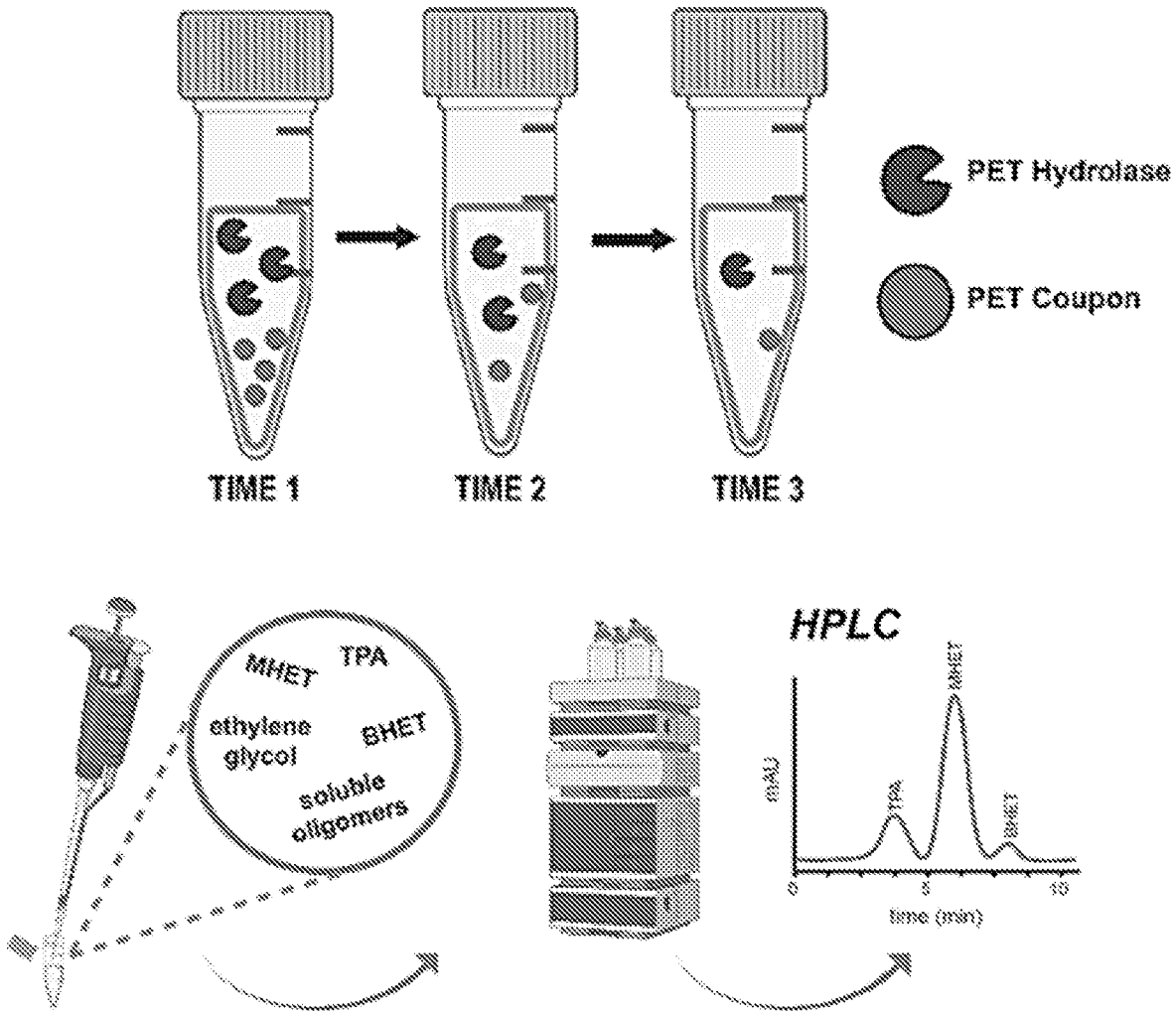
Official Use Only/Export Controlled Information/Department of Commerce EAR99

FIG. 1C



Official Use Only/Export Controlled Information/Department of Commerce EAR09

FIG. 2A



Official Use Only/Export Controlled Information/Department of Commerce EAR99

FIG. 2B

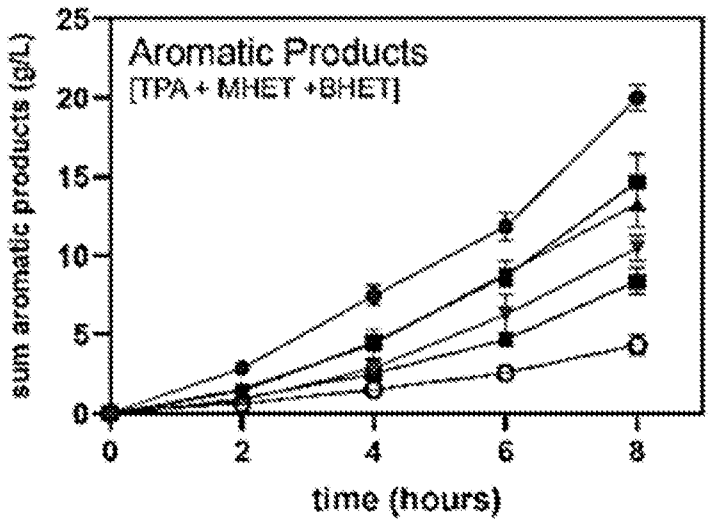


FIG. 2C

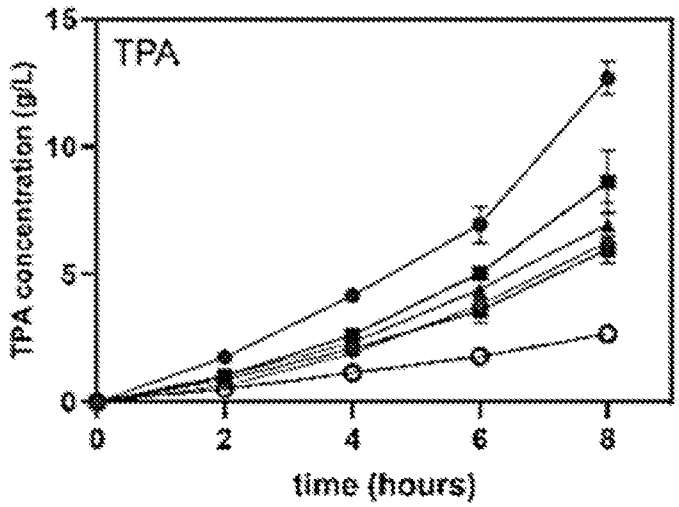
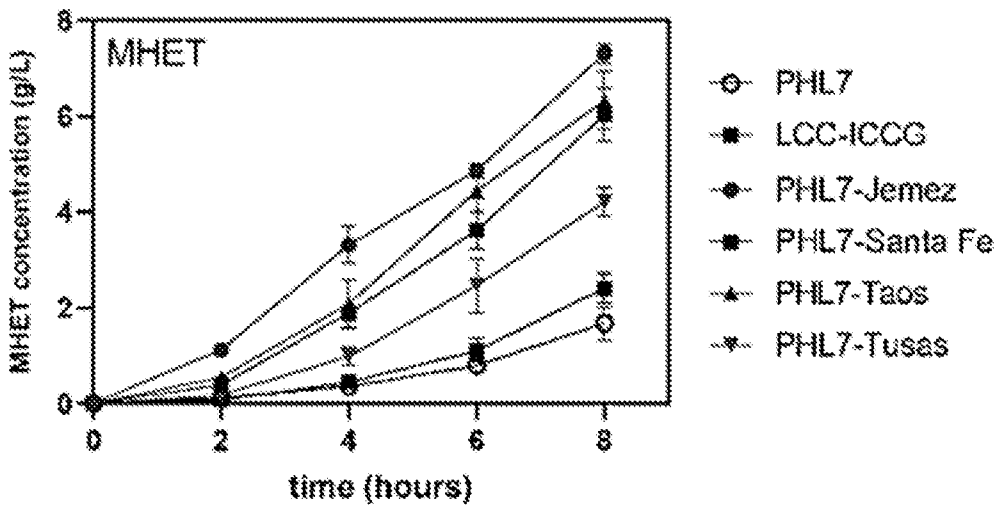


FIG. 2D



Official Use Only/Export Controlled Information/Department of Commerce EAR99

FIG. 3A

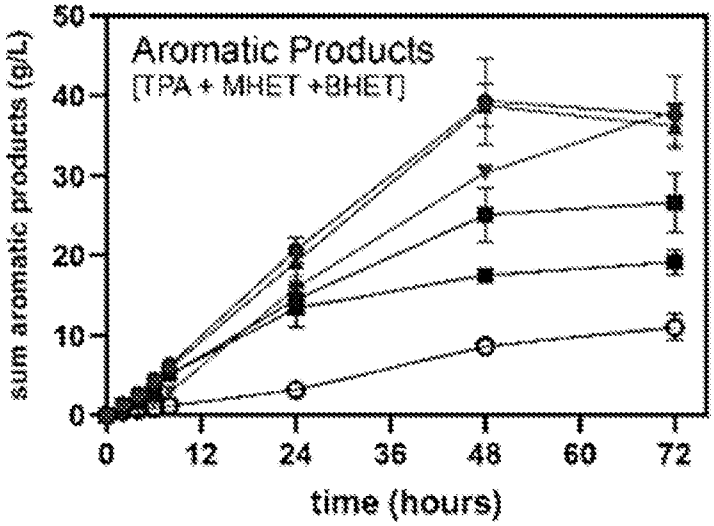


FIG. 3B

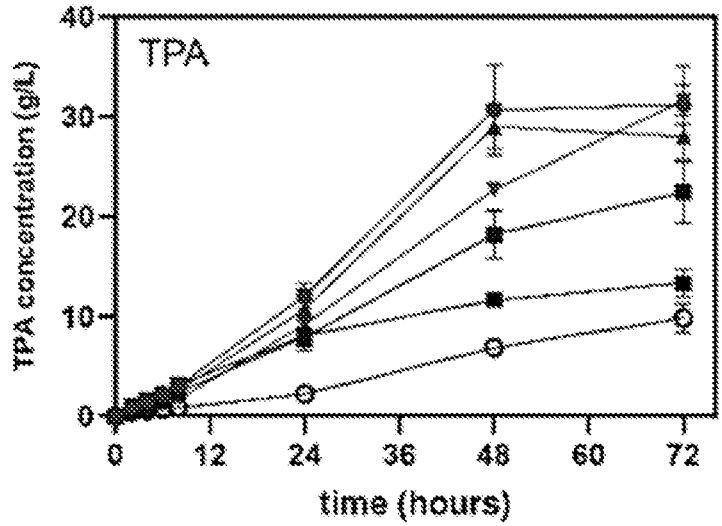
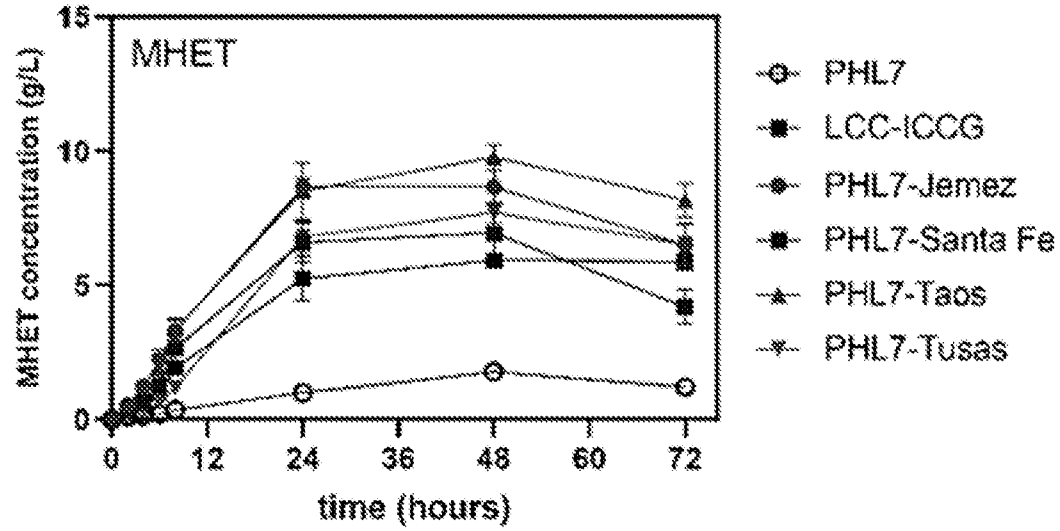


FIG. 3C



Official Use Only/Export Controlled Information/Department of Commerce EAR99

FIG. 4A

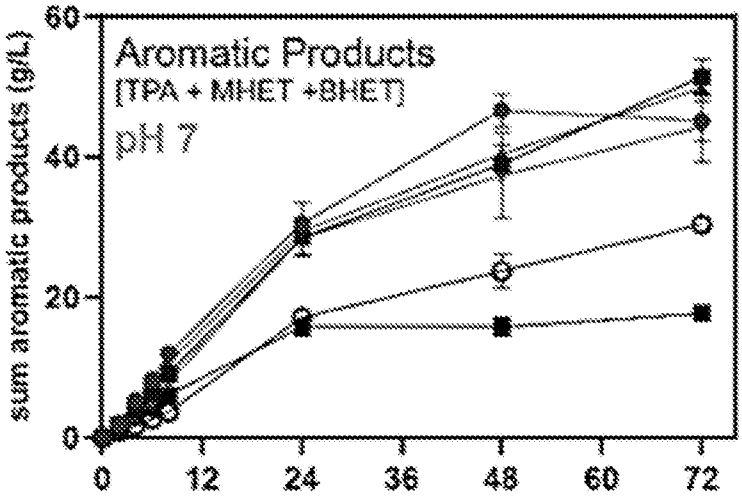


FIG. 4B

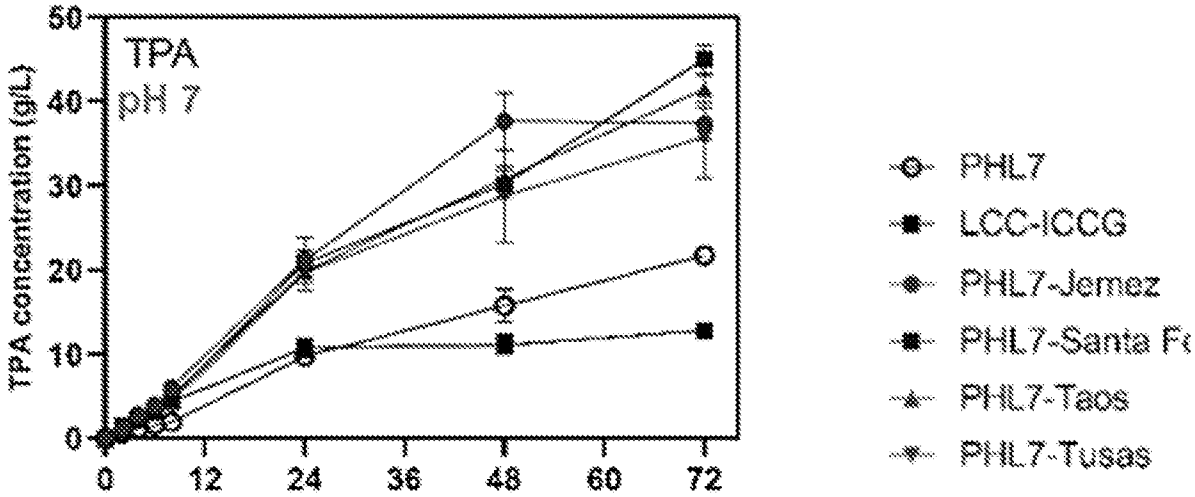
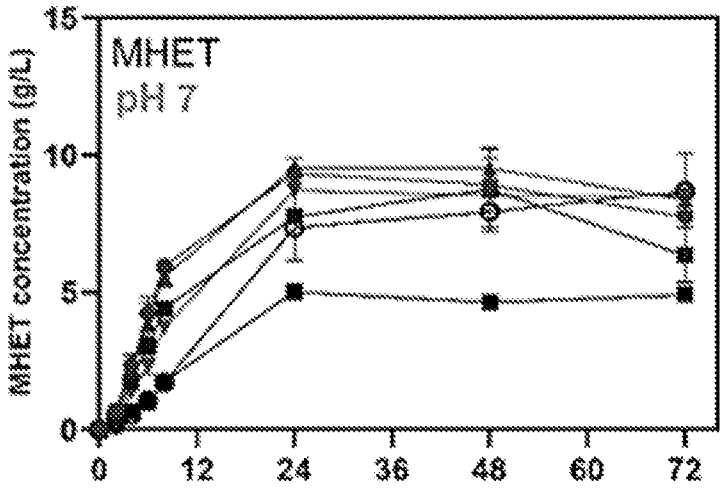


FIG. 4C



Official Use Only/Export Controlled Information/Department of Commerce EAR99

FIG. 4D

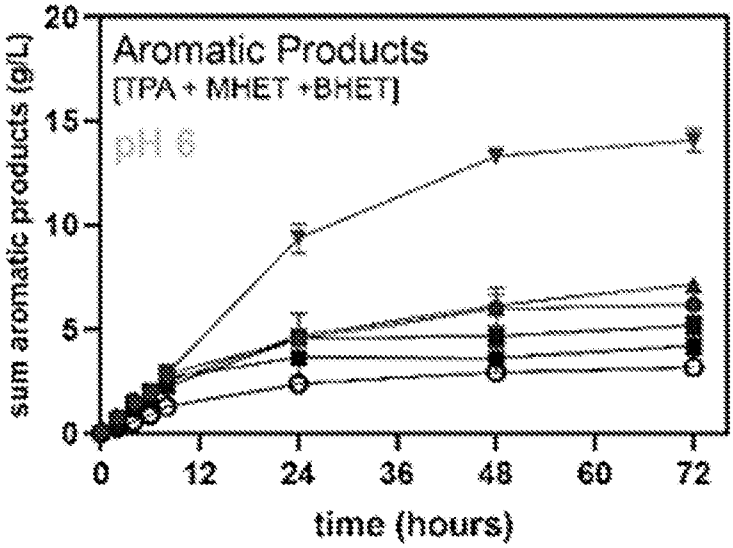


FIG. 4E

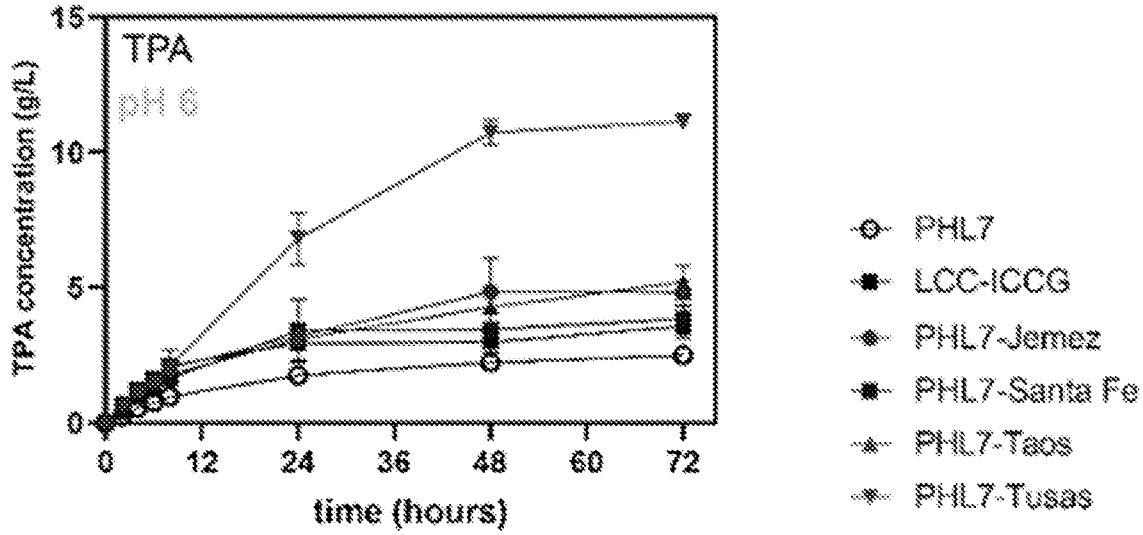
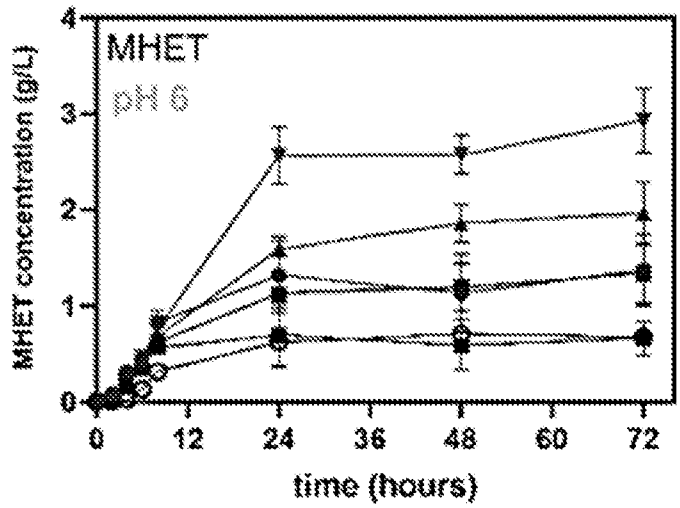
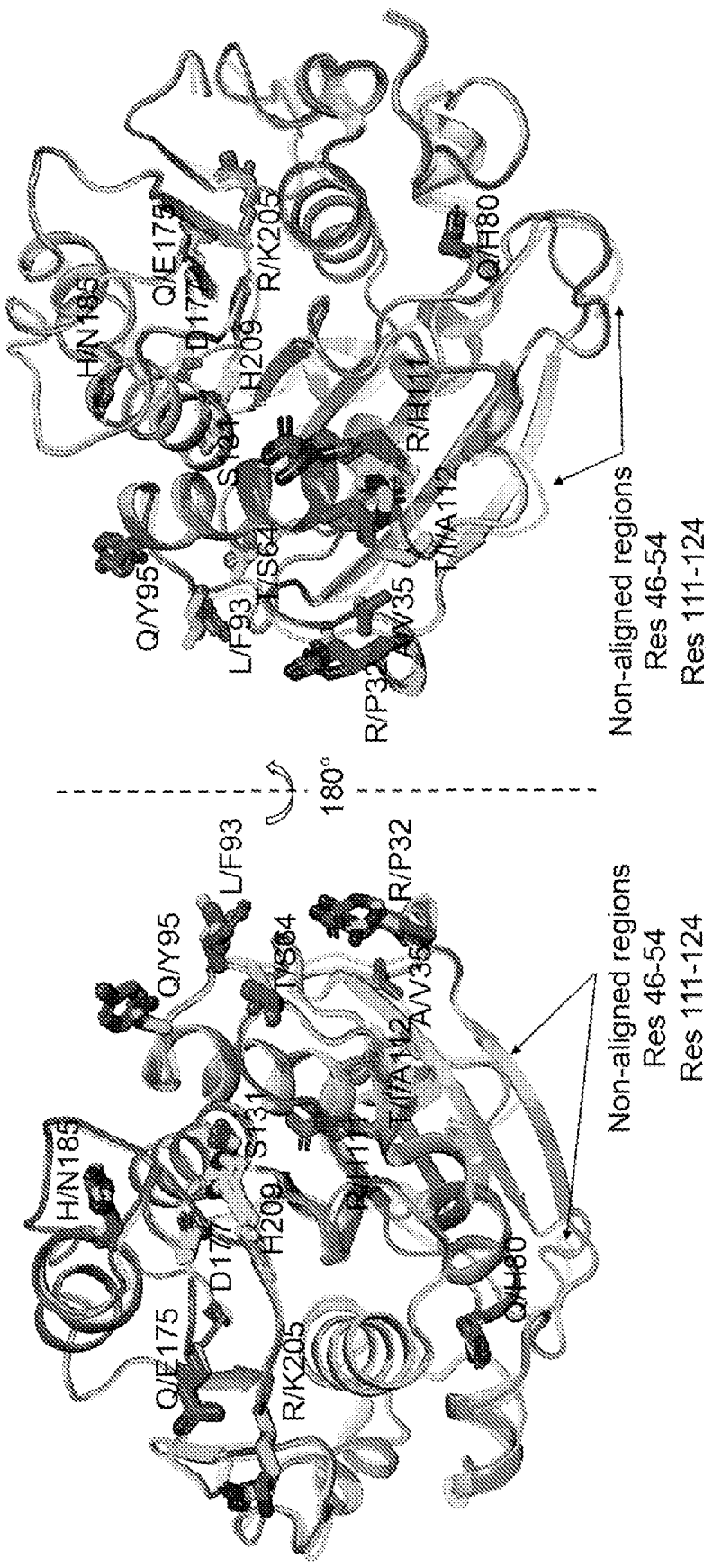


FIG. 4F



Official Use Only/Export Controlled Information/Department of Commerce EAR99

FIG. 5A



Official Use Only/Export Controlled Information/Department of Commerce EAR99

FIG. 5C

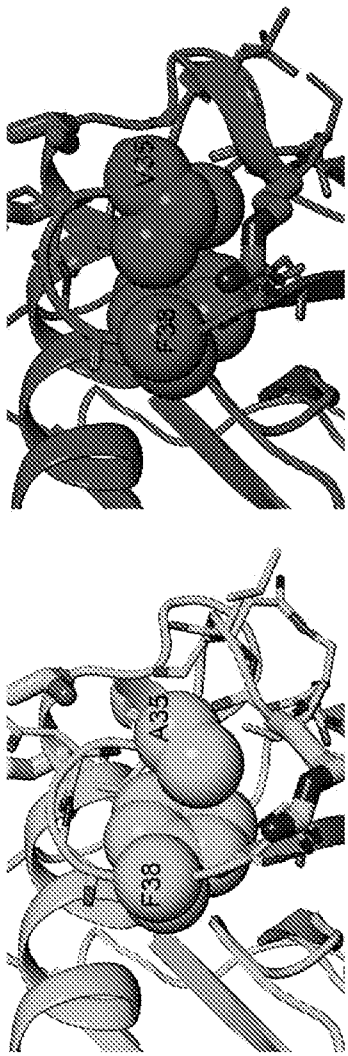
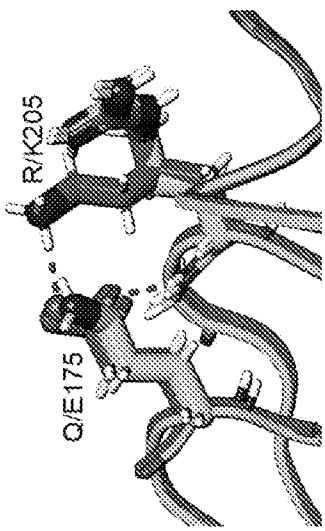


FIG. 5B



Official Use Only/Export Controlled Information/Department of Commerce EAR99

FIG. 6A

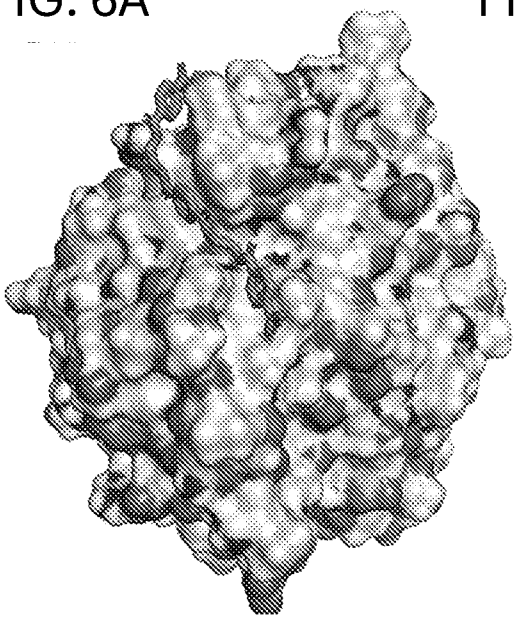


FIG. 6B

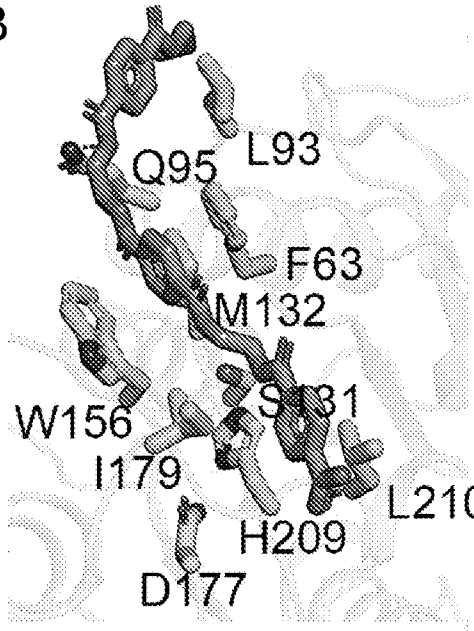


FIG. 6C

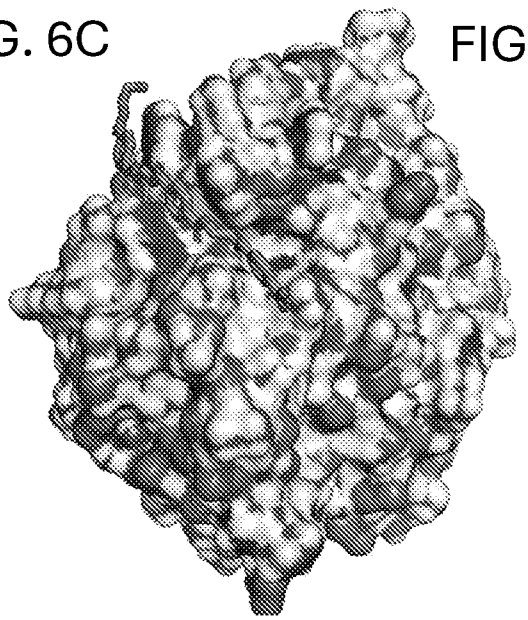
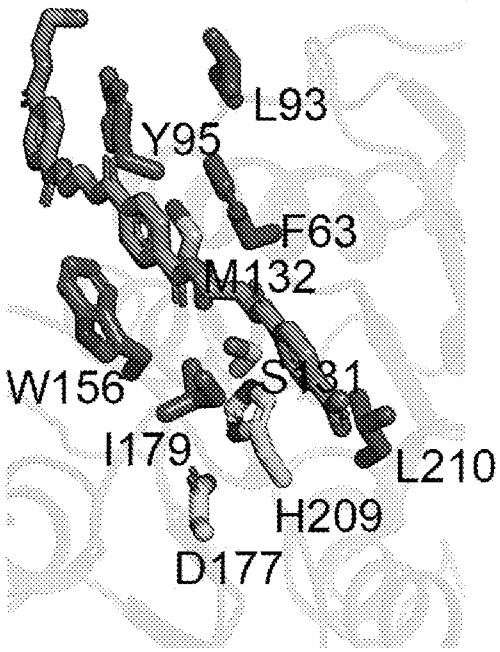


FIG. 6D



Official Use Only/Export Controlled Information/Department of Commerce EAR99

FIG. 7A

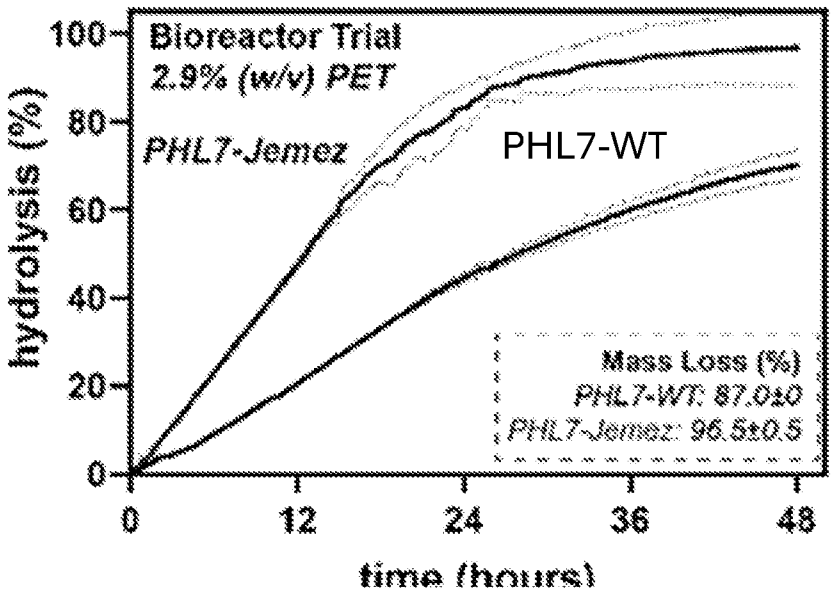


FIG. 7B

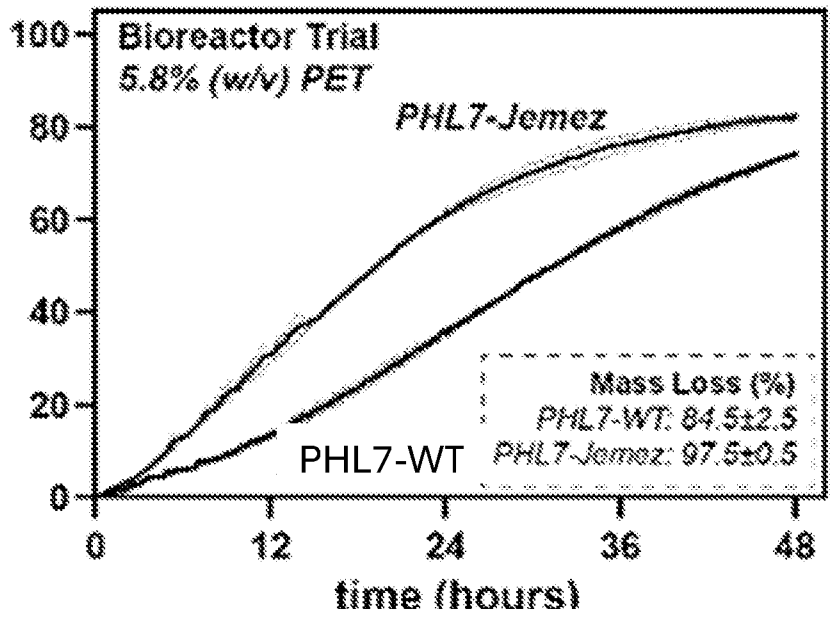
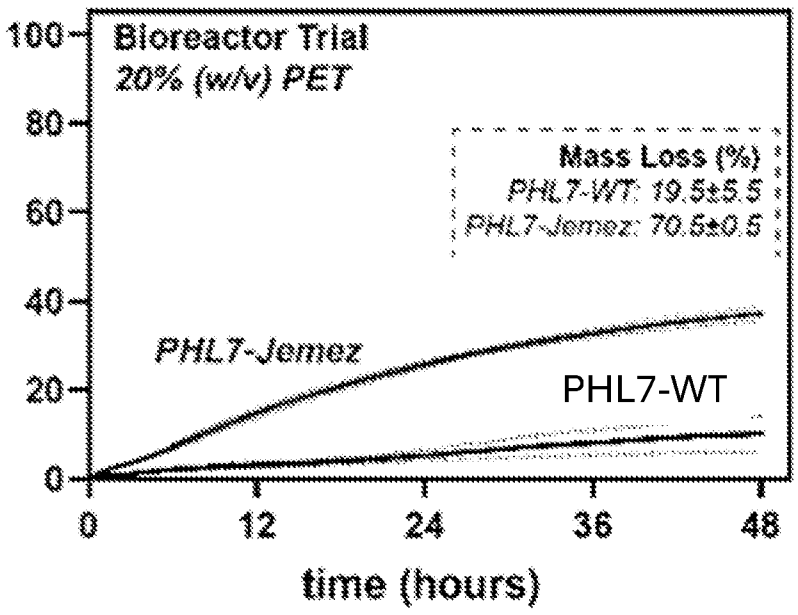
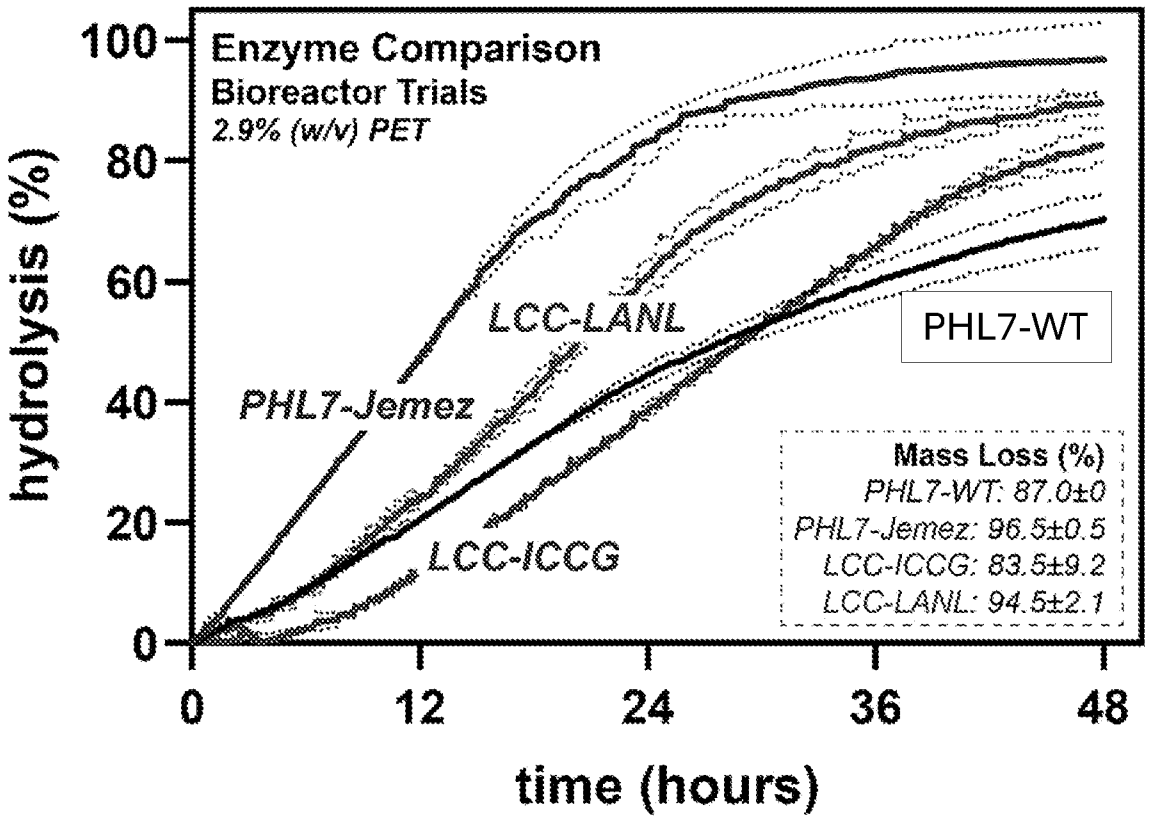


FIG. 7C



Official Use Only/Export Controlled Information/Department of Commerce EAR99

FIG. 8



Official Use Only/Export Controlled Information/Department of Commerce EAR99

FIG. 9A

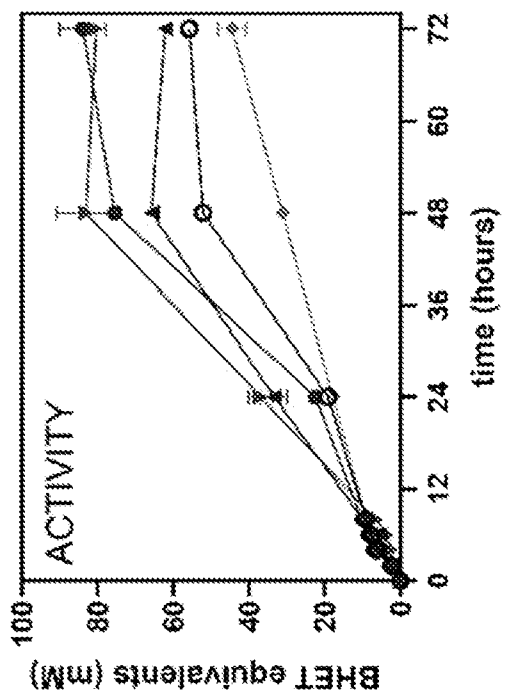
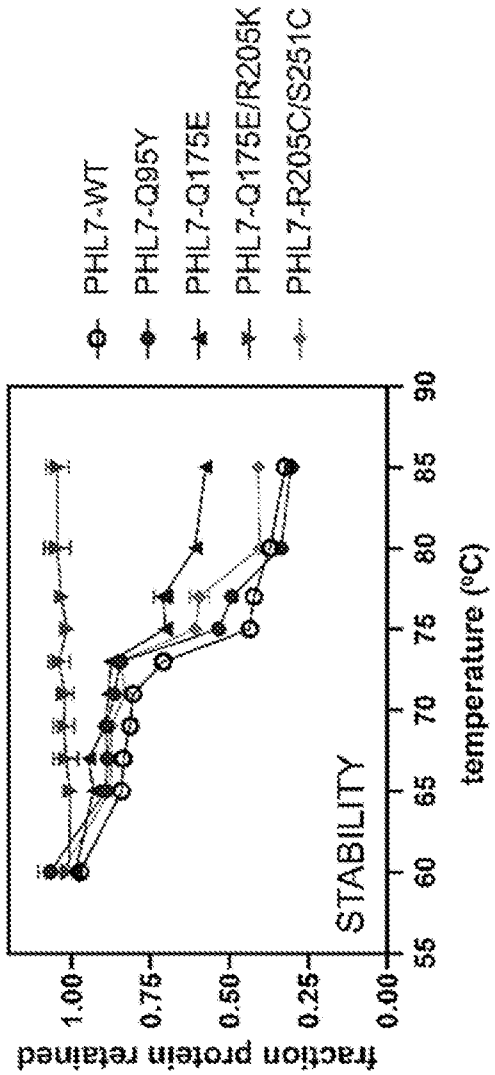


FIG. 9B



Official Use Only/Export Controlled Information/Department of Commerce EAR99

FIG. 10A

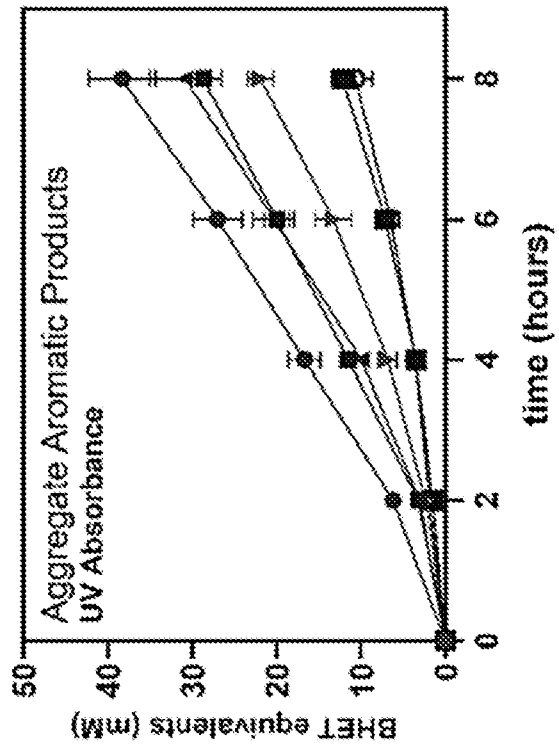
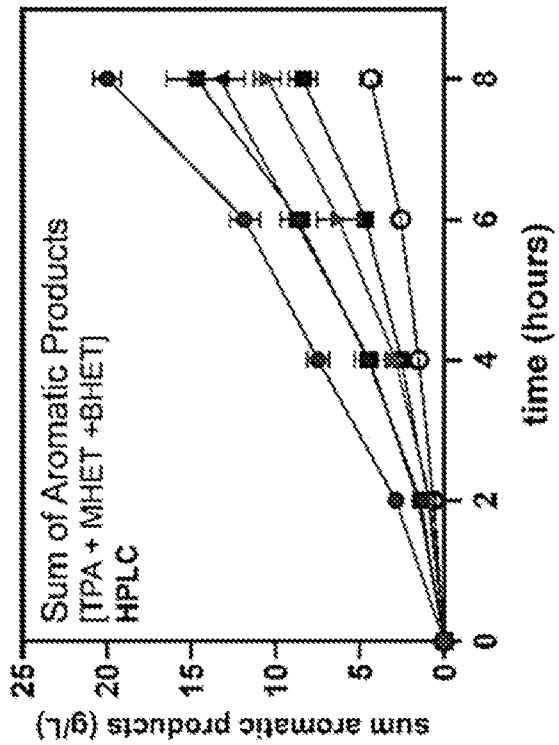
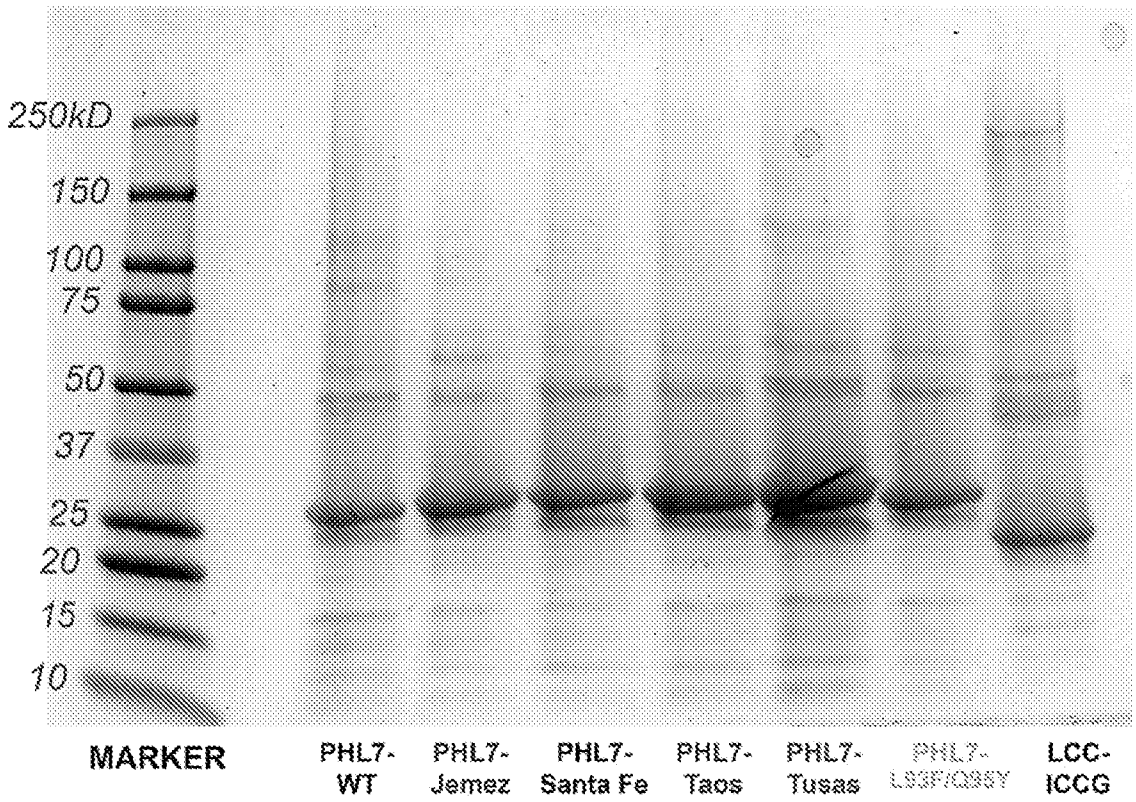


FIG. 10B



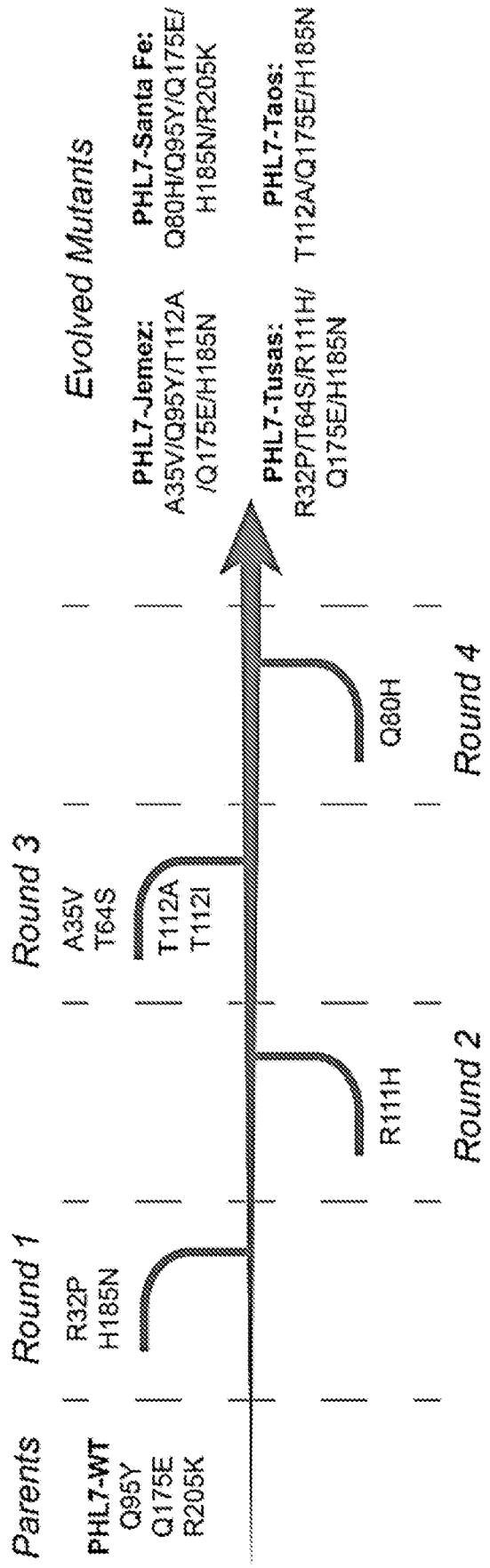
Official Use Only/Export Controlled Information/Department of Commerce EAR99

FIG. 11



Official Use Only/Export Controlled Information/Department of Commerce EAR99

FIG. 12



Official Use Only/Export Controlled Information/Department of Commerce EAR99

FIG. 13A

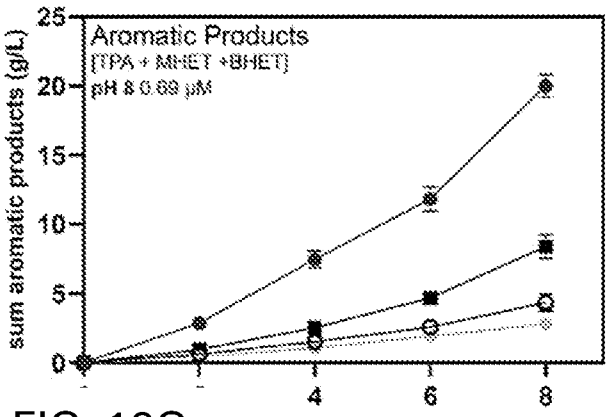


FIG. 13B

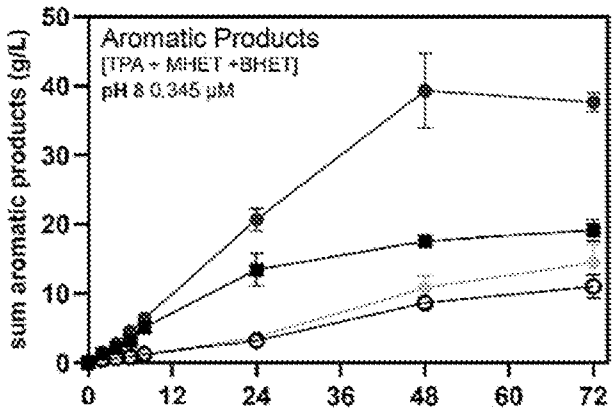


FIG. 13C

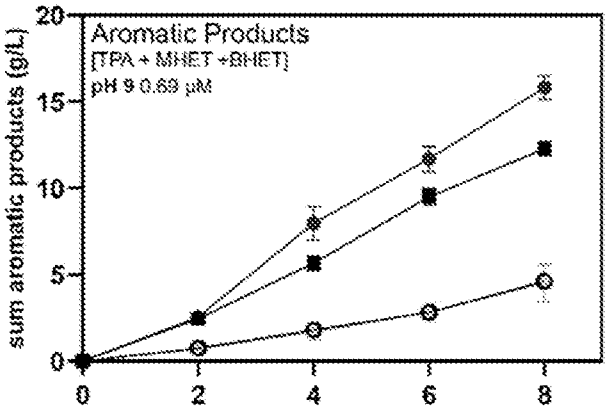


FIG. 13D

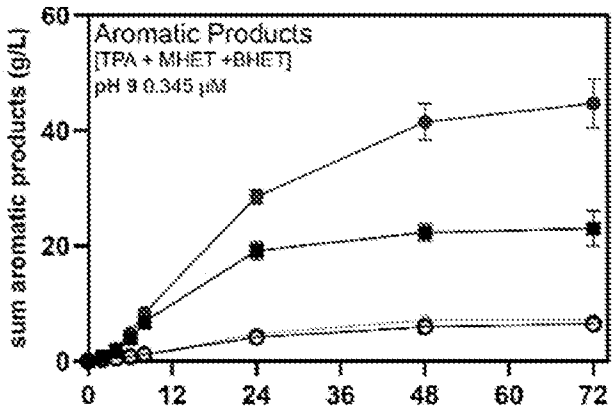


FIG. 13E

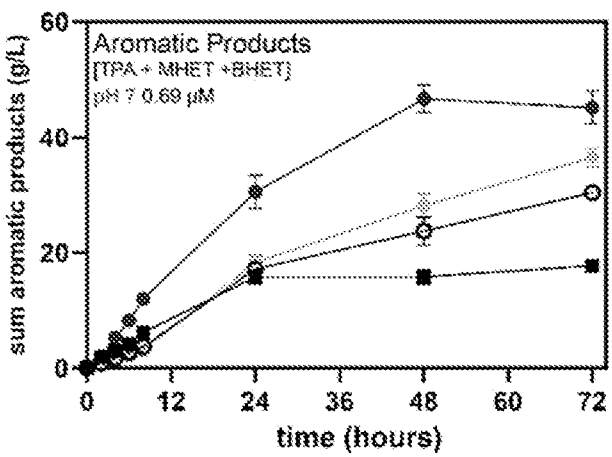
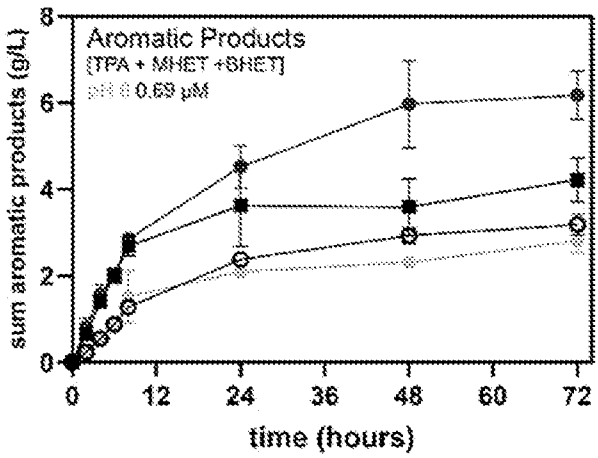
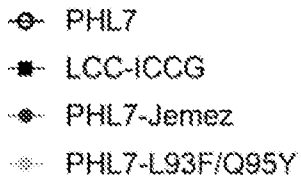


FIG. 13F





Official Use Only/Export Controlled Information/Department of Commerce EAR99

FIG. 14A

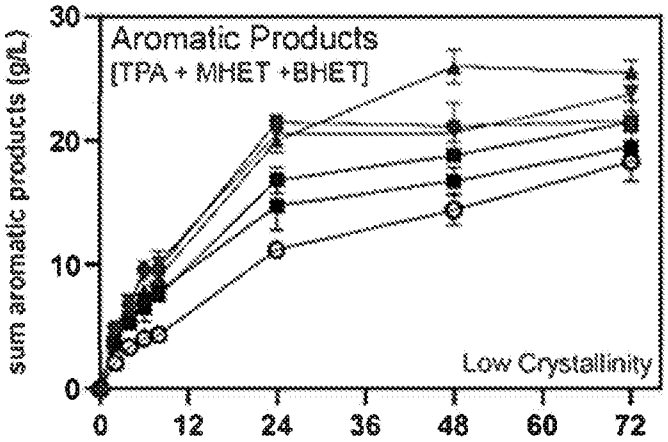


FIG. 14B

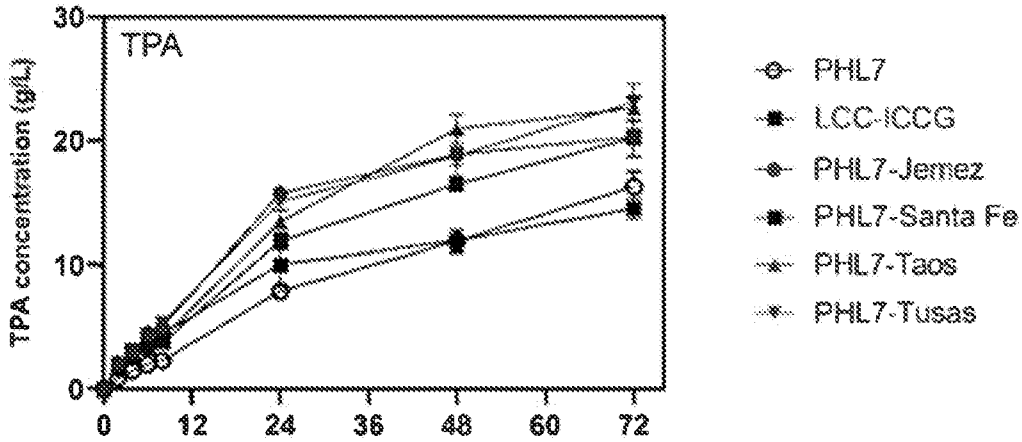
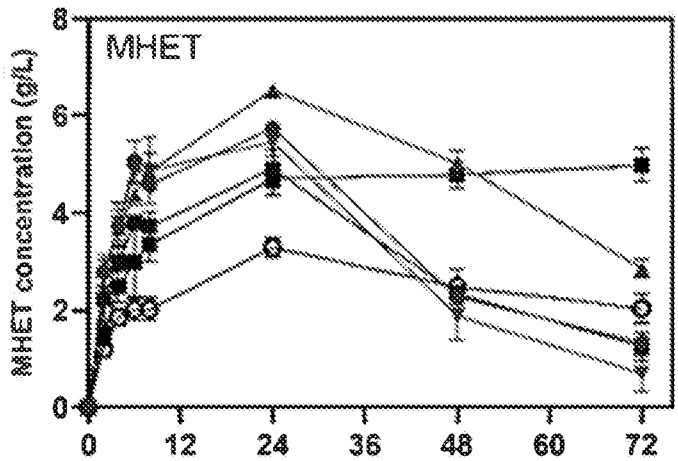


FIG. 14C



Official Use Only/Export Controlled Information/Department of Commerce EAR99

FIG. 14D

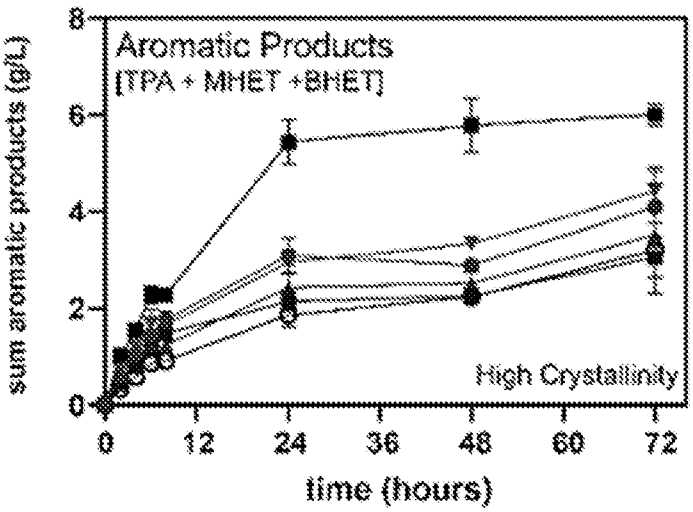


FIG. 14E

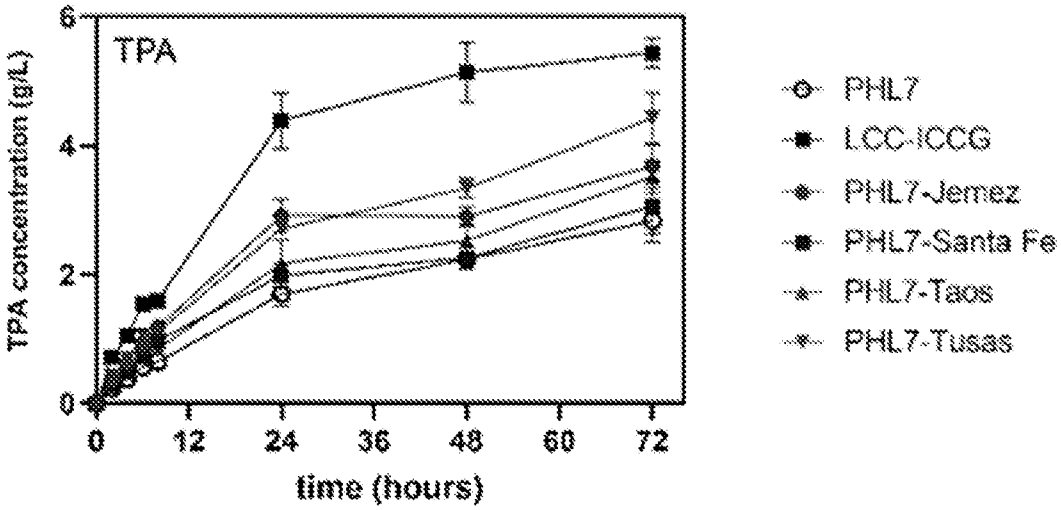
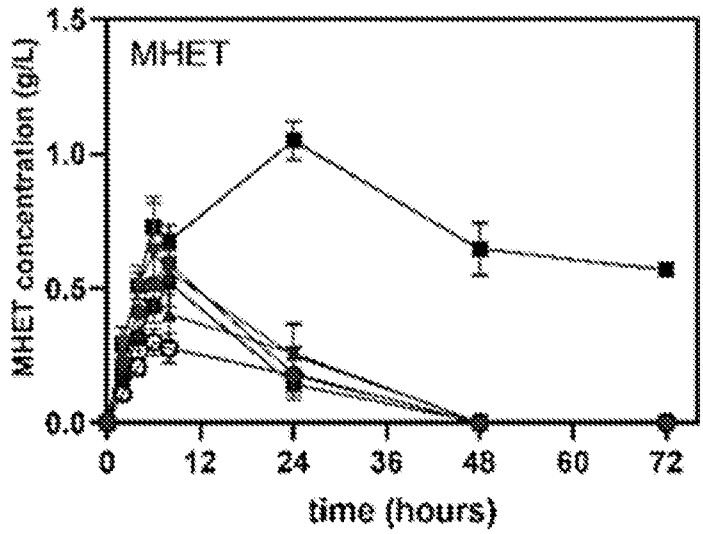


FIG. 14F



Official Use Only/Export Controlled Information/Department of Commerce EAR99

FIG. 15A

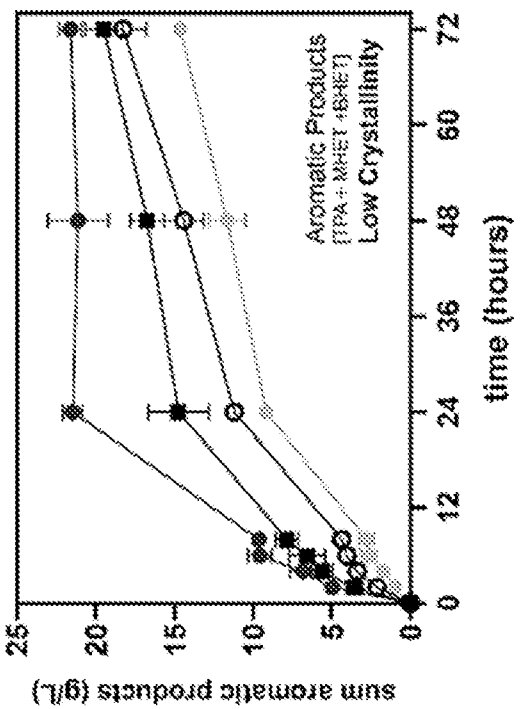
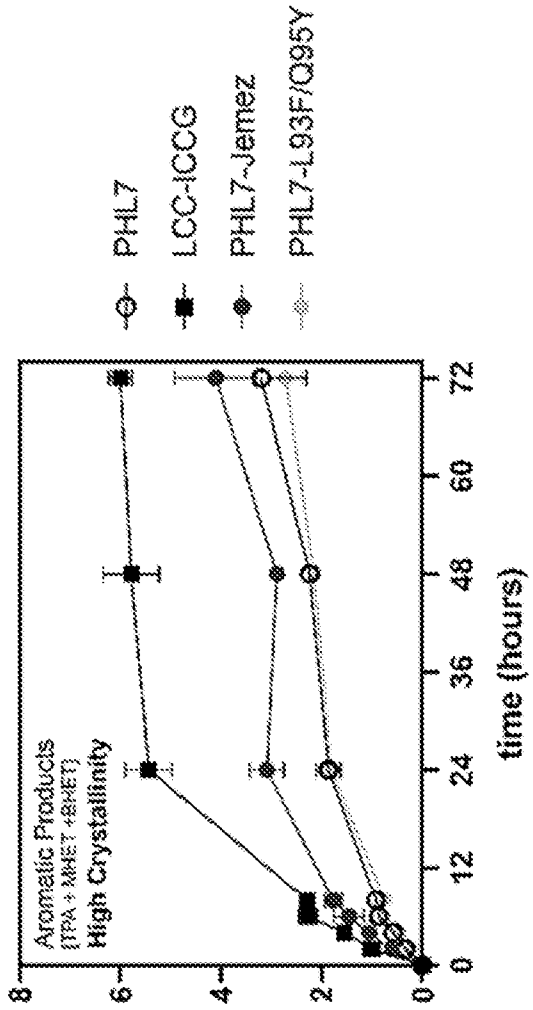


FIG. 15B



Official Use Only/Export Controlled Information/Department of Commerce EAR99

FIG. 16A

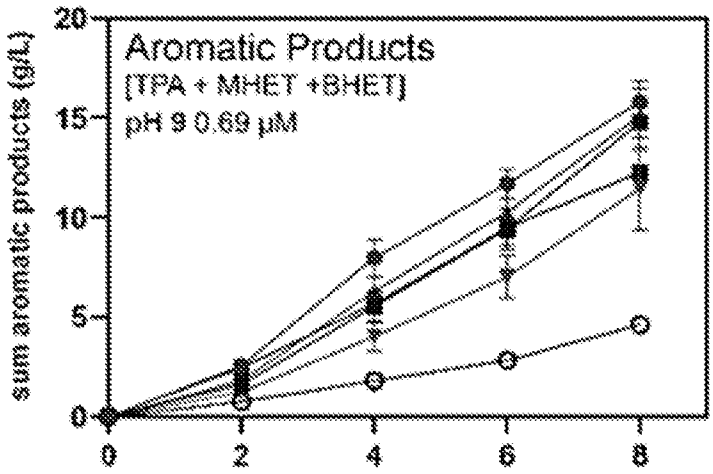


FIG. 16B

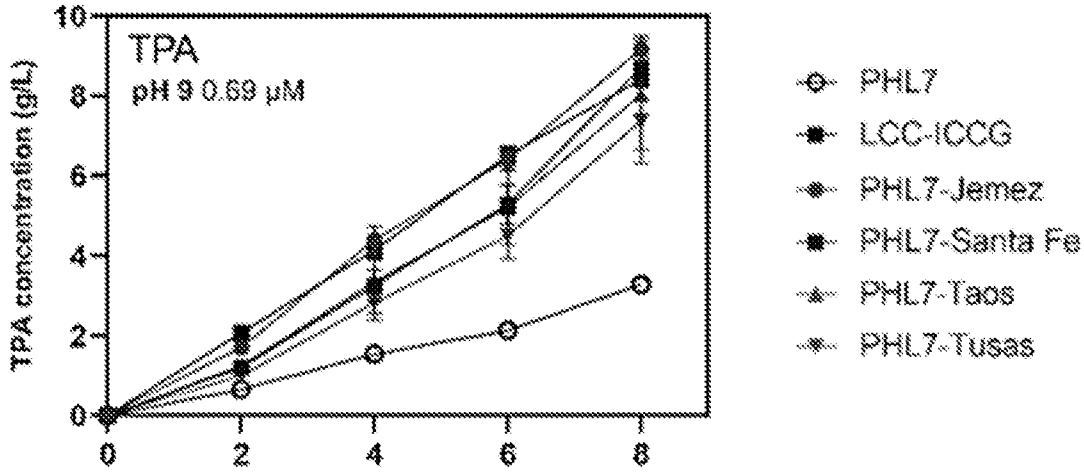
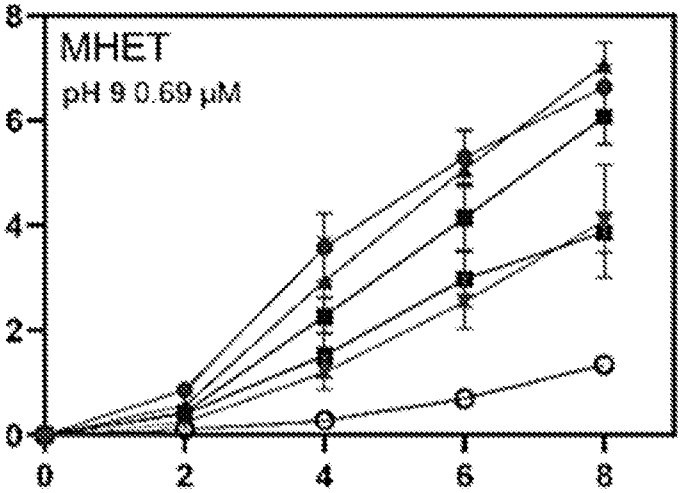


FIG. 16C



Official Use Only/Export Controlled Information/Department of Commerce EAR99

FIG. 16D

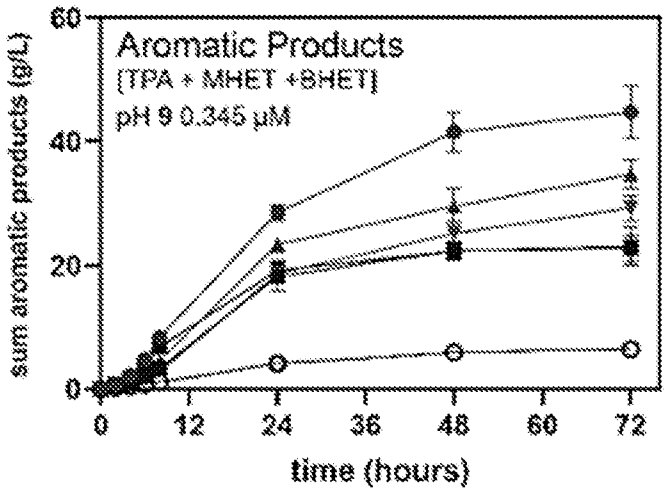


FIG. 16E

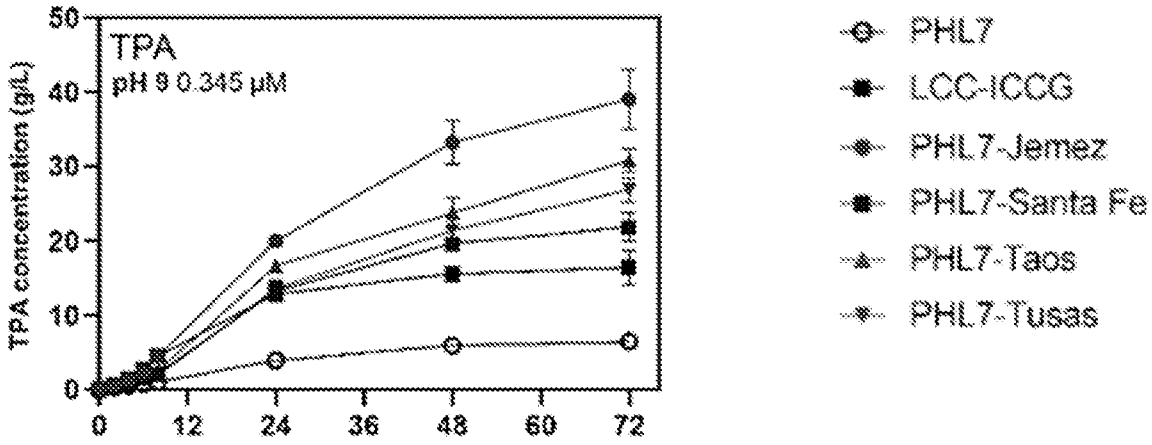
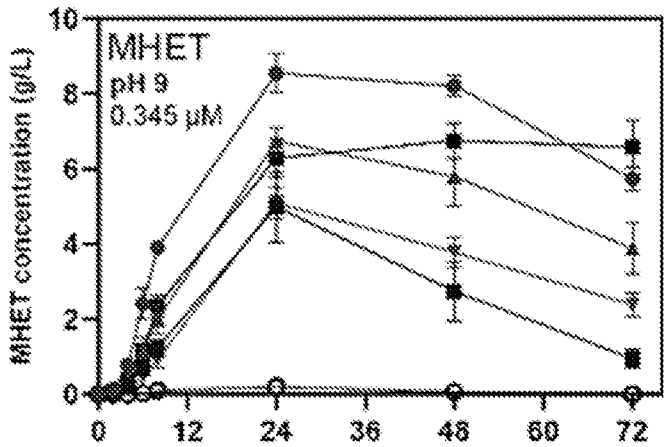


FIG. 16F



Official Use Only/Export Controlled Information/Department of Commerce EAR99

FIG. 17A

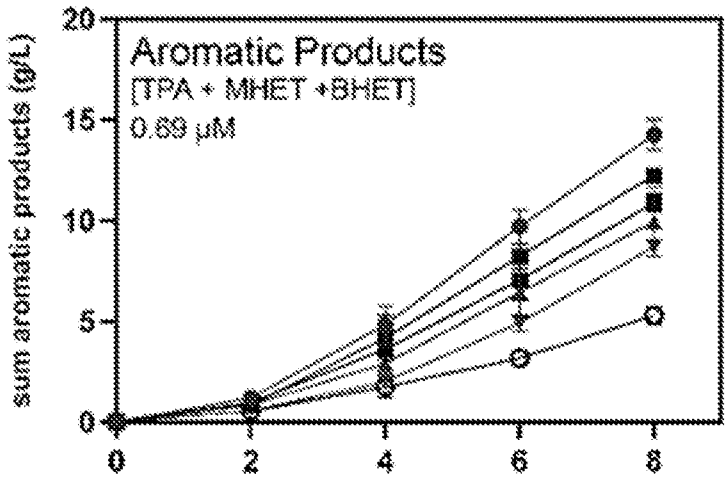


FIG. 17B

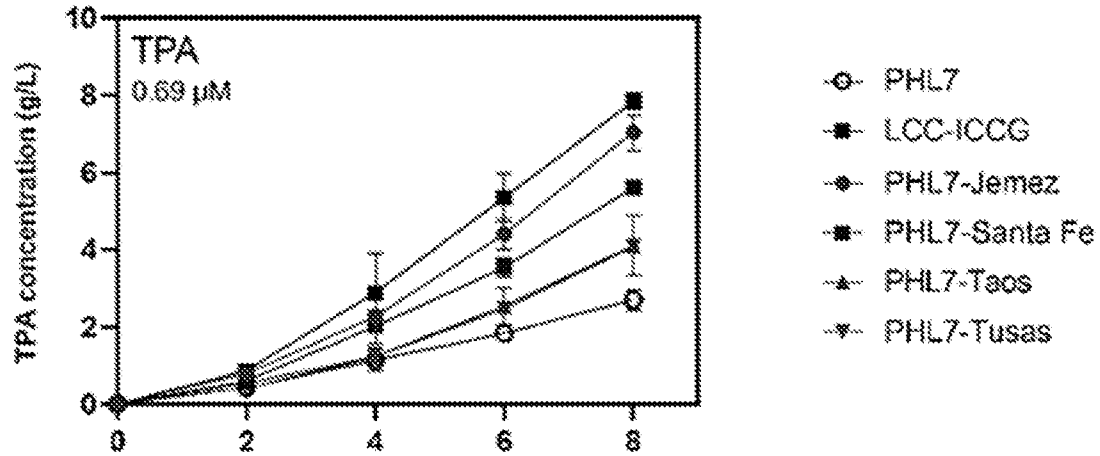
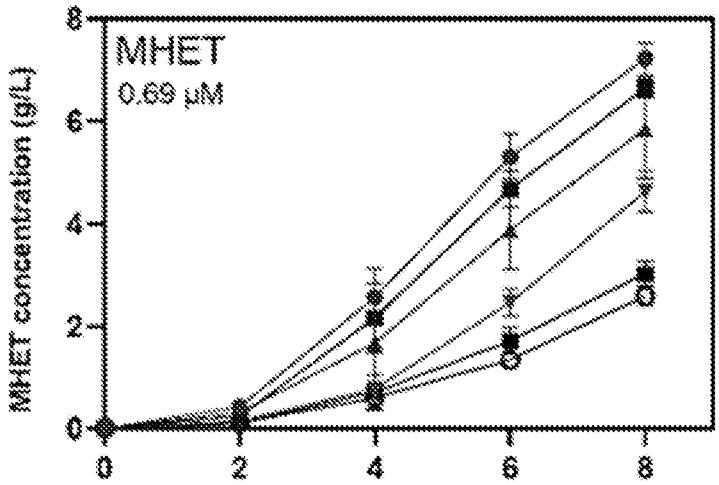


FIG. 17C



Official Use Only/Export Controlled Information/Department of Commerce EAR99

FIG. 17D

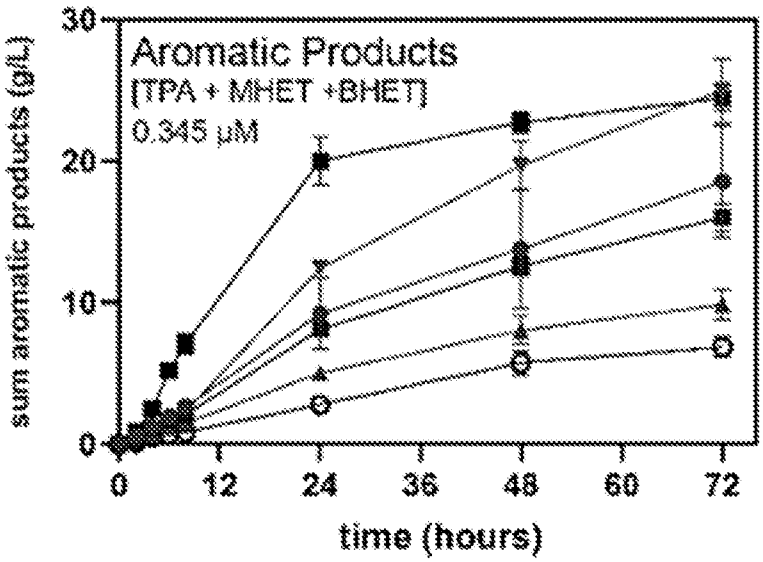


FIG. 17E

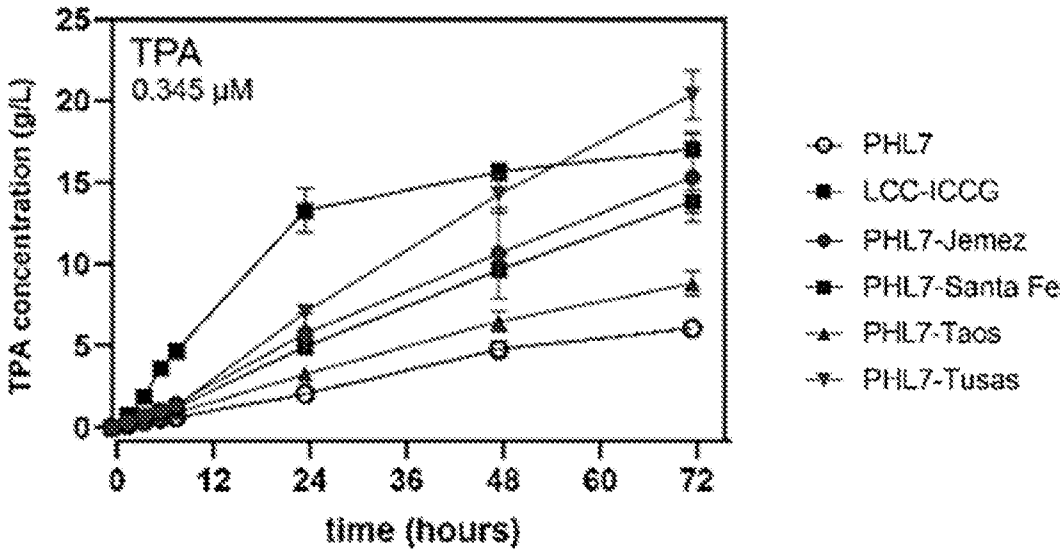
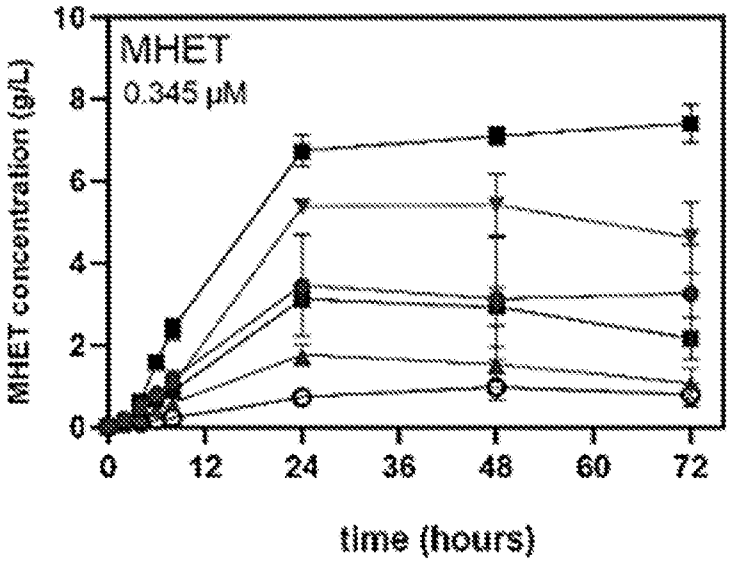


FIG. 17F



Official Use Only/Export Controlled Information/Department of Commerce EAR99

FIG. 18A

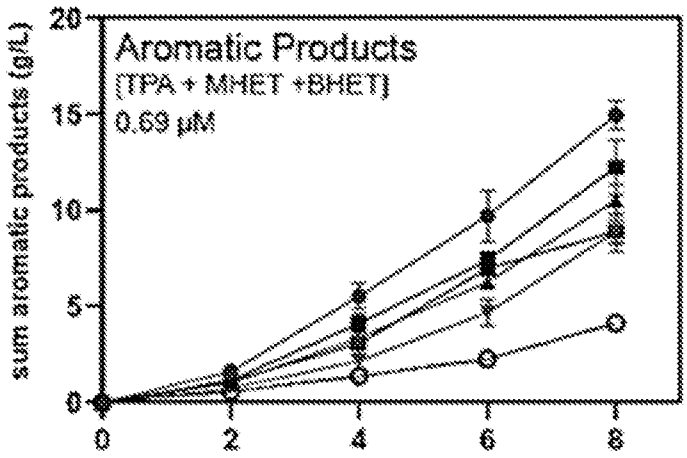
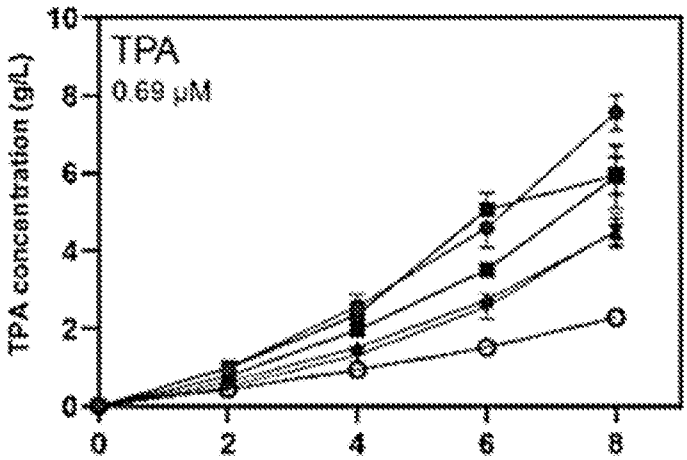


FIG. 18B



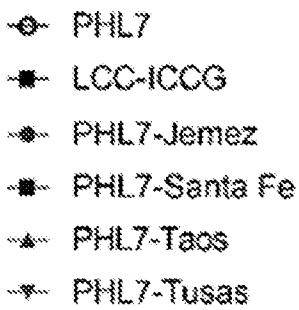
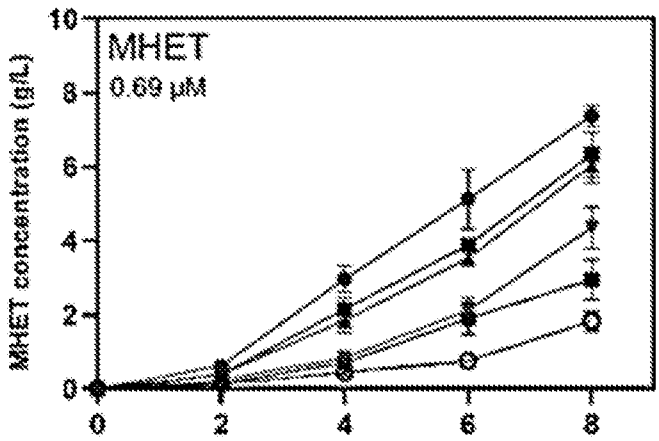


FIG. 18C



Official Use Only/Export Controlled Information/Department of Commerce EAR99

FIG. 18D

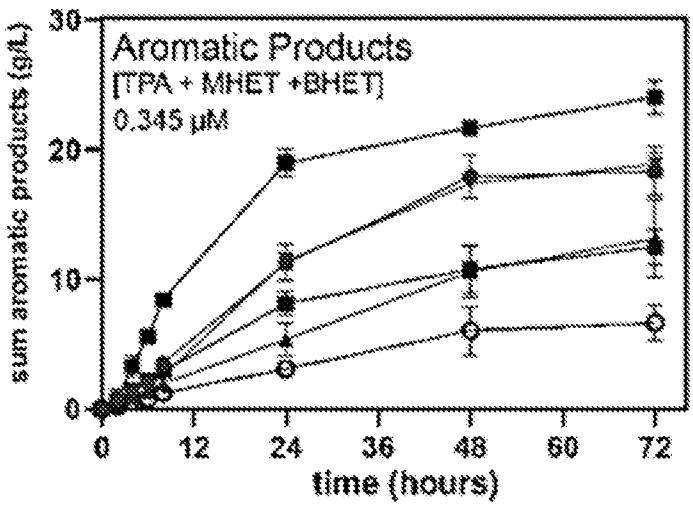


FIG. 18E

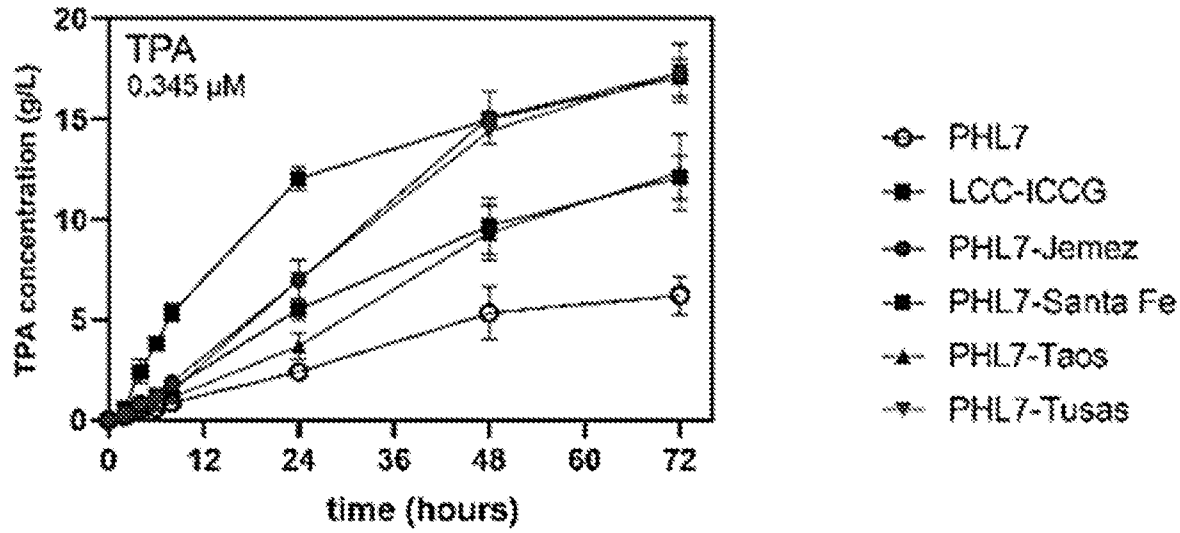
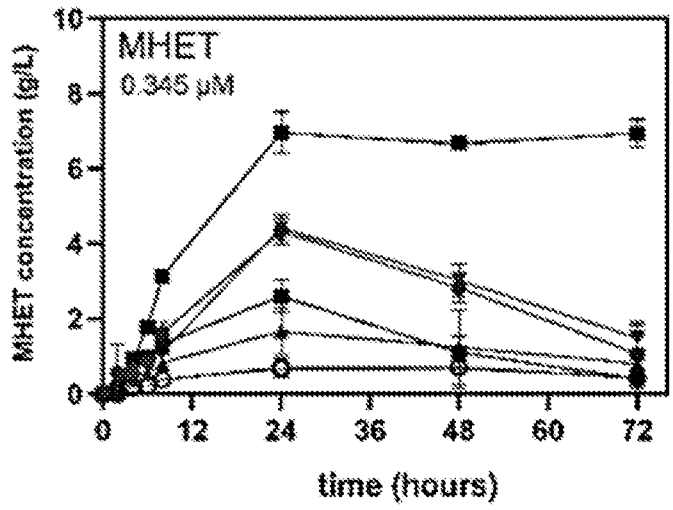


FIG. 18F



Official Use Only/Export Controlled Information/Department of Commerce EAR99

FIG. 19A

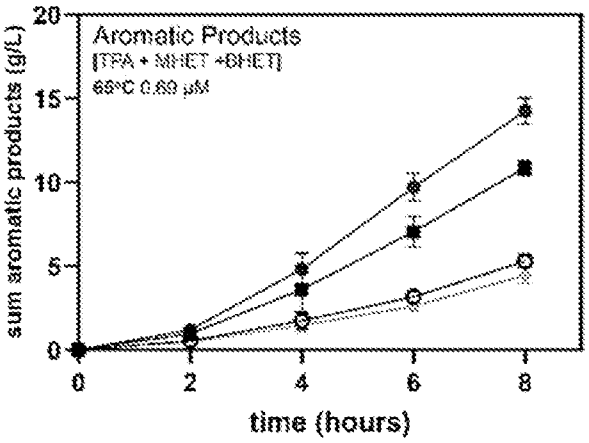


FIG. 19B

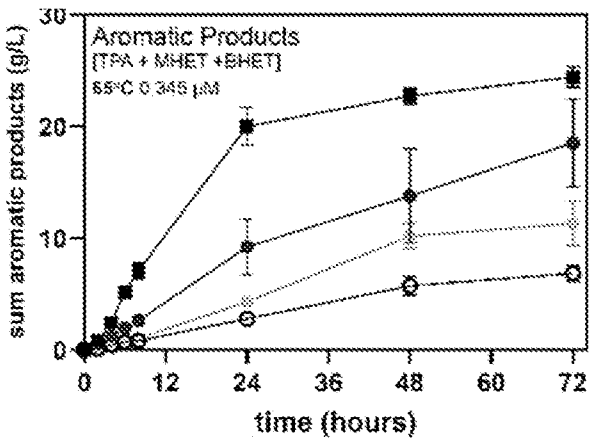


FIG. 19C

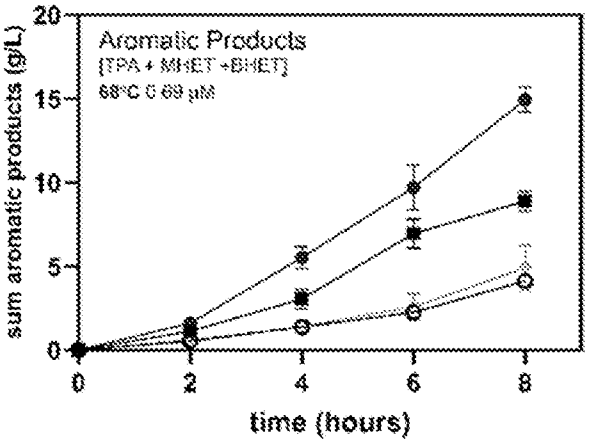


FIG. 19D

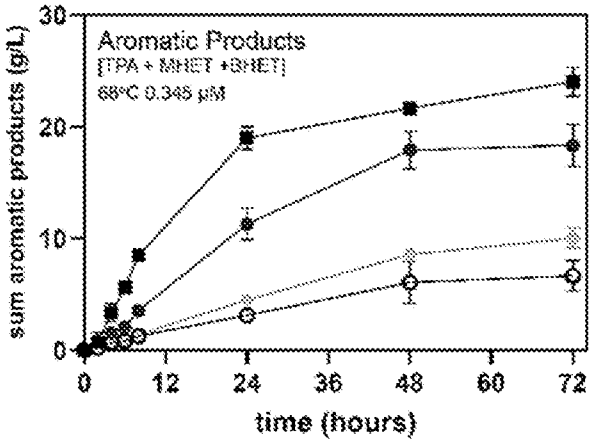


FIG. 19E

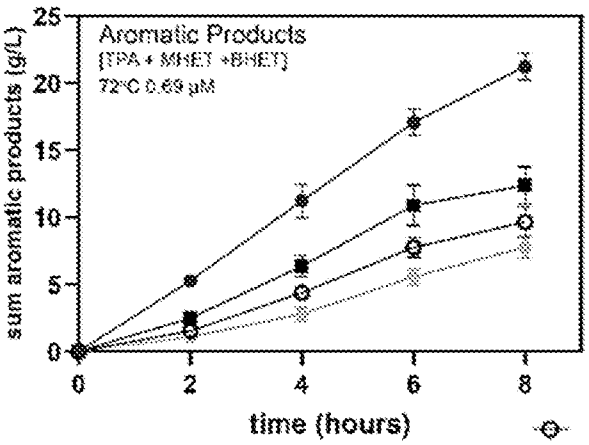
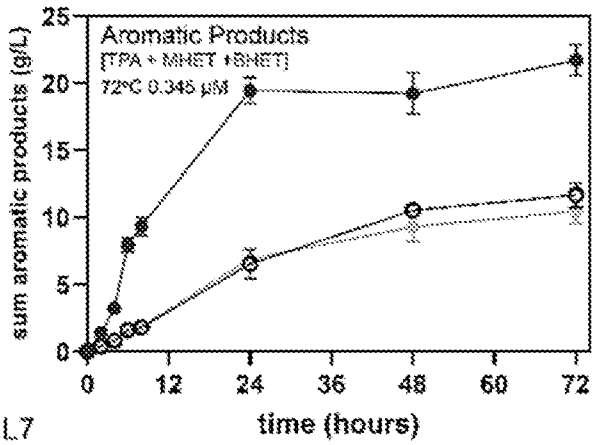
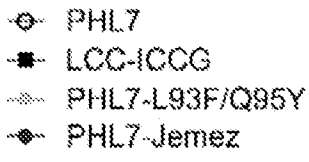


FIG. 19F





Official Use Only/Export Controlled Information/Department of Commerce EAR99

FIG. 20A

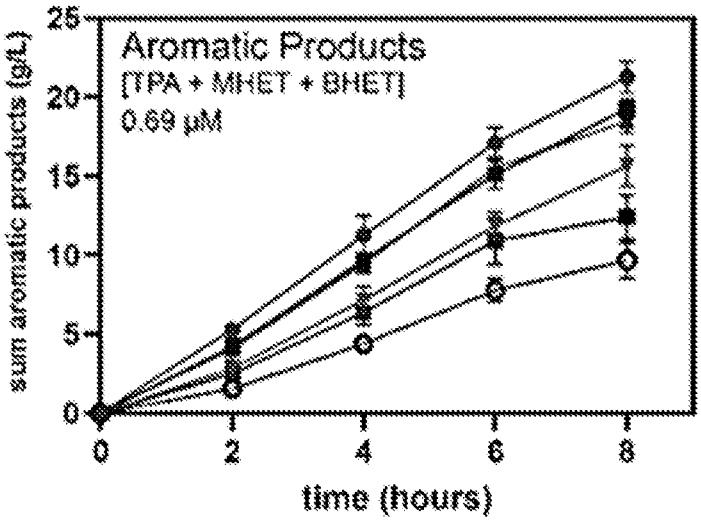


FIG. 20B

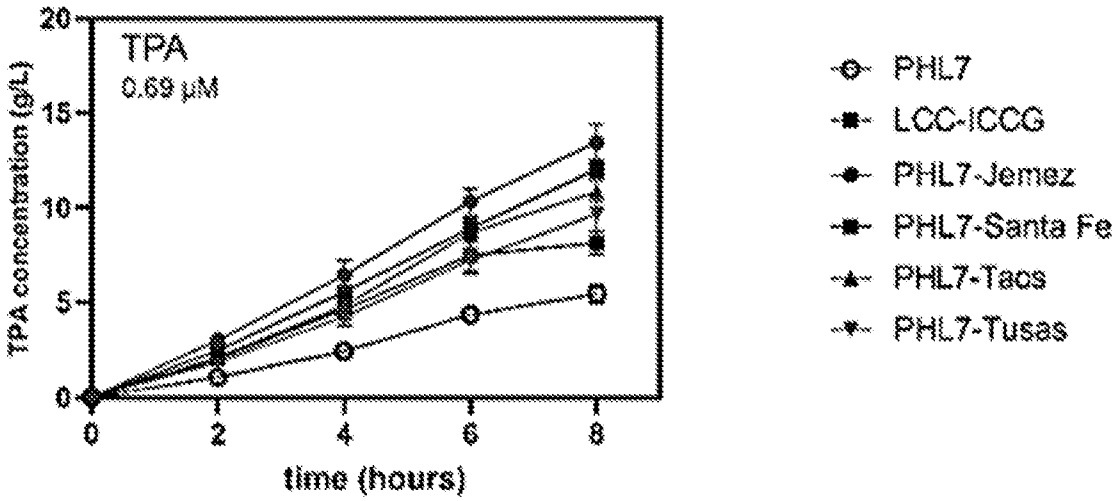
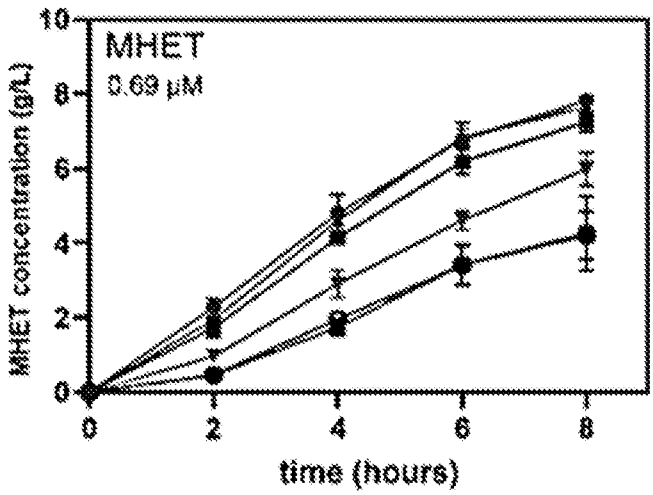


FIG. 20C



Official Use Only/Export Controlled Information/Department of Commerce EAR99

FIG. 20D

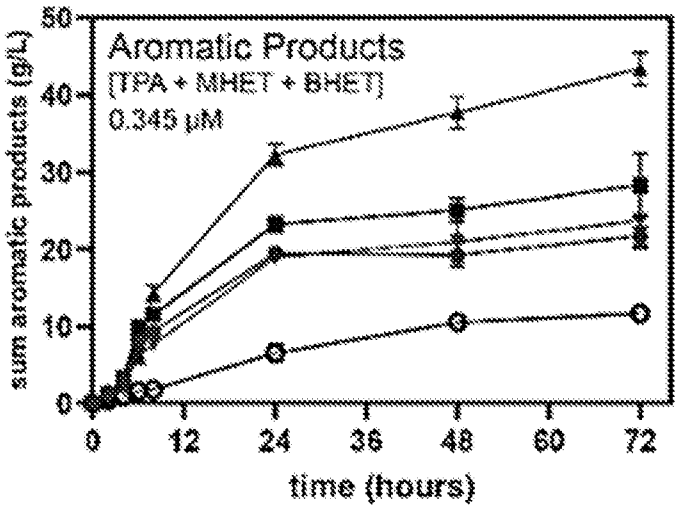


FIG. 20E

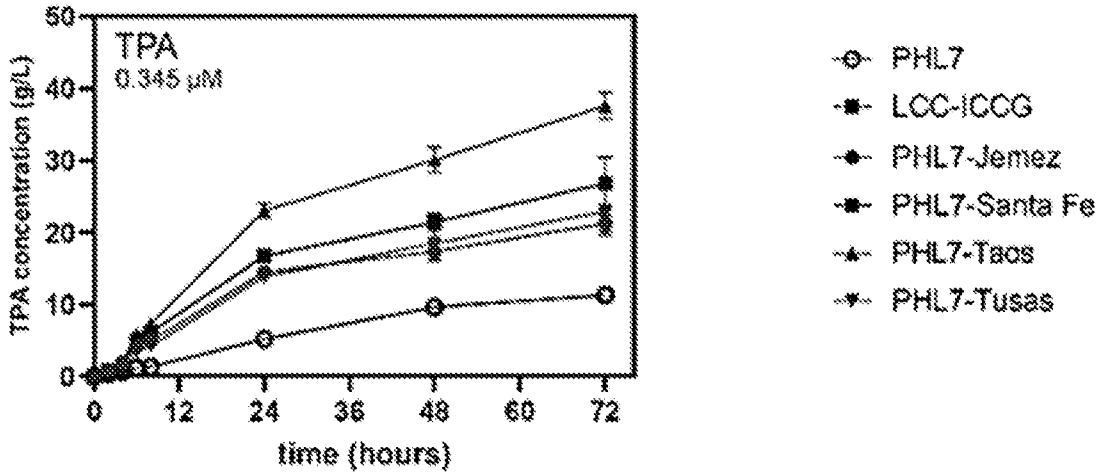
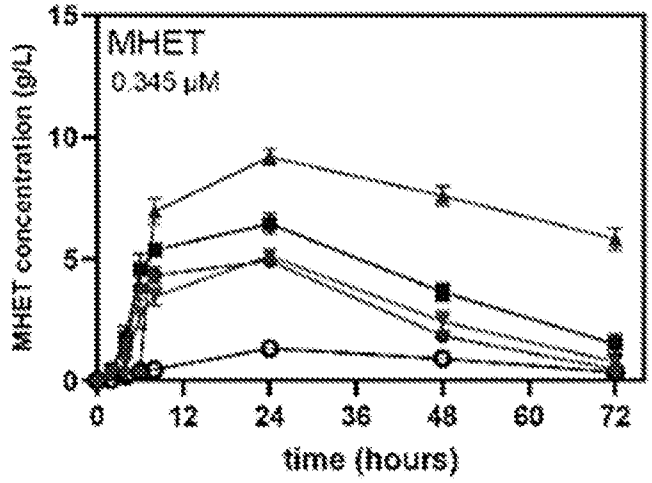


FIG. 20F



Official Use Only/Export Controlled Information/Department of Commerce EAR99

FIG. 21A

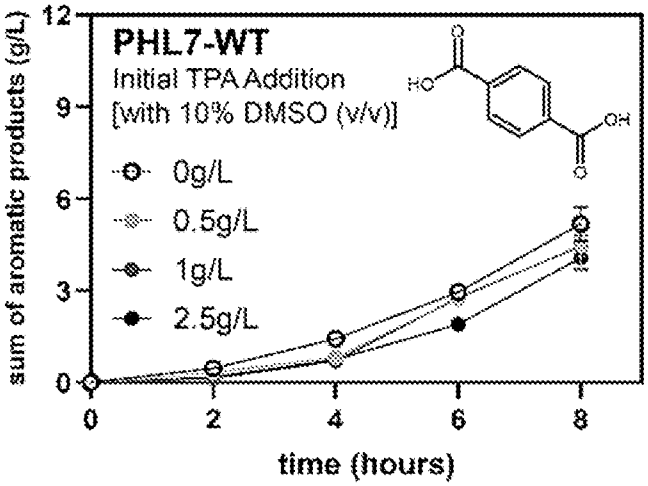


FIG. 21B

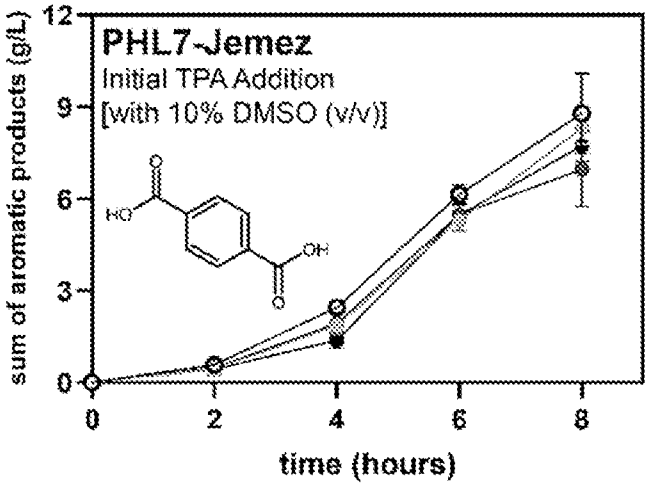


FIG. 21C

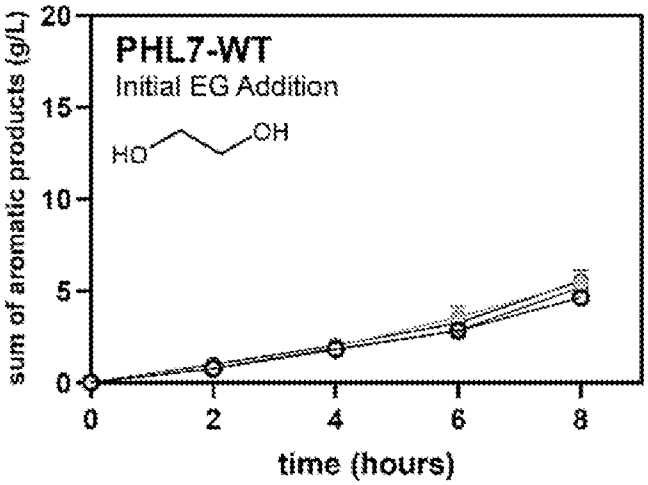


FIG. 21D

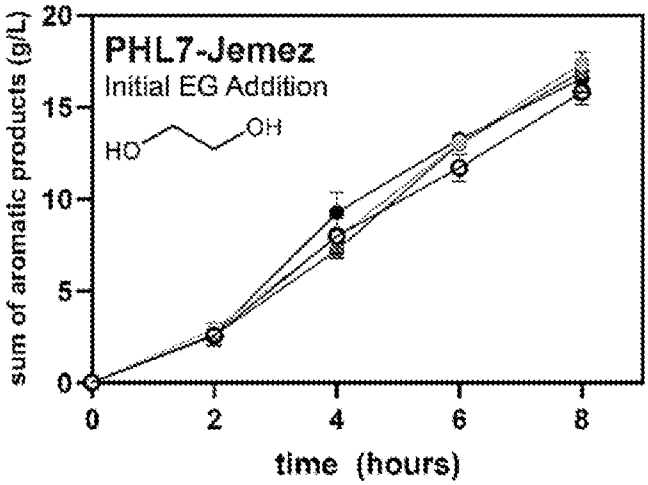


FIG. 21E

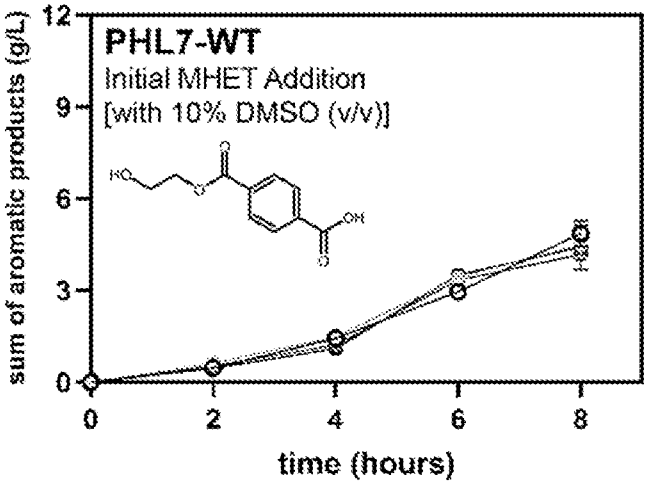
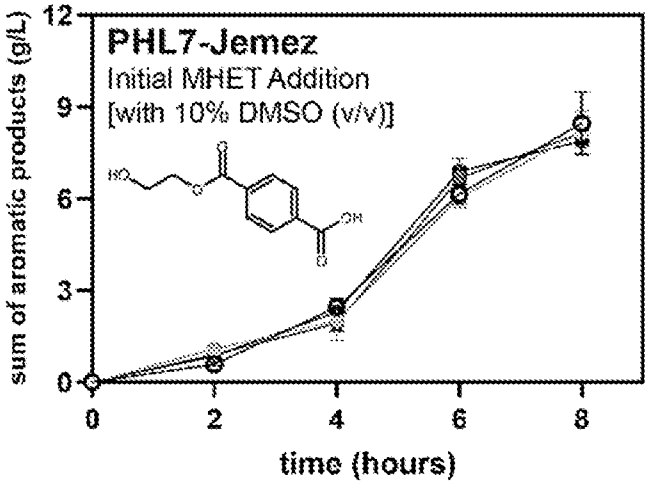


FIG. 21F



Official Use Only/Export Controlled Information/Department of Commerce EAR99

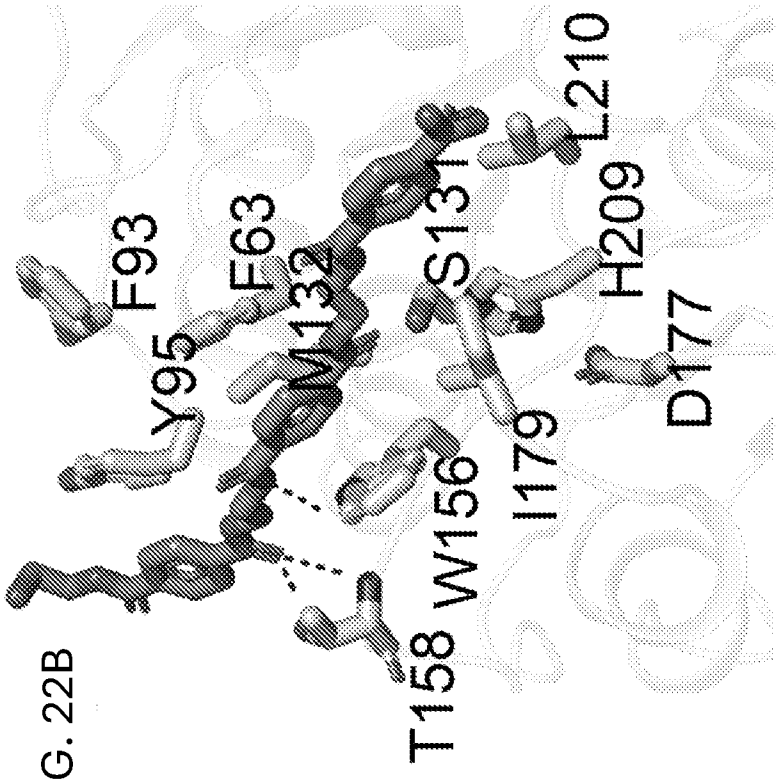


FIG. 22B

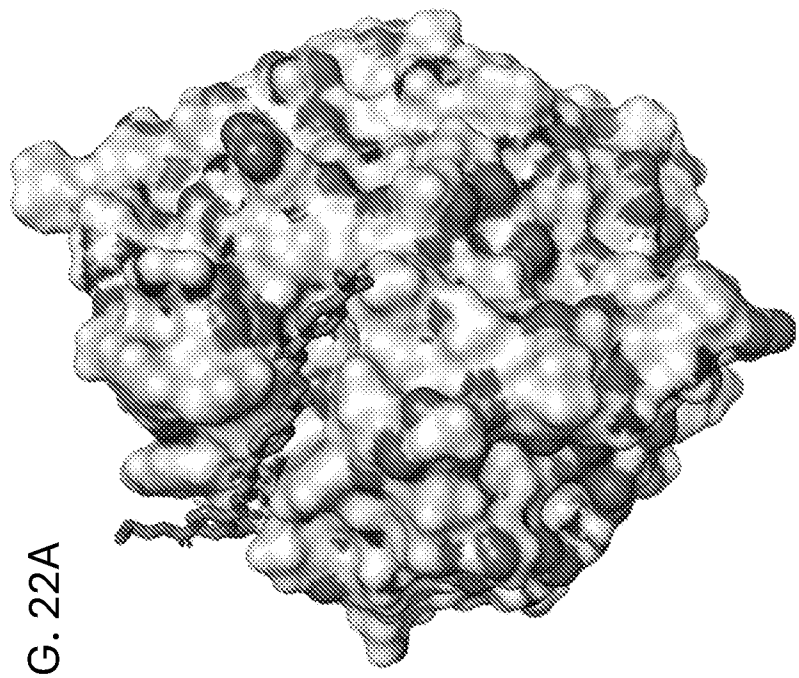


FIG. 22A

Official Use Only/Export Controlled Information/Department of Commerce EAR99